Azadeh Hassan Raeisi

Investigation of Hydrophobically Modified Polyacrylamide Gels Prepared in Micellar Solutions of a Cationic Surfactant

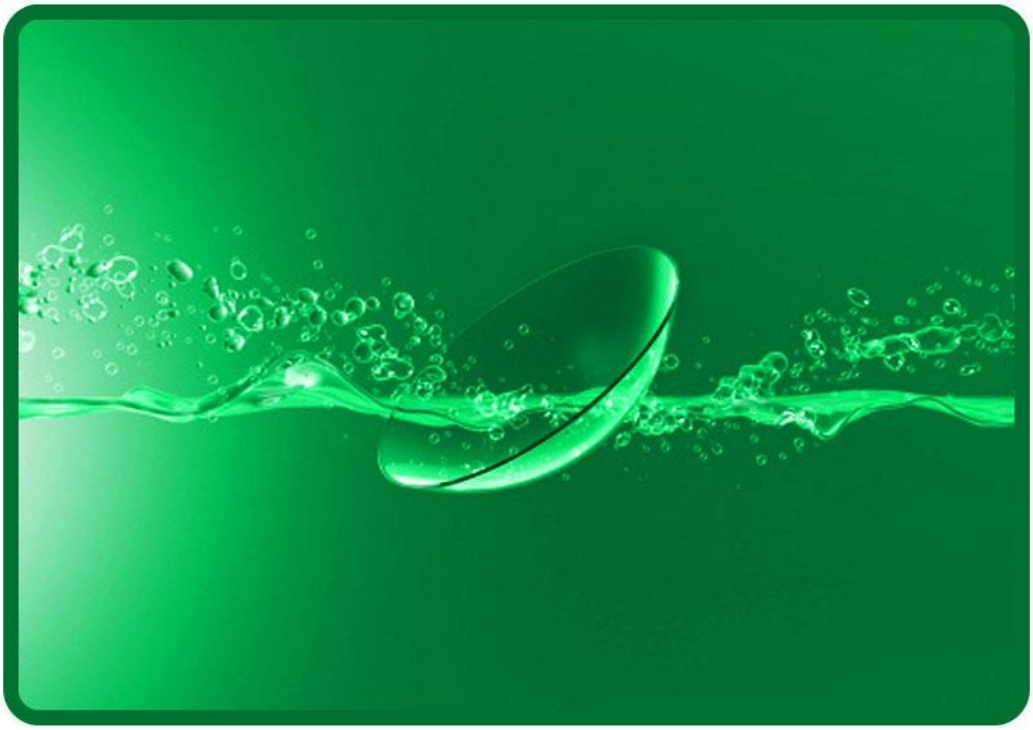

Investigation of Hydrophobically Modified Polyacrylamide Gels Prepared in Micellar Solutions of a Cationic Surfactant

Doctoral Thesis

Doctor rerum naturalium (Dr. Rer. Nat.)

Submitted by
Azadeh Hassan Raeisi
From Tehran

Approved by the Faculty of Natural and Materials Sciences,
Claustah University of Technology,

Date of oral examination
25.04.2014

Chair person of the Board of Examiners
Prof. Dr. D. E. Kaufmann

Chief Reviewer

Prof. Dr. Wilhelm Oppermann

Reviewer

Prof. Dr. Diethelm Johannsmann

The Faculty of Natural and Materials Sciences

at Clausthal University of Technology

Prof. Dr. ....., President

Prof. Dr. ....., Dean

awards

Ms .....

born in ..... on .....

the degree

Doctor rerum naturalium (Dr. rer. Nat.)

according to the regulations of the doctoral program
upon successful completion of a doctoral thesis (dissertation)
.....
and an oral examination proving scientific qualification
obtained the final grade
.....

Clausthal-Zellerfeld, ...

....

President Dean

(Prägesiegel)

Name, Vorname **Datum: 27.02.2014**

Hassan Raeisi, Azadeh

EIDESSTATTLICHE ERKLÄRUNG

Hiermit erkläre ich an Eides Statt, dass ich die bei der Fakultät für Natur- und Materialwissenschaften der Technischen Universität Clausthal eingereichte Dissertation selbständig und ohne unerlaubte Hilfe verfasst und die benutzten Hilfsmittel vollständig angegeben habe.

Unterschrift

Abstract

The present study has been focused preparation of hydrophobically modified polyacrylamide gels in micellar solution of the cationic surfactant (CTAB) and their characterization. The investigation is considered as two stages. The first stage includes preparation of solutions and determination of optimum amount of each compound through which micellar solutions of water / CTAB / $NaNO_3$ were prepared. Viscosity of solutions containing different amounts of salt ($NaNO_3$) was measured and the results showed growth of the micelles versus salt concentration (C_{salt}) up to 0.5 M. In addition, the effect of different amounts of stearylmethacrylate (SM), as hydrophobic monomer, on the behavior of solutions was investigated via viscosity measurement and it was found that formation of hydrophobic blocks occurs as a consequence of solubility of SM within micelles. This phenomenon is an evidence of hydrophobic interactions that is believed to act as cross-links that form the network of physical hydrogels. Dynamic Light Scattering (DLS) technique was also employed in investigation of solutions that confirmed the enhancement of aggregation and formation of hydrophobic associations in the presence of salt and SM. The second stage of this study included formation of gels and evaluation of their mechanical and structural properties. In this stage also the effect of different compounds and temperature on gelation process and properties of gels were investigated. The effect of salt on solubilization of SM within the micelles and formation of physical cross-links was observed again. Increasing the initial monomer concentration (C_0) positively affected the gelation so that the elastic modulus exhibited a strong increase with raising the concentration, while its frequency dependence was decreasing. Presence of reversible cross-links resulting from the fact that hydrophobic associations can be locally solubilized also was evidenced from relaxation modulus, G (t), of the gels as a function of time. The normalized intermediate scattering function, $f(q,\tau)$, as well as the distribution of relaxation rates, G (Γ), of the gels showed that the monomer concentration has only little effect on the fast relaxation modes. DLS of gels showed two characteristic correlation times corresponding to two diffusive modes with coefficients the D_{fast} and D_{slow}. Plotted D_{fast} and D_{slow} versus initial monomer concentration also indicated the smaller mesh size of the network and longer life time of the physical cross-links. All in all, gels with a high degree of toughness and self-healing property have been obtained through this investigation.

Table of Contents

1 INTRODUCTION 1
2 THEORETICAL BACKGROUND 3
2.1 Fundamentals of hydrogels 3
2.1.1 Network formation mechanism 5
2.1.2 Hydrogels prepared by hydrophobic association 7
2.1.2.1 Effect of surfactant 10
2.1.2.2 Micellar copolymerization 12
2.1.2.3 Structural and rheological study of micelles 13
3 METHODS 16
3.1 Network rheology 16
3.1.1 Viscoelastic behavior of gels 16
3.1.2 Stress relaxation 19
3.2 Light scattering 20
3.2.1 Dynamic light scattering 22
3.2.2 Non-ergodic method 26
3.2.3 Partially heterodyne method 29
4 EXPERIMENTAL PROCEDURE 31
4.1 Substances 31
4.2 Preparation of hydrogels 34
4.2.1 Synthesis of hydrophobically modified physical gels by micellar copolymerization 34
4.2.1.1 Reaction mechanism 36
4.3 Characterization methods of hydrogels 37
4.3.1 Light scattering measurement 37
4.3.1.1 Dynamic light scattering (DLS) measurement 37
4.3.2 Rheological analysis 38
4.3.2.1 Rheological measurement 39
4.3.3 Viscometry measurement 39
5 RESULT AND DISCUSSION 41
5.1 Introduction 41
5.2 Kinetics of surfactant solution 41
5.2.1 Micellization of CTAB in the presence of $NaNO_3$ 41
5.2.2 Effect of hydrophobic monomer 45
5.2.3 Step by Step DLS characterization of hydrogel synthesis solutions 47
5.3 Gel formation 48
5.3.1 Effect of salt concentration 48
5.3.2 Variation of initial monomer concentration 50
5.3.3 Formation of physical gels at different temperatures 53
5.4 Dynamic light scattering (DLS) 54
5.4.1 Structural inhomogeneity of physical gels 54
5.4.2 Dynamics of physical gels 57

6 CONCLUSION 62
7 REFERENCES.....64
LIST OF SYMBOLS.....75

Table of figures

Figure 1. Structure of hydrophilic gels [31] 3

Figure 2. Classification of gelation mechanism [49]. 7

Figure 3. a) Schematic illustration of hydrophobic association, b) most thermodynamically favorable state of hydrophobic association [70,71] 8

Figure 4. Energy dissipation in chemically and physically cross-linked hydrogels [72]. 9

Figure 5. Monomer exchange between micelles and surfactant molecules in solution..... 11

Figure 6. Micellar copolymerization process [79]. 12

Figure 7. Different phases of surfactant depending upon its concentration [87]. 14

Figure 8. Size and shape changes of micelles in presence of $NaNO_3$. 15

Figure 9. Stress and strain versus time in dynamic loading of a viscoelastic material [103] 18

Figure 10. Elastic modulus (G′), viscous modulus (G″) and tan δ as functions of reaction time [105] 19

Figure 11. Applied strain and observed stress relaxation [101]. 20

Figure 12. Inhomogeneities of gels: a) Non-random spatial variation of cross-link density, b) Defects of network including dangling chains, loops, chains entrapments etc. c) Inhomogeneities which are dependent on cluster size, distribution and architecture of polymer chains [115] 23

Figure 13. A schematic plot of autocorrelation function obtained from DLS measurement. 25

Figure 14. Speckle patterns of a polymer solution (left) and a gel structure (right). $\langle I \rangle T$: Time-average scattering intensity, $\langle I \rangle E$: ensemble-average scattering intensity and $\langle IF \rangle T$: intensity of fluctuating part that can be determined by non-ergodic method, $\theta = 90°$. 27

Figure 15. $f(q,\tau)$ obtained by the non-ergodic method in which $gT2\ q,\tau - 1$ is shifted to an ordinate intercept of 1. 28

Figure 16. Structure of acrylamide (AAm). 31

Figure 17. Structure of technical grade stearyl methacrylate (SM). 32

Figure 18. Structure of cetyltrimethylammoniumbromide (CTAB). 32

Figure 19. Structure of ammonium persulfate (APS). 33

Figure 20. Structure of sodium nitrate ($NaNO_3$). 33

Figure 21. Structure of N,N,N',N'- tetramethylethylenediamine (TEMED). 33

Figure 22. Formation of surfactant containing physical gels in aqueous CTAB−$NaNO_3$ solutions via hydrophobic monomer (SM) [146]. 35

Figure 23. Scheme of a polyacrylamide gel: an illustration of the mechanism of polymerization with the radical mechanism by the TEMED-persulfate couple, and the radical polymerization of acrylamide. The structure of the gels is shown in the chain transfer stop [147]. 36

Figure 24. A schematic illustration of dynamic light scattering system..... 37

Figure 25. Schematic illustration of the rheometer with corne-and-plate geometry. 39

Figure 26. The size of the micelle increases with increasing the concentration of counterions and decreasing temperature [73]. 42

Figure 27. Viscosity of the micellar solutions as a function of $NaNO_3$ concentration at room temperature. 43

Figure 28. Viscosity as a function of the shear rate for 3.3 w/v% surfactant aqueous solutions with different salt concentrations at 25 °C. 44

Figure 29. Variation of viscosity as a function of hydrophobic monomer concentration added to the solution of CTAB and $NaNO_3$. 45

Figure 30. Schematic illustration of reorganization of micelles from rod-like to spherical by adding SM in the presence of salt and CTAB [156,157]. 46

Figure 31. Viscosity variation versus shear rate with different SM amounts for systems containing 3.3 w/v% of CTAB and 0.3 M of $NaNO_3$ at 25 °C. 47

Figure 32. (a) Normalized intermediate ensemble-average scattering function $f(\tau)$, calculated from $gT2\tau$ for various preparation steps at scattering angle of 90°. (b) Characteristic decay time distribution function, G(Γ), obtained with a measurement time of 2 h at θ = 90° for different steps of solution preparation. Temperature = 25 °C. 48

Figure 33. Optical image of synthesized physical gels at different salt concentrations ranging from 0.1 to 1.0 M at room temperature. 49

Figure 34. Values of G´ and G˝ and the loss factor (tan δ) of hydrogels as a function of initial monomers concentration at 35 °C. $NaNO_3$ = 0.3 M, CTAB = 3.3 w/v%, ω = 6.3 rad.s^{-1} and γ_0 = 0.01. 51

Figure 35. Characterization of the elastic modulus of hydrogels with different initial monomer concentrations by rheological measurements. Elastic modulus (G´) as a function of reaction time (a) and frequency ω (b) measured after 3 hours of reaction time. $NaNO_3$ = 0.3 M, CTAB = 3.3 w/v%. 52

Figure 36. Relaxation modulus G(t) as a function of time for various monomer concentrations. In prepared gels $NaNO_3$ = 0.3 M, CTAB = 3.3 w/v%. 53

Figure 37. Temperature dependence of the static (a) and viscous (b) moduli of hydrogels as a function of the monomer concentration. $NaNO_3$ = 0.3 M, CTAB = 3.3 w/v%. 54

Figure 38. Variation of the time averaged scattering intensities, $\langle I \rangle T$, with sample position of physical gels synthesized with different initial monomer concentration. The solid line indicates the ensemble-averaged scattering intensity, $\langle I \rangle E$ and the dashed line represents the fluctuating components of the scattering intensity, $\langle IF \rangle T$. $\theta = 90°$ and $T = 35°C$. 56

Figure 39. Normalized intermediate ensemble-average scattering function $f(\tau)$, calculated from $gT2\tau$ for different monomer concentration at a scattering angle of 90° (green curves) and characteristic decay time distribution function, G(Γ), obtained with a measurement time of 2 h at θ = 90° on a gel formed with different initial monomer concentrations. Temperature = 35 °C. 58

Figure 40. Sub-chains or blobs that their motion between two entangled or cross-linked point leads to fast relaxation [163]. 59

Figure 41. (a) Relaxation rate of the fast (Γ_{fast}) and slow (Γ_{slow}) modes plotted versus q^2 for different monomer concentration. (b) Diffusion coefficient of each relaxation mode plotted against initial monomer concentration..... 61

1 Introduction

Synthetic hydrogels with superior mechanical properties have a wide range of applications in tissue engineering, drug delivery, contact lenses, sensors and actuators, mainly because of their similarity to biological tissues [1,2]. Poor mechanical strength and lack of self-healing ability, however, hinder the use of hydrogels in many application areas. The poor mechanical performance of hydrogels is a consequence of their low resistance against crack propagation that originates from the lack of an efficient energy dissipation mechanism in a chemically cross-linked network. The design of hydrogels with a good mechanical performance such as a high degree of toughness is, therefore, crucially important in many existing and potential application areas of soft materials [3-6].

To obtain a gel with a high degree of toughness, one has to increase the overall viscoelastic dissipation along the gel sample by introducing dissipative mechanisms at molecular level. Our focus has been on increasing the mechanical performance of hydrogels formed by free-radical cross-linking copolymerization (FCC). Hydrogels formed by free-radical cross-linking copolymerization process always exhibit an inhomogeneous cross-link density distribution, known as spatial gel inhomogeneity [7-13]. In the polymerization technique used in this work, micellar cores of surfactant molecules serve as an environment that enhances aqueous solubility of hydrophobic monomers. This effect results from effective attraction of hydrophobic monomers in aqueous media, known as hydrophobic interactions. The network of this kind of gel is formed from cross-linking of the hydrophilic backbones via the mentioned hydrophobic groups. The reversible physical cross-link points lead to a physical hydrogel with superior mechanical properties as well as the capability of self-healing and remodeling [14-18].

In this study, physically cross-linked hydrogels with enhanced mechanical properties were obtained by copolymerization of acrylamide (AAm) and stearylmethacrylate (SM) in micellar solution. The process was carried out by utilizing cetyl trimethylammonium bromide (CTAB) as surfactant and in the presence of sodium nitrate ($NaNO_3$). $NaNO_3$ causes the growth of the CTAB micelles and enhances the solubility of hydrophobic monomers within the micelles. The physical gels tend to dissolve in concentrated surfactant solutions while they are not soluble in water owing to their strong hydrophobic interactions. Because of the temporary nature of the hydrophobic associations, such gels exhibit a high degree of toughness and self-healing properties [19,20].

Hydrophobic interactions play a dominant role in the formation of large biological systems. These interactions can be generated in synthetic hydrogels by incorporation of hydrophobic sequences within the hydrophilic polymer network chains. Recently, it has been shown that hydrogels formed by hydrophobic associations, exhibit a high degree of toughness due to the mobility of the junction zones within the gel network, which contributes to the dissipation of the crack energy along the hydrogel network [19,21,22].

Knowing that addition of an electrolyte into aqueous ionic surfactant solutions weakens the electrostatic interaction and causes the micelles to grow, it was tried to polymerize long chain carbon compounds in the presence of an electrolyte. Results of the present study indicate that acrylamide can be copolymerized with large hydrophobes such as stearylmethacrylate (SM) in a micellar system provided with an electrolyte added in sufficient amount. Strong hydrophobic associations between the blocks of SM prevent dissolution in water and flow, while the dynamic nature of the junction zones between the network chains provides strong and long-lived hydrophobic associations resulting in efficient self-healing capability [23-26].

In terms of the instrumentations, DLS (Dynamic Light Scattering), viscometer and rheometer were used in order to determine the dynamic and mechanical properties of synthesized hydrogels, respectively. The correlation functions determined by DLS revealed markedly slow relaxations -seemingly diffusive- occurring on time scales of the order of mili-seconds to hours and dependent on the total monomer concentration of the gel. These long correlation times are an indication of the life-time of the hydrophobic associations that serve as cross-linkages. The relaxation rates were also observed macroscopically in frequency-dependent rheological measurements. When DLS measurements were performed on a time scale appreciably shorter than the longest relaxation times, speckle patterns typical of the inhomogeneous and non-ergodic nature of physically cross-linked gels were observed.

2 Theoretical background

2.1 Fundamentals of hydrogels

Due to its wide range of applications, the term “gel” has various definitions in each area of science such as chemistry, physics and biotechnology. The most common definition of gels is the one proposed by Tanaka in 1992 [27]. According to this definition, a “gel” is a network of cross-linked linear polymers with the capability of absorbing high quantities of a solvent as swelling agent. If the solvent is water, the system is called “hydrogel”. A hydrogel can be assumed as a giant structure of inter-connected polymer molecules developed in three dimensions through a continuous phase. Because of the high amount of water as well as the ease of processing and biocompatibility, hydrogels have become superior candidates for a wide range of applications such as pharmaceutics, food chemistry, cosmetics, medicine and biotechnology. Therefore, developing advanced processes to improve functional and mechanical properties of hydrogels is a key challenge in all fields of materials science [28-30].

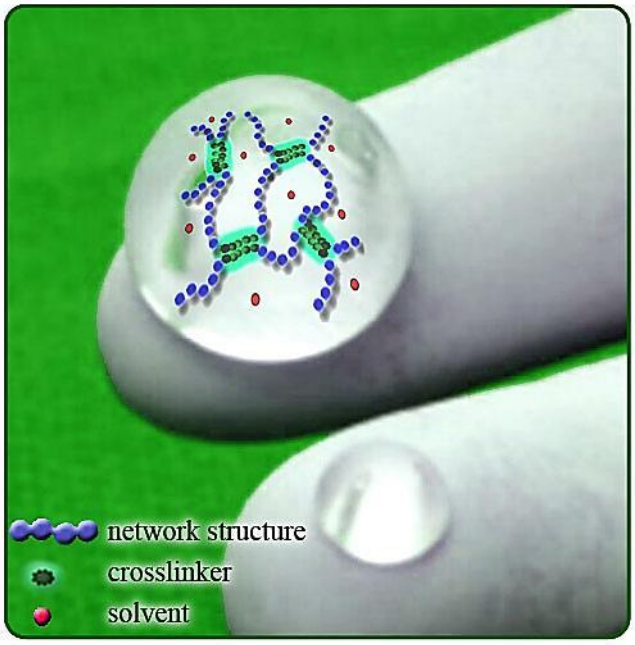

Figure 1. Structure of hydrophilic gels [31].

Although gels were used since ancient centuries, the first scientific study of gels was performed by Thomas Graham in the 19th century who employed sol-gel method to produce silica gel [32]. During 1940’s and 1950’s scientists such as Flory [33,34], Huggins [35,36] and Treloar [37,38] continued the investigation of gels. Treloar studied elasticity in

the polymer networks and Flory's studies were in the area of physical chemistry of macromolecules. Flory and Huggins succeeded to establish the Flory-Huggins theory of polymer solutions[1].

Based on this theory a volume phase transition[2] in the network was predicted by Dusek and Patterson [40]. The volume phase transition was first observed by Tanaka in slightly ionized Polyacrylamide (PAAm) gels immersed in an acetone-water mixture at 1981 [41]. Simultaneously mechanical and swelling behavior of chemically cross-linked poly-gels was studied by Horkay and Zrinyi [42]. During the last decades and after Tanaka's discovery gels with the ability to respond to an external signal were prepared. In the late 1980's swelling and phase transition of gels were mostly studied. Recently gels are being intensively investigated in order to enhance the structural and functional properties and broaden their applicability [4,43-46].

Hydrogels can absorb a great amount of water without being dissolved which resulted from swelling of the polymeric network. The most important characteristic of a gel is its water holding capacity. On molecular level, existence of water in a hydrogel occurs in two different forms: bonded to polar hydrophilic groups as "bond water" and filling the vacant space between polymer chains and pores as "free water" [47]. Polar hydrophilic groups become hydrated in the presence of water. These hydrated groups provide the primary bond water which causes the network to swell and provide contacts between hydrophobic groups with water. These groups are also capable of interacting with water molecules to form hydrophobically bond water or secondary bond water. Due to the osmotic driving force, the network can still absorb water. Through this process swelling happens that opposes the covalent or physical cross-links and causes the entropy decrease because of decreasing the possible configurations of chains. On the other hand increasing the entropy of the system due to polymer and solvent mixing as well as a change of enthalpy through mixing affects the swelling. Therefore hydrogel will reach an equilibrium level of swelling [42,48,49].

Another considerable characteristic of gels is elastic deformation that refers to their high deformability and recoverability. The high degree of recoverability after deformation leads to their well-known mechanical stability against external force. Low mechanical strength originates from a lack of resistance against propagation of cracks through the network as well as an inhomogeneous structure of gels [19,42].

---

[1] In 1941 Flory[33] and Huggins[35] independently developed a mathematical model of the thermodynamics of polymer solutions which determines entropy of mixing. This theory resulted in an expression of Gibbs free energy for mixing a polymer in a solvent.

[2] Volume phase transition is a change in volume of a swollen gel induced by a variation in pH, solvent composition or temperature [39].

Recent efforts towards improving the mechanical strength of gels have reported several techniques for toughening the gels, including topological gels (TP) [44], double network gels (DN) [43,50], nano-composite gels (NC) [46] and macromolecular microspheres composite (MMC) hydrogels. As a successfully utilized group with high compression strength, NC gels can be obtained by using clay particles as cross-linker of the network. It should be mentioned that another group of gels with improved mechanical strength, named tetra-polyethylene glycol or (PEG)-gels, is recently developed. PEG-gels are obtained through mixing of two types of macromers with a tetrahedron-like structure in a controlled value of pH [51,52].

Recently hydrogels with higher functionality have been developed that are able to respond when subjected to external condition changes [53]. The hydrogels that have these functionalities are called "intelligent hydrogels". They mostly respond to changes in environmental conditions. Intelligent hydrogels are also known as "responsive gels". As a unique behavior, responsive gels may respond to small changes in environmental condition by swelling or shrinking. Factors that can affect the swelling ratio of a responsive gel include: temperature, pH, light, electric or magnetic fields, solvent etc.

Due to similarities to living tissues, hydrogels are suitable candidates for prosthetic, diagnostic and therapeutic applications. Hydrogels as biomaterials benefit greatly from high water content and also a soft and rubbery nature that makes them more similar to living tissues than other synthetic biomaterials. The earliest application of hydrogels as biomaterial was in 1960, when hydrophilic networks of poly(2-hydroxyethyl methacrylate) or PHEMA were used in contact lenses [54]. Since then applications of hydrogels as biomaterial have been extended due to their exceptional similarity with living tissues. In addition molecules (e. g. drugs) can diffuse into or out of such a network that makes it possible to be used in drug delivery systems [55]. The other distinguishing biological property of hydrogels is biocompatibility [56,57]. Because hydrogels have low interfacial tension with biological environments, the driving force of protein adsorption and cell adhesion is minimal. In addition, the rubbery and soft structure of hydrogels prevents any potential irritation to the tissue [58,59].

2.1.1 Network formation mechanism

Gels have a state between solids and liquids which provides them with a useful relaxation response to the applied deformations that could be found neither in liquids nor in solids. Gels obviously present both elastic (solid-like) and viscous (liquid-like) properties which are called viscoelasticity and will be mentioned in section 3.1.1. Importantly, polymer gels can be treated as a structure of one single polymer molecule [60].

A hydrophilic network structure is formed by copolymerization of hydrophilic monomers with a cross-linker. As the first step macromolecular chains start to form through the process of gelation. But the linear macromolecular chains are still soluble in contained solvents. By linking the chains together a polymeric network develops and becomes insoluble. Hydrophilic monomers that are commonly used for this purpose are (meth)acrylates and (meth)acrylamides. Molecular groups such as –OH, –COOH, $–CONH_2$, $–SO_3H$, etc. provide the hydrophilicity [27,61,62].

Gels are classified according to different aspects such as mechanical properties, structural characteristics, method of preparation, liquid medium in gel network etc. For example according to the nature of their inter-molecular bonds (cross-linking) they can be classified into chemical and physical gels. According to their porosities, gels are classified to non-porous, micro-porous, meso-porous and macro-porous. Depending on the liquid medium in the polymer network two classes are defined: gels containing organic solvent or water. The former class is named organogel and the latter class is named hydrogel [63-65].

As mentioned earlier, gelation can take place by chemical (chemical gels) or physical (physical gels) cross-linking. Both classes are divided into several subcategories that are shown in Figure 2. Cross-links determine structural stability of gels. Physical gels with the capability of reversible deformation and self-healing have non-covalent interactions. This class includes two sub-classes of strong and weak physical gels. As some kind of strong physical bonds, lamellar microcrystals, glassy nodules or double and triple helices can be mentioned. Weak physical gels have reversible bonds between chains that are formed from temporary associations. Hydrogen bond, ionic and hydrophobic associations are examples of such weak bonds.

In contrast chemical gels have a stable and rigid structure that includes high strength covalent cross-links. Chemical gels are obtained by a chemical reaction. Formation of chemical gels may occur either by cross-linking at the time of polymerization or by cross-linking after synthesis of polymer chains. As chemical gels cannot be dissolved again, they are called permanent or irreversible gels. The main chemical processes of gelation include condensation, vulcanization and addition polymerization [31,63].

Regardless of the chemical or physical nature of bonds, all the gels have a characteristic temperature called gelation temperature that usually is shown by T_g below which the formation of a gel occurs. There is also a threshold polymer concentration, called the overlap concentration, above which the gel network will form [66].

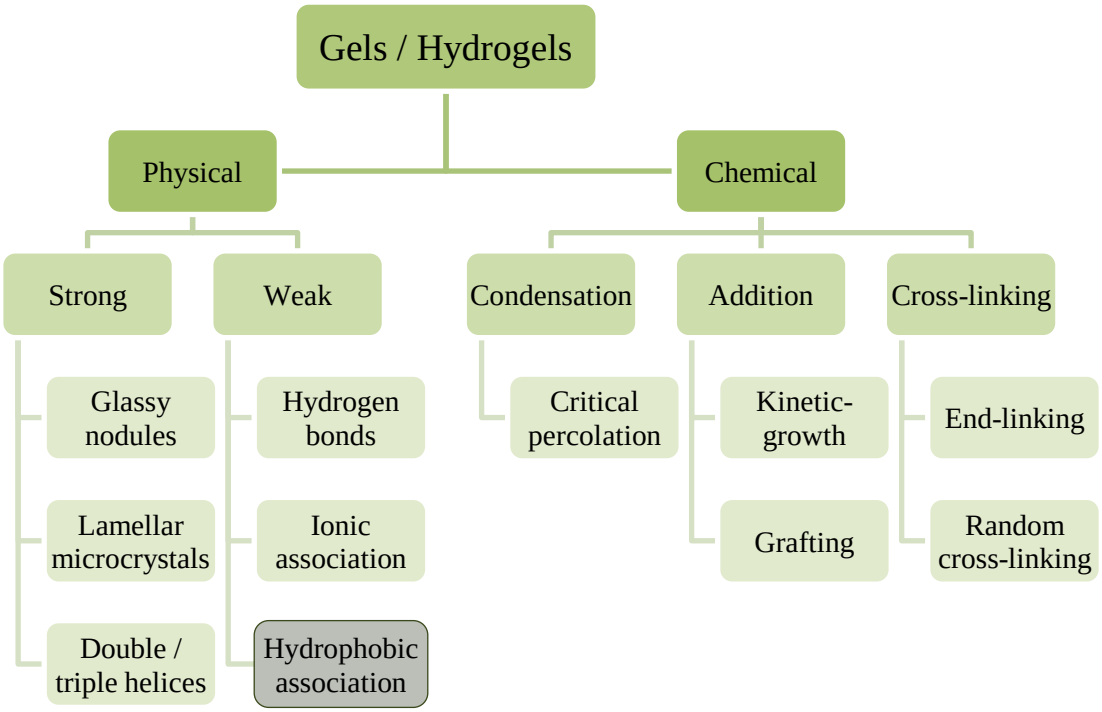

Figure 2. Classification of gelation mechanism [49].

2.1.2 Hydrogels prepared by hydrophobic association

The term "hydrophobic association" was introduced for the first time in 1953 by Kauzmann who explained the behavior of oil which associated with a separate phase in an aqueous solution [67]. Hydrophobic interactions can be defined as the association of two nonpolar molecules surrounded by a polar medium such as water [68,69]. As a result of hydrophobic interactions, nonpolar molecules tend to associate spontaneously when they are inserted into water, because the system tends to minimize the direct contact area between water and nonpolar molecules. In these conditions the hydrophobic molecules will aggregate with no or little amount of water between them. As illustrated in Figure 3 the most favorable state for the nonpolar molecules in which the nonpolars are actually associated is if there are no water molecules between the nonpolar molecules. Displacement of water molecules around a nonpolar compound at room temperature increases the entropy. As the enthalpy change of this process is not notable, the free energy decreases ($\Delta G < 0$) based on the following equation:

$$\Delta G = \Delta H - T\Delta S \quad (1)$$

That implies a thermodynamically favorable process. It is of importance to notice that the hydrophobic molecules do not need to attract each other and the effect of

surrounding water sticks them together. An increase of temperature or addition of salts affects the hydrophobic association tendency [14].

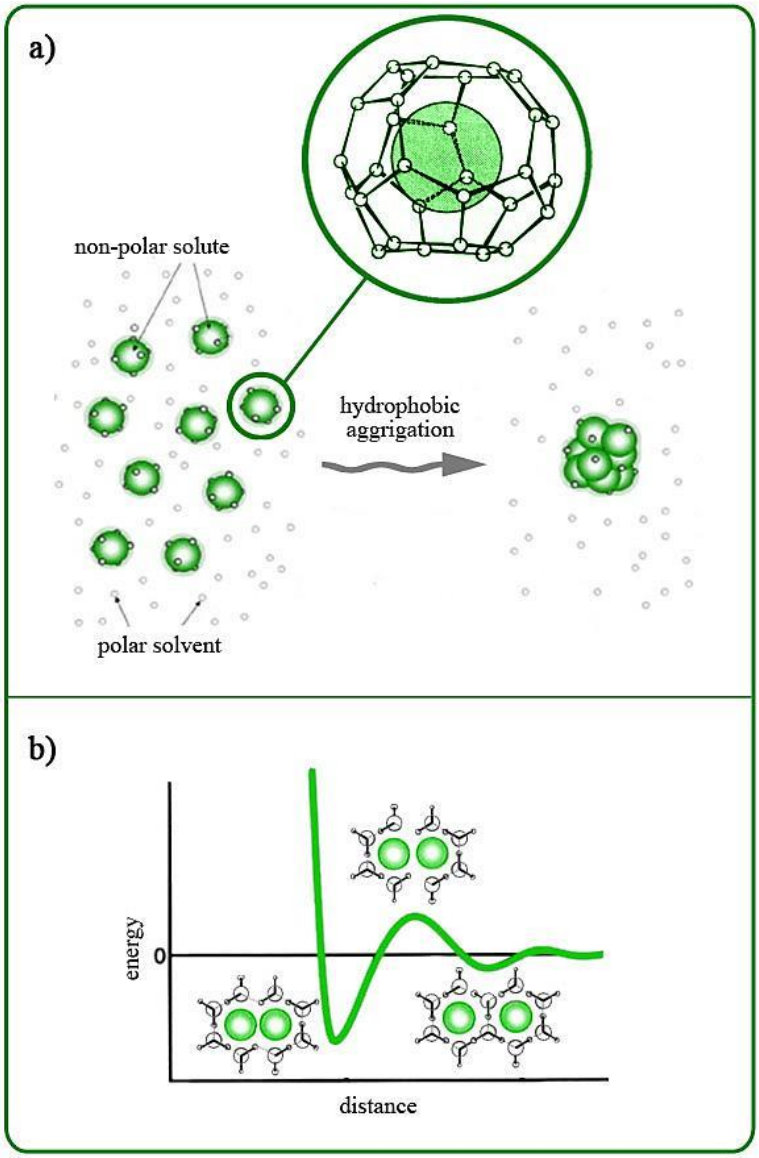

Figure 3. a) Schematic illustration of hydrophobic association, b) most thermodynamically favorable state of hydrophobic association [70,71].

Hydrophobically associated polymers have been the subject in extensive studies during the last two decades. Weak mechanical properties and the lack of reforming capability of hydrogels that are two critical defects of hydrogels can be modified concerning physical nature of hydrogels rather than their chemical nature. In these hydrogels, surfactant molecules are organized into aggregates to form micelles. A micelle is a structure that includes hydrophobic chains of the surfactant molecules surrounded by hydrophilic heads in an aqueous environment. Micelles can be considered as

hydrophobic groups that make a network from hydrophilic backbone via cross-linking. These physical cross-link points as well as the capability of self-healing and remodeling of hydrogels result in the superior mechanical properties of hydrogels. It has been even evidenced that a higher hydrophobic group content in hydrogels leads to an improved mechanical strength [15].

In order to explain unique functionalities of hydrophobically associated network in hydrogels, a comparison between chemical and physical gels is necessary. Gels can be classified in several ways regarding their different aspects and properties. As already mentioned above, according to the nature of polymer network's bonds, hydrogels are divided into chemical and physical gels. The former class is cross-linked by permanent covalent bonds while the latter class is cross-linked by weak bonds such as hydrogen bonds, hydrophobic interactions or van der Waals forces or a mixture of them. Chemically cross-linked hydrogels have poor mechanical performance originated from very low crack propagation resistance. In fact, there is no efficient mechanism of energy dissipation through such networks. In contrast, physical gels prepared by hydrophobic sequences within hydrophilic chains exhibit higher toughness benefited from the mobility of cross-links within the gel network. In these gels the energy of crack can be dissipated within the gel network effectively. This difference between chemical and physical gels is illustrated in Figure 4. During the synthesis process of a physical gel, hydrophobic monomers distribute along the hydrophilic polymer backbone. This incorporation develops strong and long-living hydrophobic associations [3,22].

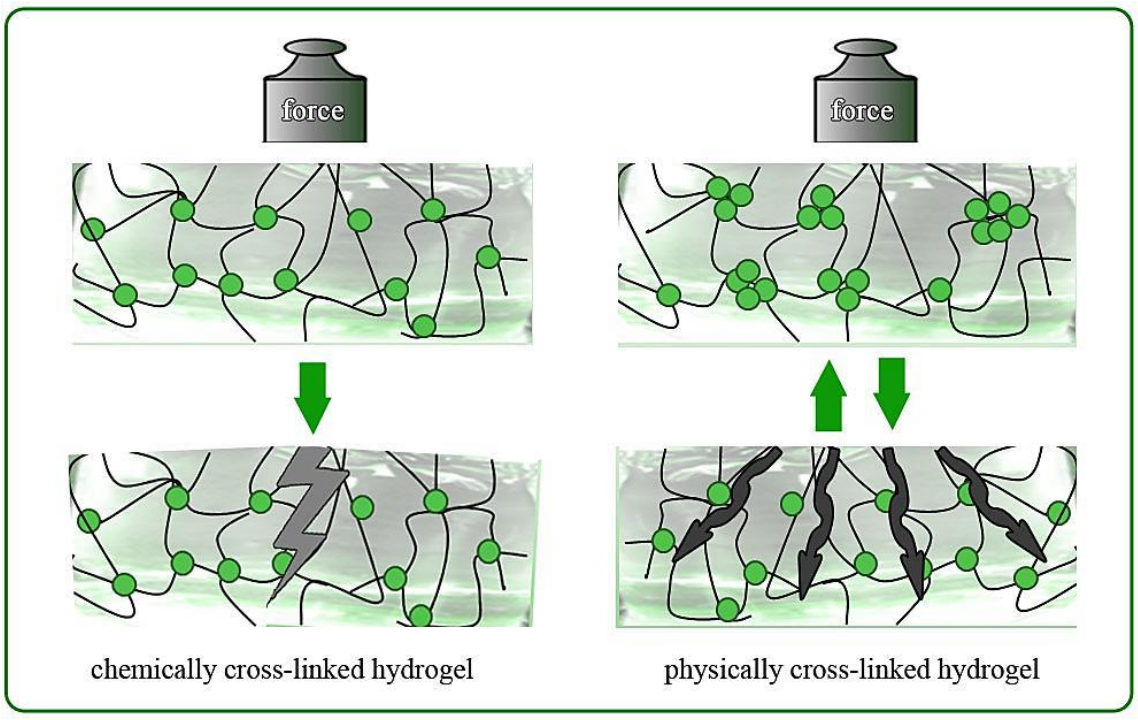

Figure 4. Energy dissipation in chemically and physically cross-linked hydrogels [72].

In a study performed by Tuncaboylu et al. [19] it was suggested that surfactants stabilize the physical cross-links in the gels prepared by copolymerization of large hydrophobic monomers stearyl methacrylate with the hydrophilic monomer acrylamide in a micellar solution of sodium dodecyl sulfate (SDS). In the presence of the surfactant, the hydrophobic sections of the network can easily be solubilized and become weak and reversible at 35 °C. While with no surfactant hydrophobic associations are as strong as covalent cross-links. This indicates that mechanical properties of hydrogels such as relaxation behavior and self-healing properties can be adjusted by controlling the amount of surfactant in the gel network.

2.1.2.1 Effect of surfactant

Surfactants are substances with amphiphilic molecules. An amphiphilic molecule includes a hydrophilic head and a slender hydrophobic tail. In an aqueous solution, above a specific concentration, which is called critical micelle concentration (CMC), the surfactant molecules organize into aggregates and form micelles. Micelles may be formed into different sizes and shapes such as spherical, worm-like, vesicle, etc. The configuration of micelles depends on the size of the head-group, length of the surfactant's tail, concentration of the surfactant and temperature [73].

As surfactants create a thin monolayer on the surface of the solutions, they are also called surface active materials. Surfactants are divided into three classes: 1. anionic surfactants including salts like sodium dodecyl sulfate, 2. cationic surfactants including quaternary ammonium salts-hexadecylpyridinium bromide and 3. ampholytic such as long-alkyl amino acids [74].

There is a dynamic breaking and reformation process in the aggregates caused by permanent exchange of surfactant's molecules, so that monomers simultaneously leave and enter into the micelle by diffusion process (Figure 5). This dynamic process results in micelles with fluctuating particles and variable shape and size. The net exchange, however, is equal to zero. Thermal fluctuations within the system are consequences of these dynamic processes [74,75].

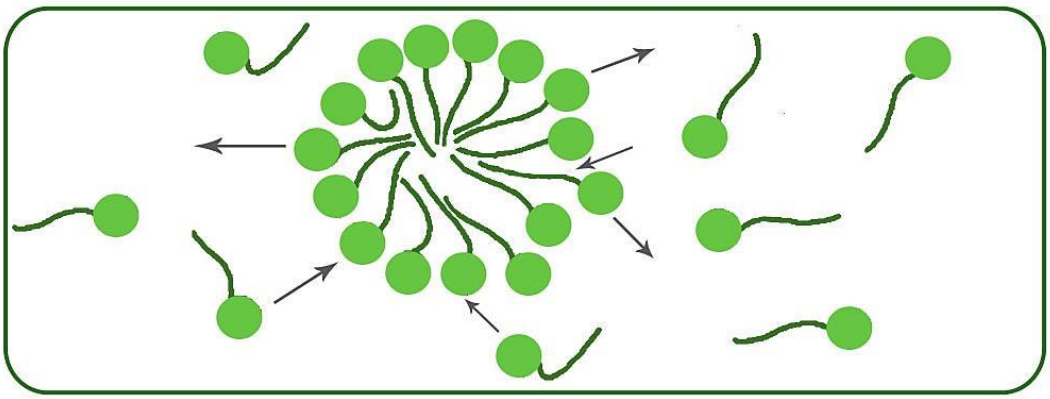

Figure 5. Monomer exchange between micelles and surfactant molecules in solution.

In the present study hexadecyltrimethylammonium bromide (CTAB) was used in order to obtain an aqueous micellar solution.

Among different surfactants CTAB was employed because of its superior micellization behavior, as suggested by M. A. Bahri et al. [76]. They have compared microviscosity of SDS, DTAB and CTAB and found out that a solution containing CTAB presents higher microviscosity values than that of DTAB and SDS. It is claimed that CTAB forms cylindrical or rod-like, more organized and less hydrated micelles.

Under suitable conditions in a solution, the aggregates will reorganize as rod-like geometry. At low concentrations the size of the aggregates is much smaller than their distance and the system exists in a sol state. By increasing the concentration, the length of rod-like micelles increases and becomes comparable to the distance between micelles and the solution starts to exhibit elastic properties [74,75].

Because of the cylindrical or rod-like structure of micelles of CTAB in solution, surfactant tails organize towards the central axis of micelles. This type of organization allows the other chains to be added to the micelle without increasing the compacting degree. But the situation is different in micelles with spherical configuration in which any additional chains into the micelle will reduce free space inside the micelle and subsequently increase the local viscosity. Generally speaking, the higher microviscosity of the CTAB containing solution is due to the higher number of carbon atoms in their tails[1]. Further, there is no doubt that by increasing the hydrophobic chain length of the surfactant, the critical micelle concentration (CMC) will decrease. In contrast micellar

[1] 16 carbon atoms in CTAB's tail and 12 carbons in tails of DTAB and SDS

size decreases by increasing the hydrocarbon chain length of the surfactant's molecule [74,77].

2.1.2.2 Micellar copolymerization

In the micellar copolymerization process the solubilization of a hydrophobic monomer is performed in the presence of a surfactant. The effect of surfactants on the microstructure of co-polymers was first reported by W. Peer in 1987 [78]. The micellar copolymerization reaction was then first introduced by Candau et al. [79] in 1993 based on a technique developed by Turner et al. [80].

For gels prepared by the micellar copolymerization method in this work, stearyl methacrylate was used as hydrophobic monomer and CTAB as surfactant as illustrated in Figure 6. This monomer is soluble within the micelles formed by the CTAB surfactant. As there is a high concentration of hydrophobic monomers within the micelles, hydrophobic blocks are distributed randomly along the hydrophilic polymer backbone. This incorporation between large hydrophobic blocks and hydrophilic polymer backbone forms strong and long-living hydrophobic associations [20].

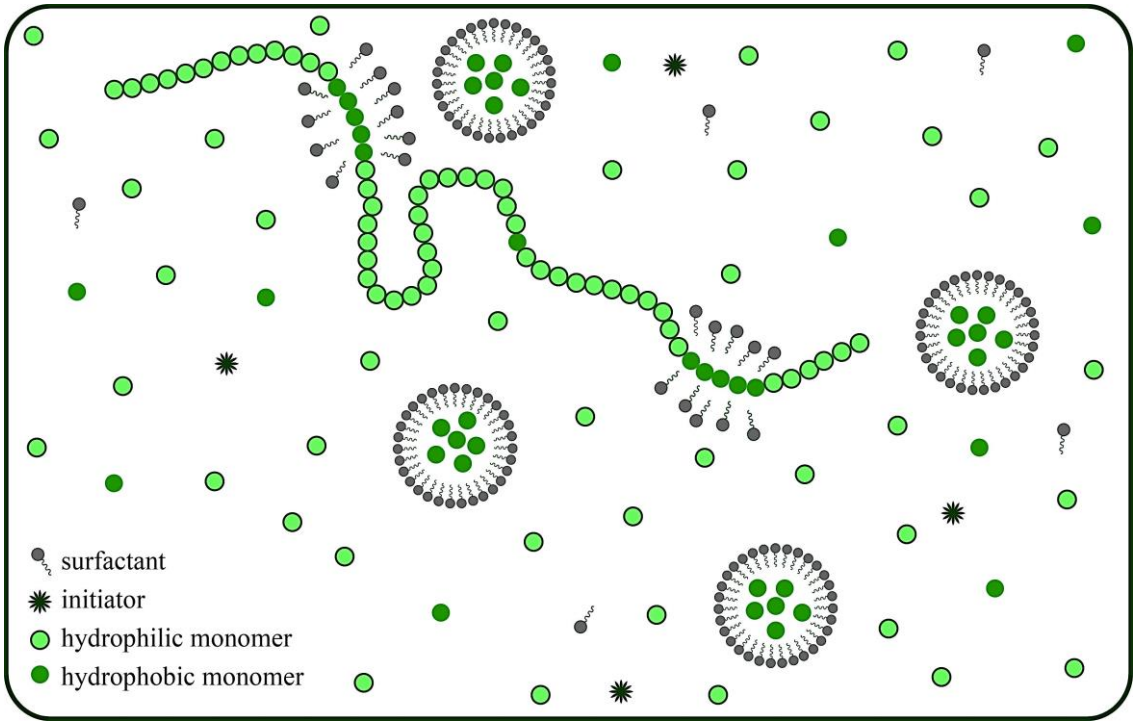

Figure 6. Micellar copolymerization process [79].

There is a clear difference between micellar copolymerization and solution copolymerization. In micellar copolymerization process, the polymer chain is formed by hydrophobic blocks and hydrophilic chains. In comparison to that in a solution copolymerization process, the hydrophilic and hydrophobic monomers will distribute randomly into the polymer chain [81].

2.1.2.3 Structural and rheological study of micelles

Micellar copolymerization of hydrophilic monomers such as acrylamide requires the hydrophobic monomers to be solubilized into the micelles. Large hydrophobic monomers such as stearyl methacrylate are not able to copolymerize with acrylamide in aqueous solution of CTAB at room temperature. This phenomenon is related to the low solubility of monomers within aqueous medium which is due to the small size of micelles that are not able to provide solubility for large hydrophobic molecules [82-84].

Viscoelasticity of a micellar solution can be induced by three mechanisms: by a second oppositely charged surfactant [85], counterions or uncharged compounds such as esters and aromatic hydrocarbons [75,86].

At an adequate concentration of amphiphilic molecules in water, the hydrogen bonded structure of water is disturbed by the hydrophobic group of surfactant molecules. Therefore the hydrophobic chains will be directed away from the water which decreases the free energy. In fact this process aims to reach a balance between micellization favoring forces (such as van der Waals and hydrophobic forces) and those opposing it (such as kinetic energy of molecules and electrostatic repulsion) [77].

The concentration at which micelles firstly appear is called critical micelle concentration (CMC). At concentrations above the CMC micelles become stable. Figure 7 shows the different possible organizations of surfactant molecules at different concentrations [87].

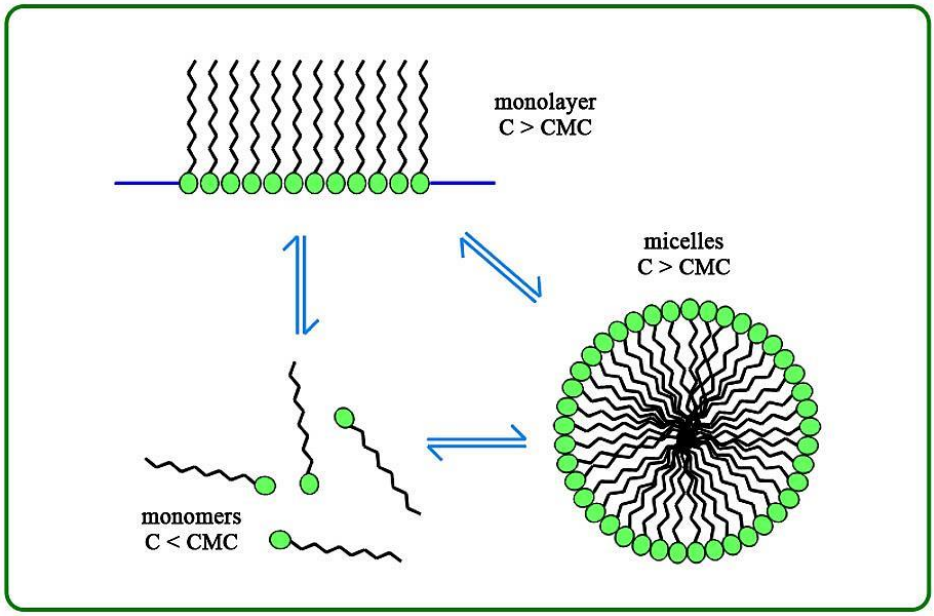

Figure 7. Different phases of surfactant depending upon its concentration [87].

In addition to CMC, counterions also strongly affect the size and shape of the micelles.

Formation of worm-like micelles in CTAB solution was an attractive area of research during the last two decades [88]. Addition of salt to this system causes lengthening of the micelles (Figure 8). This one-dimensional growth of the micelles is attributed to screening of head–head repulsion between amphiphiles and thereby reducing the interfacial curvature of the micelles. By varying the shape of the micelles, rheological properties of the solution will be affected. Low shear viscosity versus concentration of salt exhibits a maximum which indicates that by increasing the salt concentration the micelles become enlarged [89-92].

The decrease in viscosity is believed to be due to fluid cross-links (such as stearyl methacrylate in the present work) that are arranged as a branched micelles network. This network shows weak rheological response, which will be discussed in detail in section 5.2.2[93-96].

During the procedure of hydrogel synthesis formation of worm-like micelles of CTAB in presence of sodium nitrate ($NaNO_3$) has been also investigated. The observed results are in good agreement with the literature which can be a strong evidence of the mentioned theories. Similar studies reported different techniques for evaluating the aqueous solutions of CTAB such as rheology, small-angle neutron scattering (SANS) and cryo-transmission electron microscopy (cryo-TEM). In this study the effect of different concentrations of counterions and hydrophobic monomers in aqueous solutions

were investigated via viscometery, while its effect on obtained hydrogels were evaluated by rheometery measurement.

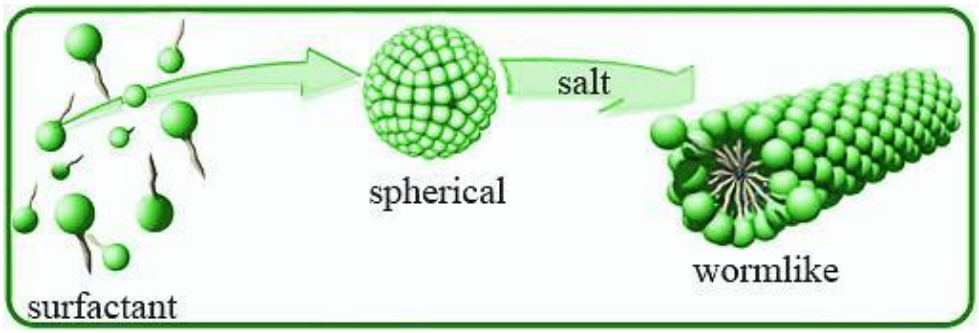

Figure 8. Size and shape changes of micelles in presence of $NaNO_3$.

3 Methods

3.1 Network rheology

The mechanical properties of hydrogels can be evaluated with the theories of rubber elasticity and viscoelasticity [97]. The former is based on time-independent and the latter is based on time-dependent recovery of structural orientation. Hydrogels are mechanically weak materials. Poor mechanical strength as well as the necessity that the sample should not de-swell during the procedure, requires special test adjustments.

The viscoelasticity theory explains the relation between elasticity, flow and molecular motion of polymers. Polymers often exhibit viscoelastic behavior against the applied stresses. This viscoelastic response depends on several parameters such as time scale of imposed stress (or strain). The time dependence of applied mechanical motion is as determinative as its magnitude in evaluating the mechanical properties. Under an applied stress (or strain) segments of the polymer chains move and by removing the applied condition, the system starts to a time-dependent recovery. Studying this behavior of hydrogels provides useful information for network characterization [98,99].

3.1.1 Viscoelastic behavior of gels

Polymer gels do not behave as an ideal elastic material which can be described by Hooke's elasticity law or as an ideal viscous material according to Newton's law. Gels are called viscoelastic materials which have both viscous and elastic properties [100,101]. For a fully elastic material the stress depends only on applied deformation and is independent of the rate of strain. In contrast in a viscous material the stress is dependent on the rate of applied strain. In case that a substance exhibits both elastic and viscous properties, it is called a viscoelastic material. The viscoelastic properties of materials are mostly explained in rheology [102].

A fully elastic or Hookean material completely saves the energy of deformation and recovers to its initial form after the pressure is removed. Based on Hooke's law, shear strain, γ, is a linear function of shear stress, σ:

$$\sigma = G \cdot \gamma \tag{2}$$

The parameter of proportionality is the shear modulus G, which indicates the resistance of material against deformation. Almost all solids are fully elastic as long as the shear strain is low.

An ideal viscous liquid exhibits a completely irreversible response to shear stress. The energy of this deformation will be dissipated. A liquid that exhibits viscous behavior is

called Newtonian liquid. Newton's law shows the relation between viscosity and shear rate in a viscous liquid:

$$\sigma = \eta \cdot \frac{d\gamma}{dt} = \eta \cdot \dot{\gamma} \tag{3}$$

in which σ is the stress and $\dot{\gamma}$ is the shear rate. η is the viscosity which expresses resistance of the liquid against flow.

Elasticity is a time independent property, while viscoelasticity is a property that depends on time and is affected by the shear frequency in an oscillatory experiment. For a Hookean material, applied stress and resulted strain have the same phase and therefore the relation between stress and strain as functions of time are related to each other by equation 4. The time dependent deformation can be expressed by a periodic equation in which γ_A is maximum deformation and ω is the angular frequency.

$$\sigma(t) = G \cdot \gamma(t) = G \cdot \gamma_A \sin(\omega t) \tag{4}$$

In case of a Hookean material, the deformation will always stay in the same phase with the stress.

For an ideal viscous material the shear stress which oscillates with the same angular frequency causes a strain with a phase difference of π/2. That means when strain is in its maximum or minimum level, shear stress is zero and vice versa.

$$\sigma(t) = \eta \cdot \dot{\gamma}(t) = \eta \cdot \gamma_A \cdot \omega \cdot \sin(\omega t + \frac{\pi}{2}) \tag{5}$$

In case of a viscoelastic system, the phase difference between stress and strain, δ, is in the range of 0 to π/2. Then the equation should be written as:

$$\sigma(t) = \sigma_0 \cdot \sin(\omega t + \delta) \tag{6}$$

It shows that the stress and strain are in different phases which equals δ, but the oscillation frequencies of stress and strain are the same. This situation is shown in Figure 9.

Based on stated theories the stress can be divided into two components: elastic component and viscous component that correspond to δ=0 and δ=π/2, respectively. Thus the shear modulus is separated into two values, G′, corresponding to the elasticity and G″, corresponding to the viscosity of the system. Because the energy of an elastic deformation will be saved within the system, G′ is also called the storage modulus. Through a viscous deformation energy will not be recovered, therefore G″ is called loss

modulus. In this way the relation between stress and deformation (strain) can be expressed as:

$$\sigma(t) = \gamma_A[G'(\omega) \cdot \sin(\omega t) + G"(\omega) \cdot \cos(\omega t)] \quad (7)$$

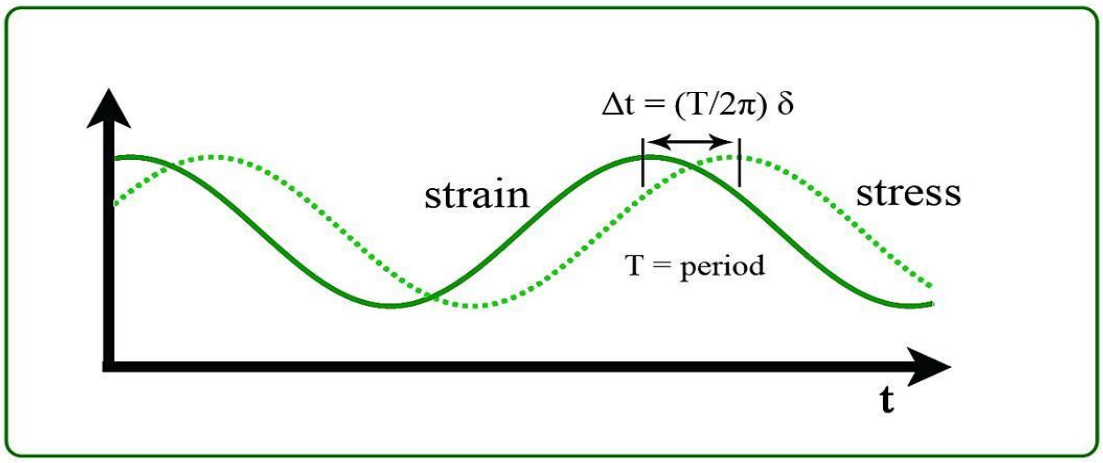

Figure 9. Stress and strain versus time in dynamic loading of a viscoelastic material [103].

The shear modulus also can be obtained as a dynamic parameter and a complex quantity, G^* that includes two elastic and viscous modulus:

$$G^* = G'(\omega) + i \cdot G"(\omega) \quad (8)$$

The ratio $(G")/(G')$ is called loss tangent which can be obtained by equation (9). In this equation δ is the loss angle or loss factor and depends on the material's character. Loss tangent is indicative of viscoelasticity of the material.

$$\tan \delta = \frac{G''}{G'} \quad (9)$$

As illustrated in Figure 10, during the course of gelation a gel-forming system shows a range of properties from close to ideally viscous ($G' = 0\,, tan\ \delta \to \infty$) to close to ideally elastic ($G" = 0\,, tan\ \delta = 0$). In case of $G" \gg G'$, the system is a viscoelastic liquid ($\infty > tan\ \delta > 1$) and in case of $G' \gg G"$ it is a viscoelastic solid. At the gel point $G' = G"$ that corresponds to $tan\ \delta = 1$.

At the gel point, where the gel network starts to form and liquid-like behavior turns to solid-like, G′ and G″ are approximately equal and show identical frequency

dependence. By means of the following relation the gel point can be obtained via rheology:

$$G'(\omega) \sim G''(\omega) \sim \omega^n \tag{10}$$

n is called relaxation exponent adapting values between 0 and 1 [104].

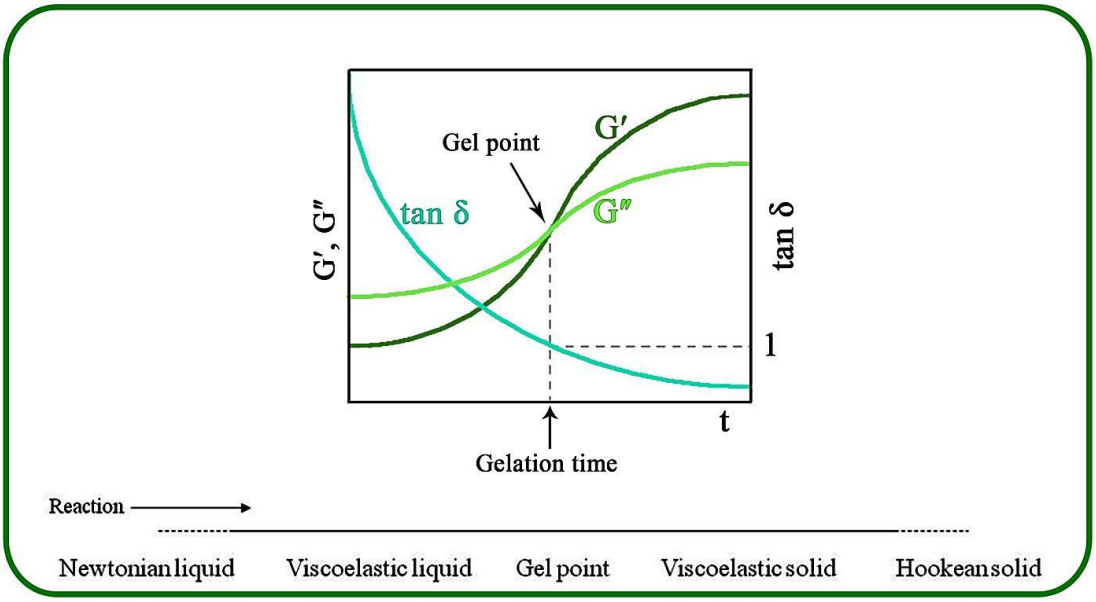

Figure 10. Elastic modulus (G′), viscous modulus (G″) and tan δ as functions of reaction time [105].

Measuring of viscoelasticity can be performed using different rheological methods such as: viscometry, creep, relaxation and oscillation. Viscometry is mainly used for liquid materials. In this technique shear rate is kept constant and a constant stress is measured. Creep and relaxation techniques can be used for both liquids and gels. The creep technique is performed in constant stress to measure the time dependent strain. Through the relaxation technique, a constant strain is applied and time dependent stress will be measured. The oscillation technique can be used to evaluate the viscoelasticity of any kind of soft materials. By this technique a periodic stress or strain can be applied and a periodic strain or stress will be measured.

3.1.2 Stress relaxation

If a rapid strain is applied to a material, the stress relaxation test determines the required stress as a function of time in order to maintain the material at that level of strain [102]. An applied strain with magnitude of γ, establishes a stress in the material. In the case of

an ideally elastic material, the stress, based on Hooke's law, will jump to the value of $G \cdot \gamma$ and will not decrease (relax) as long as the strain is imposed. In contrast for an ideally viscous material, the applied strain causes a stress which will instantaneously decrease (relax) to zero. Viscoelastic materials exhibit a time dependent releasing trend of stress, $\sigma(t)$. Therefore the stress relaxation modulus is also defined as $G(t)$ which is obtained by:

$$G(t) = \frac{\sigma(t)}{\gamma} \tag{11}$$

This equation is a time-dependent generalization of Hooke's law. A schematic illustration of applied strain and resulting stress is shown in Figure 11 [100,101].

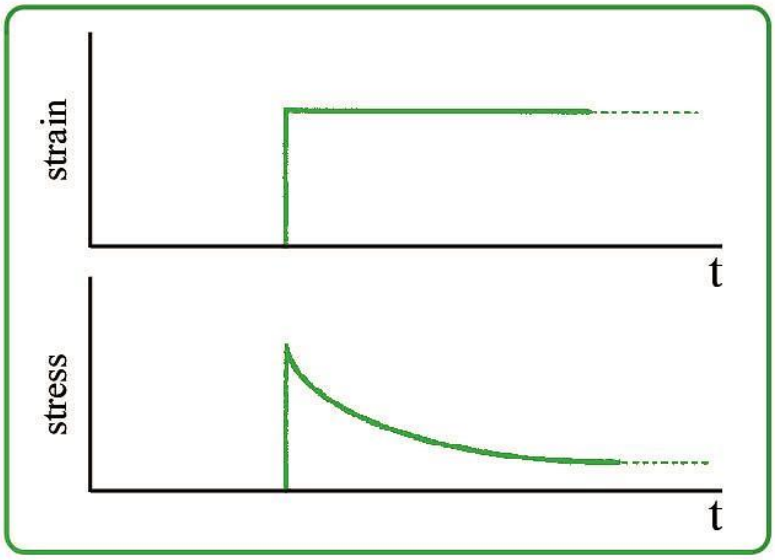

Figure 11. Applied strain and observed stress relaxation [101].

In hydrogels, the type of cross-links strongly determines the stress relaxation behavior. The modality of cross-links in gels may be ionic or covalent. Ionic cross-links will break under applied deformation and stress relaxation will result in reformation of ionic cross-links. In contrast stress relaxation in a gel with covalent cross-links occurs through migration of water within the gel network [106].

3.2 Light scattering

The term Light Scattering (LS) refers to the scattered light from non-absorbing macromolecules or colloidal particles suspended in a solution. This technique can be used for studying the swelling behavior of gels and colloidal particles coated with a

layer of smart gels [107,108]. Because of differences between the refractive index of solvent and solute, the incident light will be scattered by a dilute macromolecule solution [109,110]. Size, molar mass and an estimated shape of the particles or macromolecules can be determined from data resulted through analyzing the scattered light.

The structure of the material determines the extension of scattering. So that scattered light from liquids and gases is due to the density fluctuations which are caused by thermal movements of the molecules. In a mixture of dissolved polymer in a suitable solvent there are more fluctuations in concentration which are caused by diffusion of the polymer coils. This additional fluctuations result in more intense scattering.

Generally speaking, light scattering can give information about the gelation process, the point at which the solution of monomers begins to act as a solid cross-linked network and also about spatial inhomogeneities, size distribution of gel particles and dynamic fluctuations due to phase transitions [111].

In case that the coils can diffuse freely the system is called ergodic, which means the time-average of the intensity of scattered light equals the ensemble-average. Introducing cross-linking agents to a polymer gel fixes the coils. Then the fluctuations of the concentration through the matrix will be frozen-in. It results in a non-ergodic system in which the polymer coils are not able to move freely.

Introducing the cross-linkers to the system causes frozen-in inhomogeneities through the gel. Under this condition scattering intensity becomes dependent on the sample position and the random distribution intensity, which is called speckel pattern, increases dramatically [112-114].

Light scattering technique classifies to the static and dynamic light scattering methods. The change of frequency in dynamic light scattering (DLS) is between $\approx 10^5$-10^7 Hz which is less than the incident light frequency ($\approx 10^{15}$ Hz). This makes the detection of DLS in the range of frequency very difficult. Therefore time correlation functions have to be used to record the data in the time domain. Due to this reason DLS technique is called also Photon Correlation Spectroscopy (PCS). Although static light scattering gives information about spatial inhomogeneities and spatial correlation, dynamic light scattering is also able to provide useful information such as dynamic correlation and connectivity correlation of polymer gels [115].

3.2.1 Dynamic light scattering

Dynamic light scattering (DLS) is a useful technique to study the dynamics of chain molecules and clustered molecules in a solvent or in a polymer gel [116]. This technique was firstly reported by Prins et al. in 1972 who observed a syneresis[1] in a gelatin gel [117]. One year after Tanaka, Hocker and Benedek found that gels should be treated as a continuum and they suggested a theory of collective diffusion of polymer networks (THB theory) [118]. This theory has become a standard method for describing the dynamics of gels which can predict the intensity correlation function (ICF), $g^{(2)}(\tau)$, as a simple exponential function. This function is applicable also for the polymer solutions in which cross linkers are introduced randomly. The inhomogeneity of gels was not taken into account by the THB theory [119] which is illustrated in Figure 12. Since the spatial inhomogeneities act as local oscillators, heterodyne-type analyses were employed often through the 1980s [120,121].

Inhomogeneity is one of the most important issues that has been investigated extensively. Real gels always show an inhomogeneous density distribution of cross-links that is known as spatial inhomogeneity. Scattering methods can be employed for investigation of gels as the spatial inhomogeneity is in close relation to the spatial concentration fluctuations [122-127]. Spatial inhomogeneities in acrylamide hydrogels may be originated from several parameters including type and density of cross-links, ionization degree, swelling ratio and temperature [7-13]. In an ideal gel, there is a constant length of network chains between the cross-links, while in a real gel there are areas with very high chain density. These areas also are stiffer and have a higher shear modulus as well as a lower degree of swelling compared to ideal gels.

Spatial inhomogeneities on sub-micron scale are mainly resulting from the gel formation mechanism through which the density of cross-links in gel may fluctuate. The quality of solvent also affects the spatial inhomogeneity of gels. Decreasing the quality of the solvent may lead to formation of larger coils that reduces the cross-linking or cause the chains coil to stretch out that increases cross-linking. Both mentioned conditions increase the elastic and spatial inhomogeneity of gels [128].

[1] The contraction of a gel accompanied by the separating out of liquid

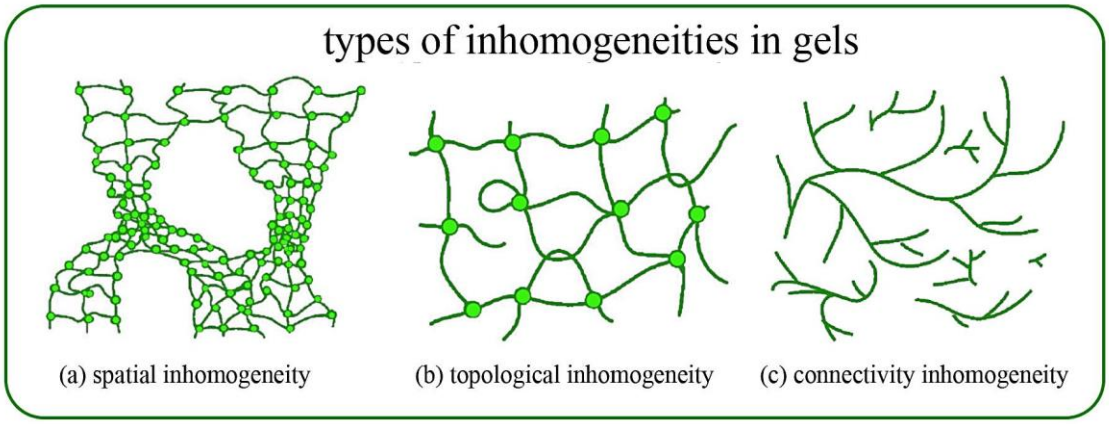

Figure 12. Inhomogeneities of gels: a) Non-random spatial variation of cross-link density, b) Defects of network including dangling chains, loops, chains entrapments etc. c) Inhomogeneities which are dependent on cluster size, distribution and architecture of polymer chains [115].

In order to take into account the effect of inhomogeneities on light scattering, different methods of data evaluation were developed. In 1989 Pusey and van Megen introduced the non-ergodic medium method [129]. Then the partial heterodyne method was proposed by Joosten et al., which was able to separate two contributions to the scattered intensity such as (liquid-like) dynamic fluctuations and the (solid-like) spatial inhomogeneities [130].

In another study [131] four methods for DLS analysis of gels have been compared with each other. The (a) non-ergodic medium method (D_{NE}), (b) partial heterodyne method (D_{HT}), (c) partial heterodyne method with the instrumental coherence correction, β, (D_{HTB}) and (d) homodyne method (D_{HM}) were described and compared. In this work the validity of non-ergodic model and heterodyne method for studying the structure of gels were investigated.

The time average scattering intensity of a gel, $\langle I(q)\rangle_T$, can be divided into two contributions as follows:

$$\langle I(q)\rangle_T = \langle I_F(q)\rangle_T + I_C(q) \tag{12}$$

$\langle I_F(q)\rangle_T$ is time-average of dynamic fluctuations (liquid-like) and $I_C(q)$ is the static component (solid-like) of the scattering intensity.

By means of measuring of intensity of scattered light in adequate quantity of sample positions and subsequent averaging, the ensemble-averages, $\langle I(q)\rangle_E$, can be calculated. It can be obtained also by simultaneous sample rotation and measurement. After performing the measurement, it is necessary to separate two contributions of scattered

light, fluctuating part and static (frozen-in) part, utilizing the intensity correlation function.

As described before, the noisy pattern resulting from DLS measurements includes information about scattered light intensity and shows a noisy pattern which is resulting from Brownian motions of the species within the sample. Treating the intensity fluctuations via a correlator provides a decaying autocorrelation function. This function is given by the following equation in which $I(q,\tau)$ refers to scattered light intensity and $\langle ... \rangle_T$ refers to the time average quantity. An example of a correlation function obtained from DLS measurement is shown in Figure 13. q is the scattering vector, θ is the angle of the detector, n is the refractive index of the medium and λ is wavelength of the light.

$$g^{(2)}(q,\tau) = \frac{\langle I(q,t)I(q,t+\tau)\rangle_T}{\langle I(q,t)\rangle_T{}^2} \tag{13}$$

$$q = \frac{4\pi.n}{\lambda_0} \cdot sin\frac{\theta}{2} \tag{14}$$

The autocorrelation function of dilute solutions is often in form of an exponential function that provides valuable information about the dynamics of the system. Since the fluctuations of the intensity of scattered light depend on thermal motions of the chains, molecules or particles, the intensity correlation function gives information about intensity correlation time ($\tau_{(2)}$). Following equations show the relation between $\tau_{(2)}$ and autocorrelation function and cooperative diffusion coefficient.

$$g^{(2)}(q,\tau) = exp\left(-\frac{\tau}{\tau_{(2)}}\right) + 1 \tag{15}$$

$$\tau_{(2)} = \frac{1}{2Dq^2} \tag{16}$$

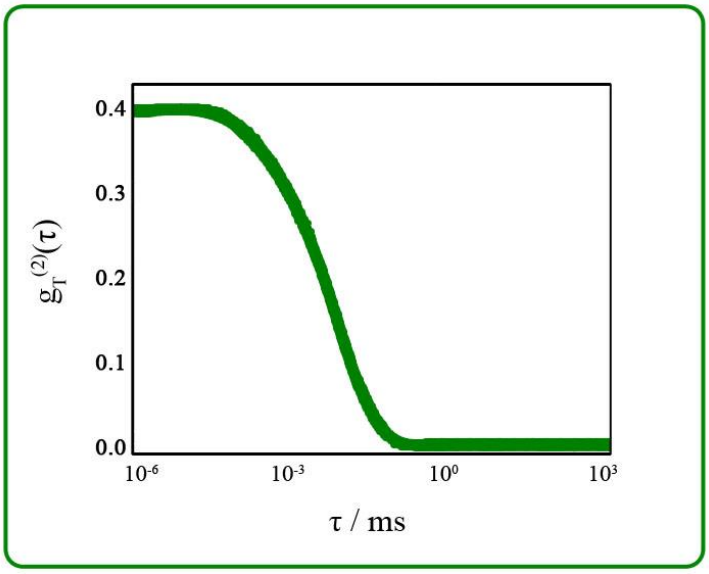

Figure 13. A schematic plot of autocorrelation function obtained from DLS measurement.

The scattered light is detected by devices with photosensitivity such as photomultiplier tubes. These devices count the number of photons which arrive at the detector. The number of photons indicates the light's intensity. However, the relevant quantity is the electric field. Intensity of light according to the equation 17 is the square of the electric field.

$$I(q,t) = |E(q,t)|^2 \tag{17}$$

The only component that makes the scattering intensity of an ergodic system, is fluctuating component. The equation $\langle I(q,t)\rangle_T = \langle I_F(q,t)\rangle_T = \langle |E_F(q,t)|^2\rangle_T$ can be applied for an ergodic system. In mentioned equation the term $E_F(q,t)$ concerns to the zero-mean complex Gaussian variable in the time domain. It is independent of sample position.

$g_T^{(2)}(q,\tau)$ of an ergodic system equals ensemble-averaged ICF, $g_E^{(2)}(q,\tau)$. The Siegert relation (equation 18) can relate the ensemble-averaged ICF to the normalized scattering function or the scattering field time correlation function $g_T^{(1)}(q,\tau)$.

$$g_T^{(2)}(q,\tau) = g_E^{(2)}(q,\tau) = \frac{\langle I(q,0).I(q,\tau)\rangle_E}{\langle I(q,0)\rangle_E{}^2} = 1 + \beta\left|g_T^{(1)}(q,\tau)\right|^2 \tag{18}$$

In this equation, β is the coherence factor of the instrument and $\langle \dots \rangle_E$ is an ensemble-average over all possible configurations of the medium.

The scattering field time correlation function, $g_T^{(1)}(q,\tau)$, can be approximated by the single exponential decaying function:

$$g_T^{(1)}(q,\tau) = exp(-\Gamma\tau) \tag{19}$$

in which Γ^{-1} is a characteristic decay time:

$$\Gamma = D_{trans}.q^2 = \frac{1}{\tau} \tag{20}$$

where D_{trans} is a translational diffusion coefficient and q is the scattering vector (eq. 14).

DLS can detect the hydrodynamic radius of polymer coils or a particle in a dilute solution. The measured size, the hydrodynamic radius R_H, is calculated by the translational diffusion coefficient, D_{trans}, which describes the center of mass movement of the whole coil by using the Stokes-Einstein equation:

$$R_H = \frac{k_B T}{6\pi\eta D_{trans}} \tag{21}$$

In this equation η is the viscosity of the solvent, k_B is Boltzman's constant and T is the absolute temperature.

In a non-ergodic system the scattering consists of two components i.e. the frozen-in (or static) component, $\langle I(q,t)\rangle_T = \langle I_F(q,t)\rangle_T + I_C(q)$ (eq. 12) and $I_C(q) = |E_C(q)|^2$. The former equation is independent of time while it depends on the position of the sample. As the different parts of the sample scatter the light differently, the speckle pattern will result from the DLS measurement. The Siegert equation cannot explain the observations, but there are basically two different approaches for justifying the fluctuating component, $\langle I_F(q)\rangle_T$, and the static component, $I_C(q)$, of polymer gels.

3.2.2 Non-ergodic method

The term "non-ergodicity" means inequality of ensemble average from time average which can successfully describe glasses and proteins [113].

Non-ergodicity of gels in relation to the DLS results has been studied by Pusey and van Megen [129] and Joosten et al. [132]. As mentioned before, the Siegert relation cannot be utilized to determine the diffusion coefficient of non-ergodic samples. Based on these studies, the time varying part of the correlation function equals the time varying part of the ensemble-averaged correlation function if the time-average intensity equals the ensemble-averaged intensity.

Polymer gels exhibit two different behaviors that arise from the liquid-like and solid-like structures of a gel. The fluctuationing component, $\langle I_F(q)\rangle_T$, corresponds to liquid-like concentration fluctuations and is ergodic while the solid-like structures determine static part of scattered intensity, $I_C\,(q)$, which is resulted from spatial inhomogeneities due the cross-linking process. The total ensemble average scattering intensity, $\langle I(q)\rangle_E$, equals the summation of these two contributions. It is obvious that in case of $\langle I_F(q)\rangle_T = \langle I(q)\rangle_E$ no static scattering results from spatial inhomogeneities which implies that the gel is behaving as an ergodic medium with no static inhomogeneities. Polymer solutions exhibit such behavior. Therefore they are called ergodic. Pusey and van Megen have proposed a model that measures scattered intensities at a high quantity of sample positions that is applied for measuring the ensemble-average of the scattered intensity, $\langle I(q)\rangle_E$, from which the degree of inhomogeneity and the diffusion coefficient can be obtained. During the measurement $\langle I(q)\rangle_E$ can be obtained by rotating the sample. Figure 14 shows an experiment performed according to non-ergodic method. As described earlier, the speckle pattern is resulted from frozen-in inhomogeneities of the non-ergodic gel. Therefore at each sample position a different quantity of time average scattering intensity, $\langle I(q)\rangle_T$, is measured. As the average of particle sizes is observed better in $\theta = 90°$, this angle is usually adjusted as scattering angle.

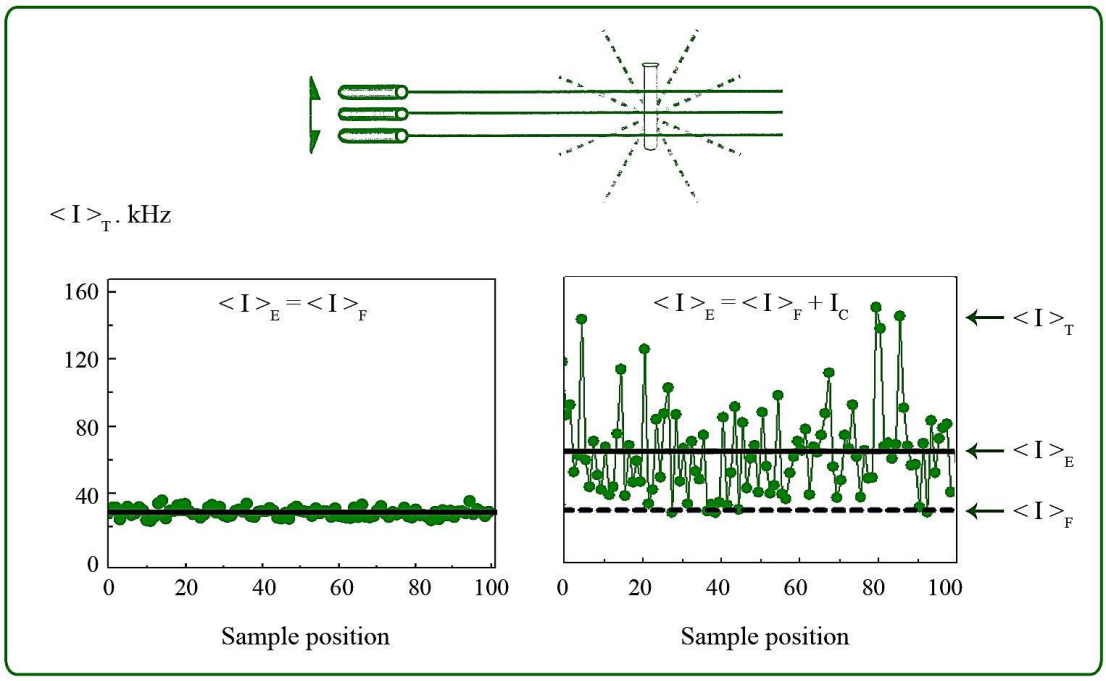

Figure 14. Speckle patterns of a polymer solution (left) and a gel structure (right). $\langle I\rangle_T$: Time-average scattering intensity, $\langle I\rangle_E$: ensemble-average scattering intensity and $\langle I_F\rangle_T$: intensity of fluctuating part that can be determined by non-ergodic method, $\theta = 90°$.

This model shows that, in the non-ergodic method, the intensity of the fluctuating part, $\langle I_F(q)\rangle_T$, is related to the time-average scattering intensity, $\langle I(q)\rangle_T$ by the following equation:

$$\langle I_F(q)\rangle_T = \langle I_F(q)\rangle_E = \langle I(q)\rangle_E[1 - f(q,\infty)] \tag{22}$$

in which $f(q,\tau)$ is the function of the normalized intermediate ensemble-average. The letter f is used in order to distinguish the intermediate scattering function of the non-ergodic medium from the field correlation function, $g_T^{(1)}$, of an ergodic medium. $f(q,\infty)$ corresponds to an asymptotic approach for $\tau \to \infty$ that is of static scattering function. $f(q,\tau)$ can also be calculated using the time average intensity correlation function that is measured at a particular position, $g_T^{(2)}$.

$$f(q,\tau) = 1 + \frac{\langle I(q)\rangle_T}{\langle I(q)\rangle_E}\left[\sqrt{\frac{g_T^{(2)}(q,\tau) - 1 - \sigma^2}{\beta}} + 1 - 1\right] \tag{23}$$

From this equation a relation between σ^2 and the ratio of intensity can be obtained. By decreasing the value of σ^2 the ratio of intensity will increase and vice versa. $\sigma^2 = g_T^{(2)}(q,0) - 1$ is the initial amplitude of the time-averaged intensity correlation function. If $g_T^{(2)}$ is converted into a normalized intermediate ensemble-averaged scattering function, $f(q,\tau)$, it shifts up to a y-axis intercept with the value of one, resulting in a nonzero offset, $f(q,\infty)$ (Figure 15).

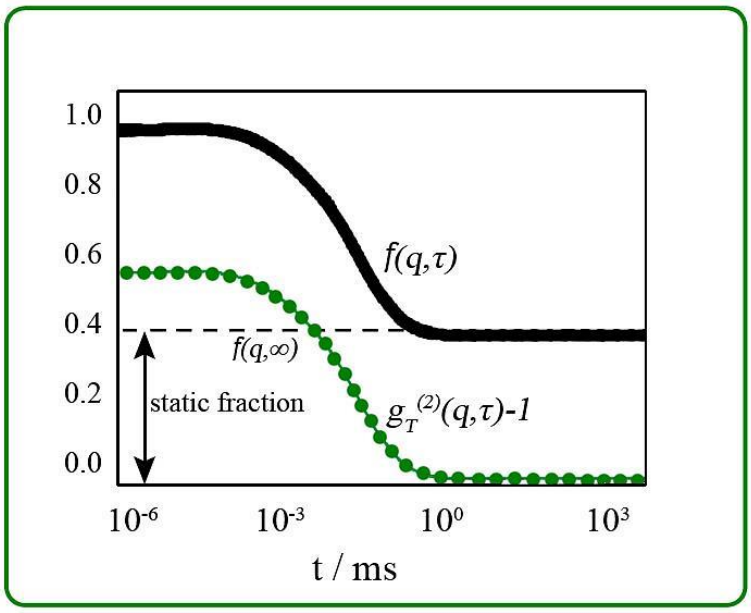

Figure 15. $f(q,\tau)$ obtained by the non-ergodic method in which $g_T^{(2)}(q,\tau) - 1$ is shifted to an ordinate intercept of 1.

The asymptotic value, $f(q,\infty)$, and the correlation time, τ, is calculated according to eq. 24 from the fitted curve in which the amplitude $A = 1 - f(q,\infty)$.

$$f(q,\tau) = f(q,\infty) + A\, exp(-\frac{t}{\tau}) \tag{24}$$

The static fraction of the polymer gel, ($\langle I_C(q)\rangle_T$), is indicated by the asymptotic value, $f(q,\infty)$, and the fluctuating part, ($\langle I_F(q)\rangle_T$), is indicated by the amplitude, A. Therefore more homogeneity of polymer gel is evidenced by lower asymptotic value. The aim of the non-ergodic method is to indicate the percentage of static and fluctuating parts of the polymer gel.

The dynamic correlation length, ζ, can be obtained by the cooperative diffusion coefficient, D, that identifies the relaxation of network chain segments according to following equation:

$$\zeta = \frac{kT}{6\pi\eta D} \tag{25}$$

where η is viscosity of the medium, kT is the Boltzmann energy.

3.2.3 Partially heterodyne method

Having determined the intensity correlation functions, the partial heterodyne method can alternatively be employed in order to separate the overall scattering intensity into its two fractions. As stated earlier this intensity is an association of scattered intensity due to fluctuations of the network and immobile domains [113,133]. This model has been developed by Joosten et al. in 1991 [130]. Scattered intensity of a non-ergodic medium is assumed to be given by summation of the fluctuating and static intensity components and the ergodicity is applied to the fluctuating part. Therefore an estimation of apparent diffusion coefficient, D_A, can be given as:

$$D_A = \frac{1}{2q^2} \lim_{\tau \to 0} \frac{\partial}{\partial \tau} ln\left(g_T^{(2)}(q,\tau) - 1\right) \tag{26}$$

By varying the sample position, different values for D_A and different local scattering intensities, $\langle I(q)\rangle_T$, will be obtained. For an ergodic system ($\langle I_F(q)\rangle_T = \langle I(q)\rangle_T$) that is homogenous and homodyne $D \approx D_A$. In case of a static, inhomogeneous and heterodyne system in which $\langle I_F(q)\rangle_T \ll \langle I(q)\rangle_T$, it is obtained that $D \approx 2D_A$. The relationship between D_A and cooperative diffusion coefficient, D, is obtained as following:

$$\mathrm{D} = \left[2 - \frac{\langle I_F(q)\rangle_T}{\langle I(q)\rangle_T}\right] D_A \tag{27}$$

Since the measurements are applied at different positions of a sample, different values of D_A and $\langle I(q)\rangle_T$ will result. By rearranging the equation above, a straight plot of $\langle I(q)\rangle_T / D_A$ versus $\langle I(q)\rangle_T$ will result. The slope and the intercept of the plotted function determine the fluctuating component of the scattering intensity, $\langle I_F(q)\rangle_T$, and D. To be able to utilize this model with high accuracy, a large number of data points are needed for plotting a straight line.

$$\frac{\langle I(q)\rangle_T}{D_A} = 2\frac{\langle I(q)\rangle_T}{D} - \frac{\langle I_F(q)\rangle_T}{D} \tag{28}$$

Both non-ergodic and partially heterodyne methods can be employed to separate the ensemble-averaged scattering intensity, $\langle I(q)\rangle_E$, into its components, $\langle I_F(q)\rangle_E$ and $\langle I_C(q)\rangle_E$.

4 Experimental procedure

4.1 Substances

Compounds and materials used in this work are briefly described below:

Acrylamide (AAm, Merk): this substance is used as a hydrophilic monomer in the micellar copolymerization reaction. Melting point of AAm is in the range of 84-85°C and its molecular weight is 71.08 g/mol (Figure 16).

As briefly described in the previous sections, the method employed herein for producing the polymer network, is copolymerization of acrylamide (hydrophilic monomers) in the presence of stearyl methacrylate comonomers (hydrophobic monomers) via radical micellar polymerization. Acrylamide is a water soluble monomer [134] and has been used as hydrophilic monomer in synthesis of hydrogels during last decades [135-140].

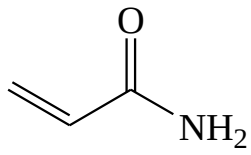

Figure 16. Structure of acrylamide (AAm).

Stearyl methacrylate (SM, Fluka): commercial stearyl methacrylate is used to improve cross-linking of hydrogels. SM consists of 65 % n-octadecyl methacrylate and 35 % n-hexadecyl methacrylate (Figure 17). Stearyl methacrylate is a water insoluble, low volatile, mono-functional methacrylate monomer with a long, hydrophobic side chain. This substance can be used to induce the following properties to polymers: adhesion, weatherability, low shrinkage, flexibility, water resistance, improved impact strength, hydrophobicity. Melting point and boiling point of SM are 18 and 310°C respectively [141].

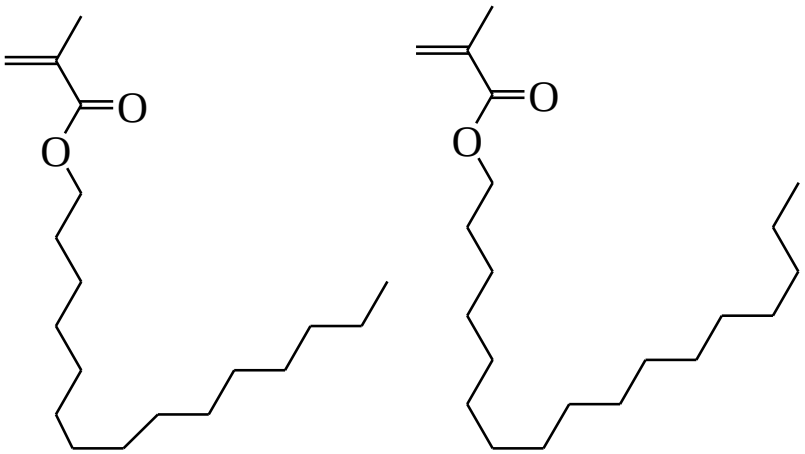

Figure 17. Structure of technical grade stearyl methacrylate (SM).

Cetyltrimethylammoniumbromide (CTAB, Sigma-Aldrich): during the procedure CTAB has been used as a cationic surfactant. The molecular weight of CTAB is 364.45 g/mol and its structure is shown in Figure 18.

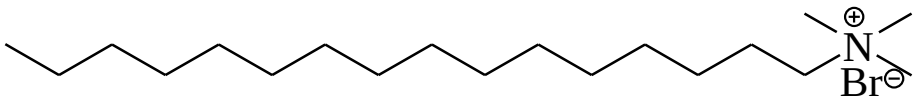

Figure 18. Structure of cetyltrimethylammoniumbromide (CTAB).

Ammonium persulfate (APS, Sigma-Aldrich): this compound is used as initiator of the micellar copolymerization reaction. APS has a molecular weight of 228.20 g/mol and a melting point of 120 ºC (Figure 19).

Polymerization of acrylamide is initiated by free radicals of ammonium persulfate which converts acrylamide monomers to free radicals. Radicals of acrylamide then react with other un-activated monomers [142]. APS is a reactive compound and tends to oxidize or decompose immediately after being dissolved in water. Therefore, APS solutions have to be freshly prepared before use.

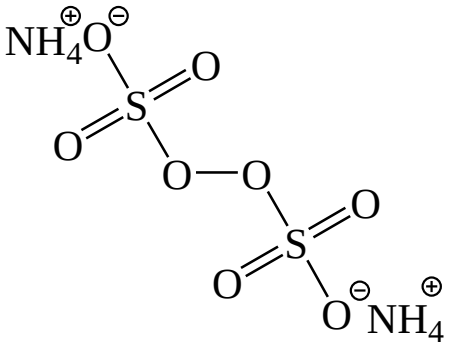

Figure 19. Structure of ammonium persulfate (APS).

Sodium nitrate ($NaNO_3$, Sigma-Aldrich): this salt is used to enhance the micelle's size. Molecular weight of sodium nitrate is 84.99 g/mol. Melting temperature of sodium nitrate is 308 °C and its solubility in water is 874 g/L in 20 °C (Figure 20).

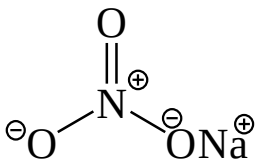

Figure 20. Structure of sodium nitrate ($NaNO_3$).

N,N,N',N'- tetramethylethylenediamine (TEMED, Sigma): this compound was used also as an accelerator of the polymerization reaction. The boiling point of TEMED is in the range of 120-122 ºC and its molecular weight is 116.21 g/mol that is shown in Figure 21.

TEMED is an essential catalyst for polyacrylamide gel polymerization that accelerates the formation of free radicals from persulfates. TEMED reacts with APS to form a free-radical of APS with an unpaired valence electron. This unpaired electron can then react with acrylamide to initiate the polymerization.

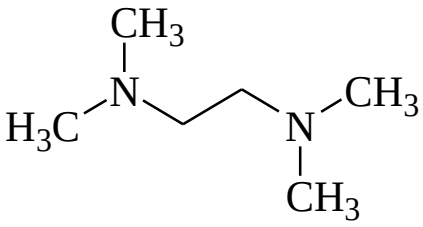

Figure 21. Structure of N,N,N',N'- tetramethylethylenediamine (TEMED).

Water: As a natural pure liquid or solvent, water has special properties owing to its molecular interactions and structuring at the surfaces. Hydrogen bonding is primarily the cause of some properties such as high boiling point, high surface tension and reluctance to solving nonpolar or hydrophobes [143]. This structure for instance leads to the creation of micelles from molecules with a polar head and a non-polar tail. Creation of micelles, inclusion of hydrophobic monomers within the micelles as well as hydrophobic interactions all benefit from the unique nature of water which makes it possible to achieve an important class of physical hydrogels called hydrophobically modified hydrogels [15,144].

4.2 Preparation of hydrogels

In the present work the synthesis of hydrophobically modified hydrogels, containing hydrophobic blocks, has been carried out using micellar copolymerization. The characterization of prepared hydrogels was conducted by rheological measurements and dynamic light scattering (DLS) techniques. By systematic variation of preparation parameters it was investigated how the properties of the physical gels are affected.

4.2.1 Synthesis of hydrophobically modified physical gels by micellar copolymerization

As mentioned above the physical gels were prepared by micellar copolymerization. In the first step CTAB (0.3 g) was dissolved in 9 mL distilled water followed by the addition of $NaNO_3$ into the solution. Optimum concentration of $NaNO_3$ was determined to be 0.3 M that increased the size of the micelles so the hydrophobic comonomer could be solubilized within the micelles [19]. Then, SM was dissolved in the resulted CTAB-$NaNO_3$ solution under stirring for 90 minutes. After addition and dissolving the acrylamide and stirring for 30 min, TEMED was added into the solution. Finally, APS stock solution (0.2 mL) was added to initiate the polymerization reaction. The SM content of the monomer mixture (SM + AAm) was fixed at 2 mol % while the total monomer concentration C_0 was varied between 5 % and 13 %. Reactions were carried out at temperatures of 25 and 35 °C. The fixed concentrations of substances mentioned above are shown in Table 1. All mentioned fixed parameters such as concentrations of CTAB, $NaNO_3$, AAm, SM[1], APS and TEMED are obtained through frequent measurements of hydrogels containing different amounts of each substance.

[1] Effect of different concentrations of AAm and SM were evaluated separately.

Table 1. Fixed total monomer concentrations, initiator and cationic surfactant during synthesis process of hydrogels.

Hydrophilic Monomer	Acrylamide (AAm)		Total concentration of monomers (SM+AAm)	11 w/v%
Hydrophobic Comonomer	Stearyl methacrylate (SM)	2 mol%		
Redox initiator system	Tetramethylethylenediamine (TEMED) concentration			0.168 M
	Ammonium persulfate (APS) concentration ($(NH_4)_2S_2O_8$)			3.5 mM
Cationic Surfactant	Cetyltrimethylammoniumbromide (CTAB)			3.3 w/v%

Figure 22 illustrates the process during which a surfactant containing physical gels in aqueous CTAB−$NaNO_3$ solutions is formed via hydrophobic interactions (SM). During the micellar copolymerization process a hydrophobic comonomer is solubilized in the surfactant micelles while the hydrophilic monomer is soluble in the aqueous medium. The hydrophobic blocks are distributed randomly in the hydrophilic polymer backbone, because of the high local concentration of the hydrophobic comonomer within the micelles. The hydrophobic blocks tend to associate and form physical cross-links to produce the hydrogel. The length of hydrophobic blocks is a function of the ratio of hydrophobic comonomer to surfactant [134,145]. Formation of such a structure was first suggested by W. J. Peer in 1987 [78].

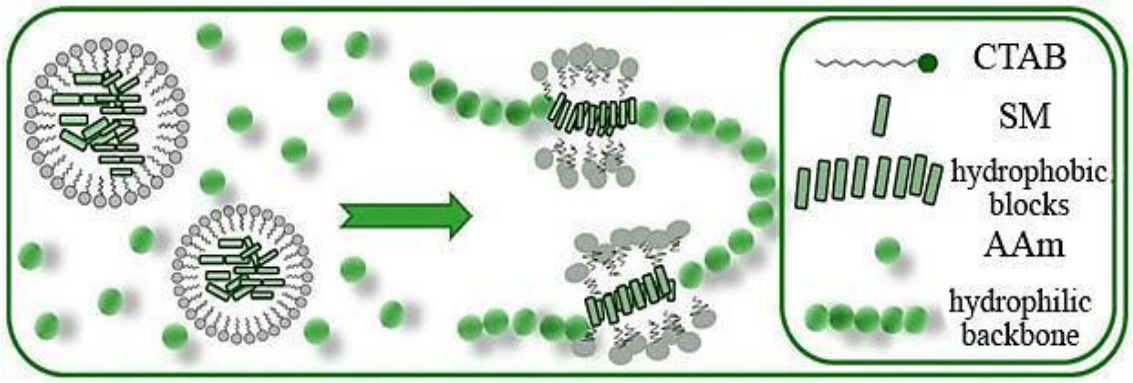

Figure 22. Formation of surfactant containing physical gels in aqueous CTAB−$NaNO_3$ solutions via hydrophobic monomer (SM) [146].

During the rheological experiments, a portion of the unreacted solution was placed between the plates of the rheometer and the reaction was monitored. Finally dynamic light scattering measurements were carried out. Therefore after adding the initiator the solution was filtered with a Nylon membrane filter with a pore size of 0.45 μm directly into the light scattering vials. After 24 hours of aging in an oven, measurements where performed in DLS at the same temperatures as the synthesis temperature (25 or 35 °C).

4.2.1.1 Reaction mechanism

The hydrogel formation mechanism is illustrated in Figure 23. Hydrophilic monomer (AAm) is copolymerized with the hydrophobic monomer (SM) by a free-radical mechanism by means of TEMED and APS.

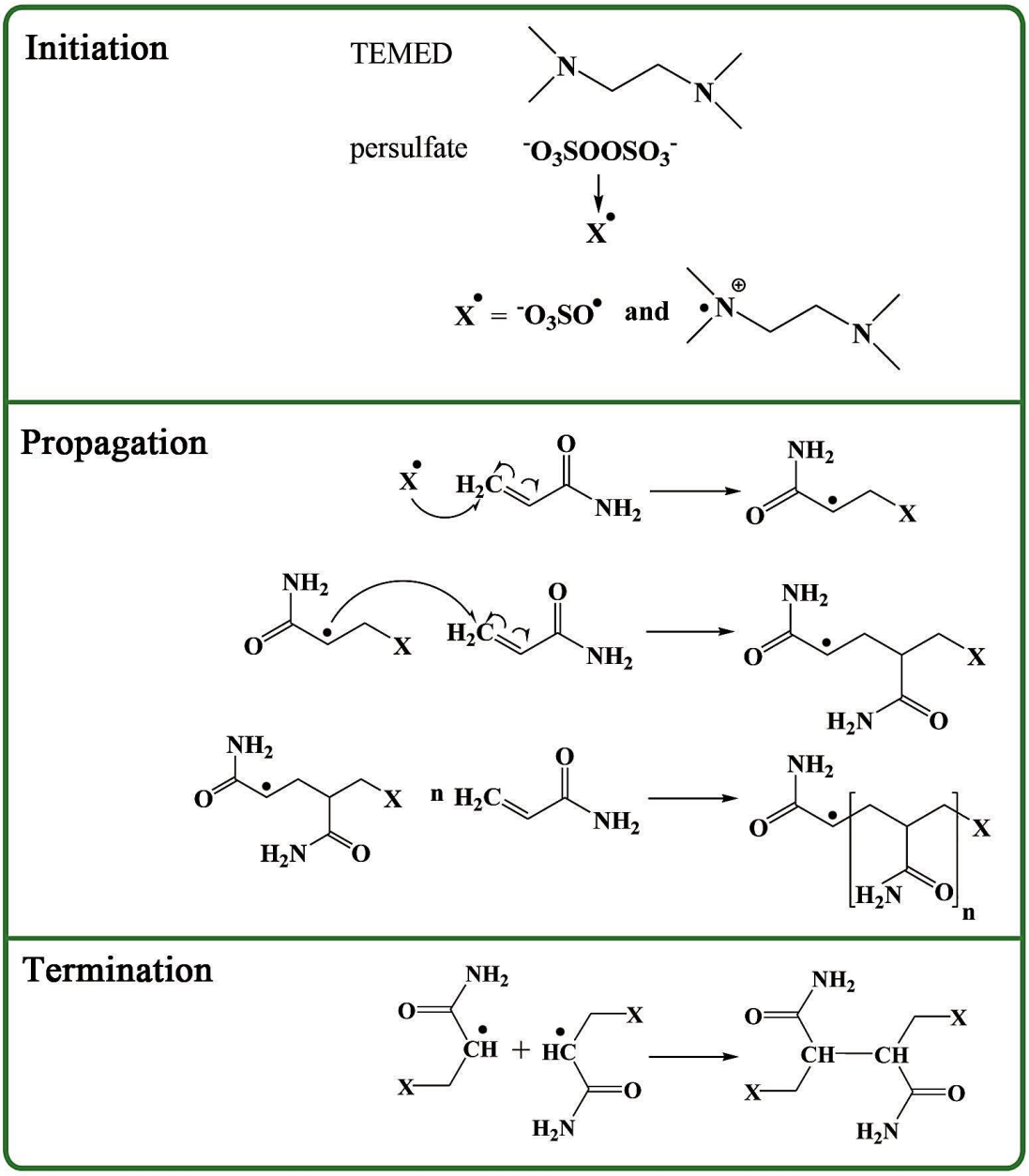

Figure 23. Scheme of a polyacrylamide gel: an illustration of the mechanism of polymerization with the radical mechanism by the TEMED-persulfate couple, and the radical polymerization of acrylamide. The structure of the gels is shown in the chain transfer stop [147].

4.3 Characterization methods of hydrogels

Obtained hydrogels were characterized by means of Dynamic Light Scattering and rheology measurement techniques. DLS analysis was carried out to evaluate the microstructure of the polymer network. Deformation of the gel structure under the influence of imposed stress was monitored and characterized by rheology measurement.

4.3.1 Light scattering measurement

4.3.1.1 Dynamic light scattering (DLS) measurement

For the DLS measurements different CTAB solutions with and without $NaNO_3$ and monomers (SM and AAm) were used. The solutions were analyzed at 25 °C.

The DLS measurements were performed with an ALV/CGS-3 compact goniometer system (ALVGmbH). This system was equipped with an ALV/LSE-5003 correlator, a cuvette rotation/translation unit for measuring the non-ergodic samples and a three-mode fiber-optical detection unit which was combined with an ALV/HIGH QE avalanche photodiode detector. Schematic DLS setup is shown in Figure 24.

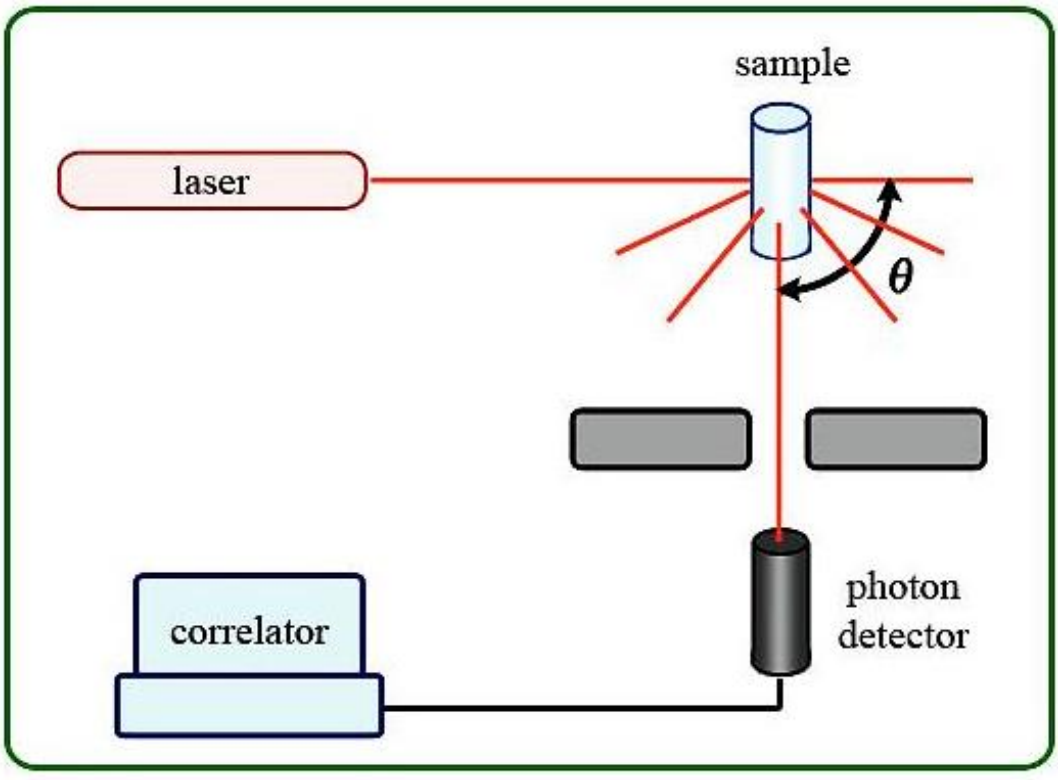

Figure 24. A schematic illustration of dynamic light scattering system.

The measurements were carried out on each hydrogel sample at the same temperature of the synthesis condition (25 or 35 °C), after a reaction time of 24 hours. Hydrogels with different concentrations of $NaNO_3$, SM and AAm were analyzed.

As the first step, measurements were done at scattering angles of 50-130°. The obtained data showed no dependence between the results of measurement and scattering angle. Therefore the result of the measurements that were performed at scattering angle of 90° will be presented in subsequent section.

Two sets of DLS analysis were performed, including measurements with and without rotation. Firstly the analysis with rotation was carried out as 100 measurements at different sample positions for 30, 100 and 600 seconds among which only the results of 600 seconds will be reported in order to obtain an ensemble average. The cuvette was constantly rotating during the measurements. Secondly measurements without rotation in 7200, 10,000 and 15,000 seconds were done at different sample positions. For each sample and each measurement time, five measurements were carried out. Each measurement was repeated three times in order to improve the accuracy of the data. Among the obtained data only the results of 7200 seconds will be presented and discussed, since there was no significant difference between results of analysis of 7200, 10,000 and 15,000 seconds.

In order to have a temperature balance before starting the measurements, the cuvettes were placed in the toluene bath for 10 minutes.

4.3.2 Rheological analysis

Viscoelasticity of a wide range of materials from high elastic solids to viscous liquids can be studied with rheology analysis. Based on mentioned description, rheology analysis is a useful method to evaluate the macroscopic properties of gels [100]. In order to characterize the polymeric matrix and the trend of diffusion which takes place in the polymers, rheological analysis was employed. This analysis investigates the flow and deformation of the materials under an applied stress during time.

The rheometer in which the gelation reactions were carried out was a Gemini 150 Rheometer system, Bohlin Instrument, equipped with a cone-and-plate geometry. Cone angle and diameter were 4° and 40 mm, respectively (Figure 25). The system was also equipped with a Peltier device for controlling the temperature. A solvent trap was employed to minimize the evaporation during all measurements.

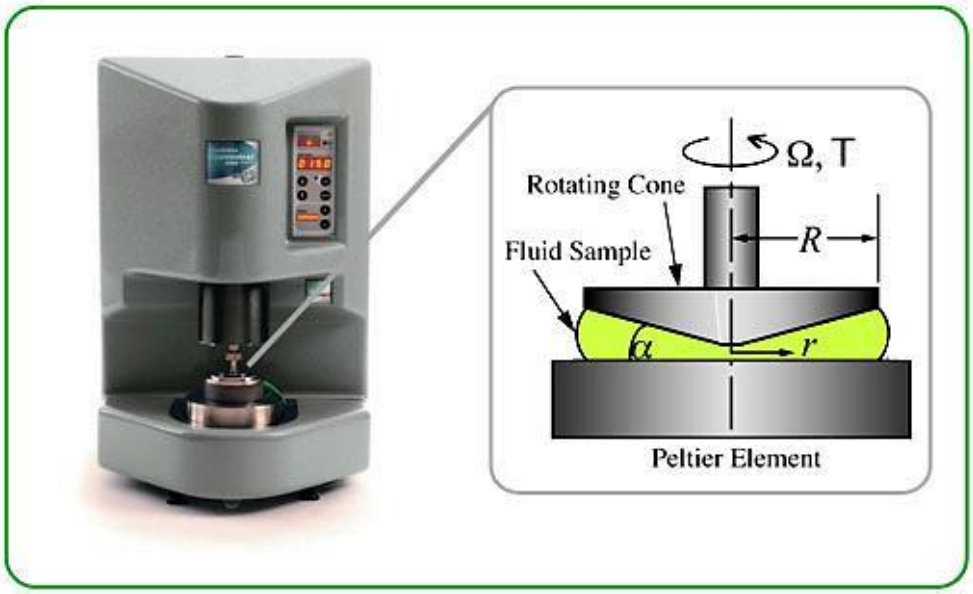

Figure 25. Schematic illustration of the rheometer with corne-and-plate geometry.

4.3.2.1 Rheological measurement

Corresponding to the angular frequency of $\omega = 6.3$ rad/s, the frequency of 1 Hz and the deformation amplitude of $\gamma_0 = 0.01$ were adjusted in order to make sure that oscillatory deformation stays within the linear regime. All reactions were monitored at temperatures of 25 and 35 °C for about 3 h. After that period, tests of frequency-sweep were performed at $\gamma_0 = 0.01$ and temperatures of 25 and 35 °C with the frequency ranged from 10^{-2} to 10^{2} Hz.

Obtained gels in rheometer were also studied with stress relaxation measurements that were performed at 25 °C. A constant amount of step-wise shear deformation (γ_0) was applied and the resulted stress $\sigma(t, \gamma_0)$ was monitored as a function of time. During the tests stain (γ_0) varied between 10 and 100. The stress relaxation experiments were performed starting from a value of the relaxation modulus with deviation less than 10% from the modulus measured at $\gamma_0 = 0.01$.

4.3.3 Viscometry measurement

Viscometry analysis was employed to measure the viscosity of CTAB / $NaNO_3$ / SM aqueous solutions with different concentrations of salt and cross-linker while the concentration of CTAB was kept constant (3.3 w/v%). The solutions were analyzed at 25 °C.

For this purpose, an Ubbelohde-viscometer with capillary diameter of 0.36 mm was used. Low viscosity samples were filtered through SCHOTT glass filters (10-100 μm) before carrying out the measurement.

5 Result and discussion

5.1 Introduction

The aim of this research is to enhance the mechanical performance of hydrogels obtained via free radical cross-linking copolymerization. For this purpose, a process was designed to synthesize smart hydrogels with a higher grade of quality. As synthetic hydrogels normally have poor mechanical properties, it is imperatively necessary to develop hydrogels with less brittleness to be applicable in any stress bearing condition. Based on the theory of crack propagation and material failure, poor mechanical properties of hydrogels originate from the lack of an efficient energy dissipation mechanism in the network. In order to enhance the degree of toughness in hydrogels, more viscoelasticity at the molecular level of the gel has to be introduced by dissipative mechanisms. Hydrogels derived from cross-linking copolymerization include inhomogeneous distribution of cross-links which is called spatial inhomogeneity. Structural inhomogeneities dramatically affect the mechanical strength of cross-linked materials.

5.2 Kinetics of surfactant solution

5.2.1 Micellization of CTAB in the presence of $NaNO_3$

In the present study sodium nitrate ($NaNO_3$) was used to enhance CTAB micelles growth which is supposed to lead to an increase in the viscosity of the solution. N. Jiang et al. investigated the effect of different salts on the formation of micelles from CTAB solution in 2005 [23]. It was found that NO_3^- ions have the most positive impact on formation of elongated micelles. Elongated micelles have a polymeric organization and can be assembled into a three dimensional network. In the presence of salts such as KBr, NaSal (sodium salicylate), $NaNO_3$ etc., CTAB micelles will grow and reorganize from spherical into worm-like configuration [148] which is briefly described in section 2.1.2.3. Interaction occurred between anions derived from salt and cationic head of the surfactant leads to strong bindings between these counterions, which in turn results in the immediate formation of a worm-like configuration of the micelles. It has also been reported that viscosity of the solution containing worm-like micelles is increased by increasing the salt concentration. By increasing the concentration of $NaNO_3$ the micellization reaction becomes more exothermic, while the entropy of the reaction is independent of the salt concentration. It is believed that the positive effect of added electrolytes on micellization is due to an increase in ionic strength of the medium. For all uni-univalent salts ionic strength of the medium and counterion condensation on micelles is the same. Therefore the observed enhanced micellization could be a strong

function of the size of NO_3^- counterions. In spite of the observations still a thorough study on the organization of cationic micelles in the presence of nitrate is lacking [96].

In contrast to the effect of salt, temperature has a reverse effect on the viscosity. It is believed that by increasing the temperature no structural transition happens in micelles rather than the reduction in their size. It is known that the size of micelles decreases monotonically by increasing the temperature (Figure 26) [23].

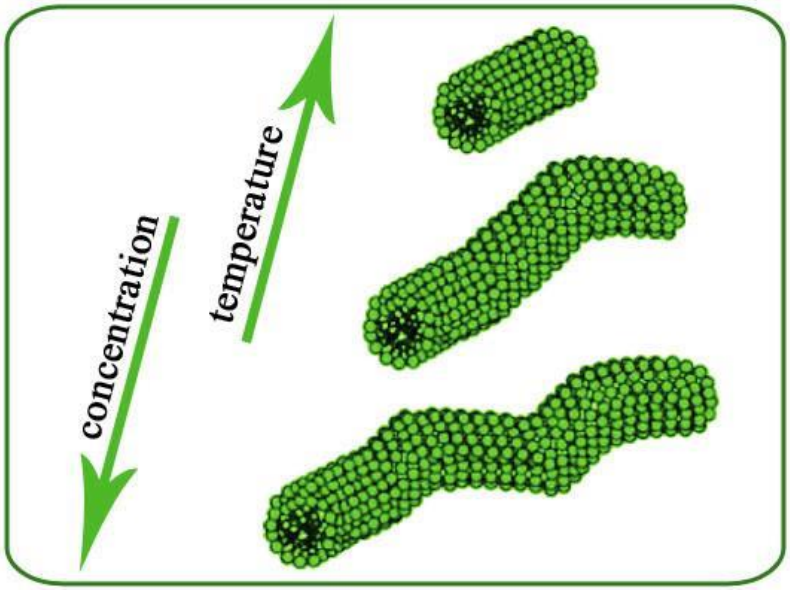

Figure 26. The size of the micelle increases with increasing the concentration of counterions and decreasing temperature [73].

The viscosity of micellar solutions prepared from water / CTAB / SM / $NaNO_3$, were measured at room temperature. Figure 27 illustrates the viscosity of each solution. As expected, different salt concentrations led to different viscosities.

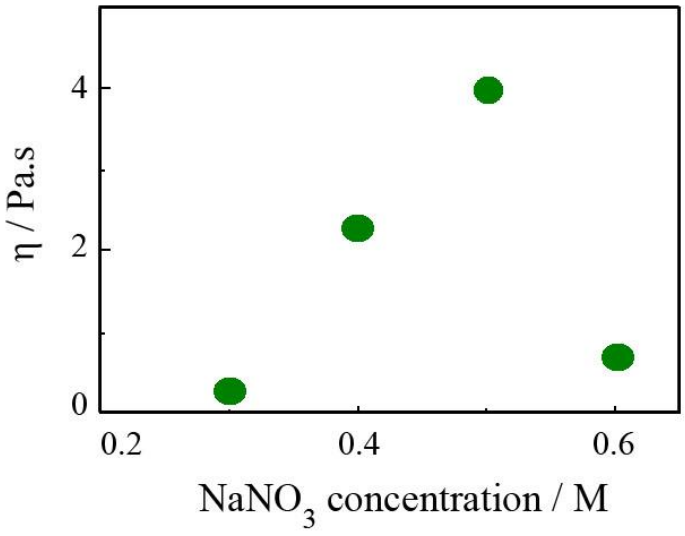

Figure 27. Viscosity of the micellar solutions as a function of $NaNO_3$ concentration at room temperature.

This analysis was carried out in order to evaluate the formation of worm-like micelles. During this analysis the concentration of CTAB was kept constant at 3.32 w/v% and each solution contained 0.043 g of SM. The constant amounts of CTAB and SM were obtained through a preliminary evaluation that was carried out on gels obtained with different CTAB and SM concentrations. Considering the gel's appearance as well as the results of oscillatory deformation tests of each gel, the optimum CTAB concentration seems to be around 3.32 w/v%. The concentration of $NaNO_3$ was varied from 0.3 to 0.6 M. By increasing the salt concentration from 0.3 up to 0.5 M viscosity was increased continually. Further increase in salt concentration resulted in a dramatic decay in viscosity.

Figure 28 shows the viscosity (η) as a function of the shear rate at different salt concentrations. If $\dot{\gamma} \rightarrow 0$, the measured viscosity is the zero shear viscosity (η_0). In non-Newtonian materials the viscosity may be shear rate dependent at higher shear rates. In contrast, at low shear rates the viscosity is independent of the shear rate standing on an almost constant amount that is called η_0. Above a critical shear rate ($\dot{\gamma}_{crit}$) viscosity starts to decrease with $\dot{\gamma}$ [149]. As it is expected, at the lowest $NaNO_3$ concentration the solution exhibits the lowest amounts of viscosity over the investigated shear rate range. The viscosity increases dramatically by increasing the $NaNO_3$ concentration up to 0.5 M, while for higher amount of $NaNO_3$ (0.6 M) the viscosity decays significantly. This behavior can be explained by the micellar growth mechanism explained in discussion of Figure 26. As stated before it is believed that addition of $NaNO_3$ increases the enthalpy

of micellization which results in the growth and elongation of the micelles. This effect is related to the "screening" of electrostatic interactions between amphiphilic groups. Screening is the reduction of the coulomb interaction strength between oppositely charged species [95,96,150,151].

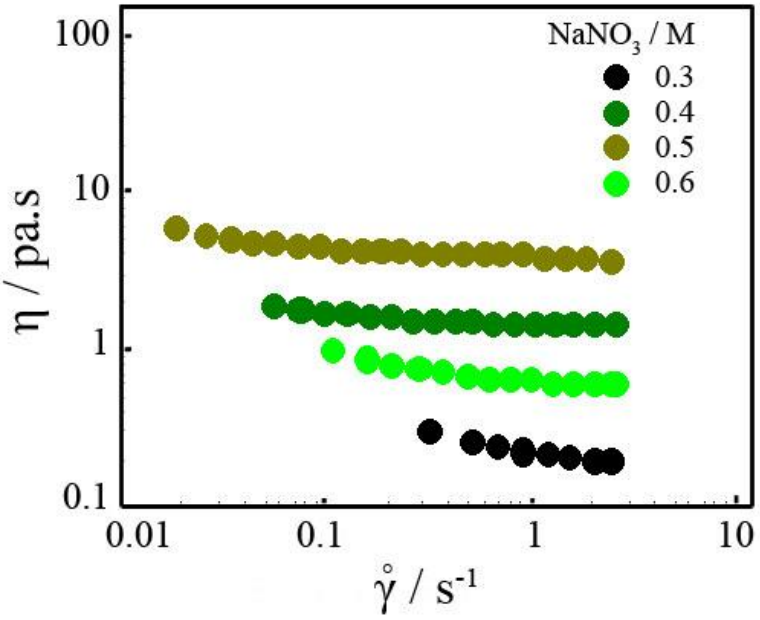

Figure 28. Viscosity as a function of the shear rate for 3.3 w/v% surfactant aqueous solutions with different salt concentrations at 25 °C.

Uni-axial growth of micelles occurring by increasing the salt concentration up to 0.5 M enhances the viscosity of the system. Enriched salt concentration heightens the curvature energy of the surfactant molecules in the end-cap of micelles. Amount of the mounted energy of the mentioned molecules is relatively higher than the molecules situated in a cylindrical body. This phenomenon causes lengthening of the micelles and formation of rod-like micelles. More increase in salt concentration leads to more lengthening of the micelles and formation of worm-like micelles. Worm-like micelles can curve freely and cause a dramatic increase in viscosity. At higher salt concentrations (>0.5 M) a decrease in viscosity of the micellar solution occurs, indicating another structural change within the system. It is believed that worm-like micelles will not lengthen anymore and branching of the micelles occurs at these high salt concentrations. As the branch points are not fixed, formation of branches reduces the viscosity [96,152,153].

A slight reduction of viscosity versus shear rate is observed that could be due to the shear alignment of micelles which is believed as worm-like micelles typical behavior [89].

5.2.2 Effect of hydrophobic monomer

After the addition of salt, stearyl methacrylate (SM) was added to the solutions. The viscosity of each solution was measured after addition of various amounts of SM. Interestingly with increasing the amount of SM in solution the viscosity decreased continuously (Figure 29).

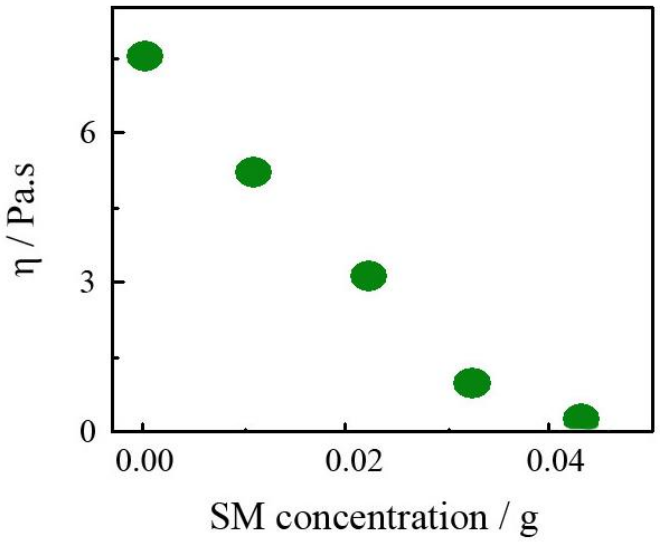

Figure 29. Variation of viscosity as a function of hydrophobic monomer concentration added to the solution of CTAB and $NaNO_3$.

It is believed that by introducing a hydrophobic substance into the solution, these molecules will diffuse and solubilize within the micelles that widely affects the organization of micelles. In fact this phenomenon is an approach for solubilizing poorly soluble molecules that have found applications in drug delivery for enhancing bioavailability of drugs [154,155]. In this procedure large hydrophobic droplets form in the aqueous solution that leads to formation of an emulsion. Although the droplet will be surrounded by the surfactant molecules, micelles still exist in the solution. As it is schematically shown in Figure 30, hydrophobic molecules reside within the non-polar core of micelles. The way these molecules are arranged within the micelles depends on their hydrophobicity and may be controlled by hydrophobic interactions, entropy change or enthalpy change. The location of hydrophobic molecules within the micelles

also affects the micelle-water interfacial tension that can influence the shape and size of the micelle [24,25,26]. Through this process the organization of micelles will change from worm-like into spherical. The association of hydrophobic monomers within the micelles' core and around the palisade layer causes an ascend in curvature of the micelles and by this way favors the rod-like to spherical transition [19].

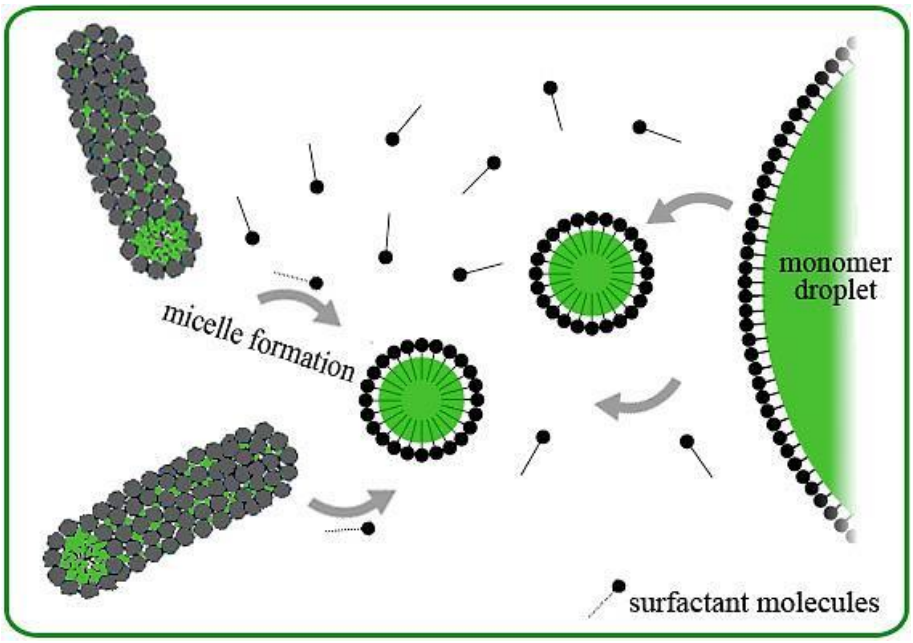

Figure 30. Schematic illustration of reorganization of micelles from rod-like to spherical by adding SM in the presence of salt and CTAB [156,157].

The first key parameter which has to be considered in evaluating the functionality of hydrophobic comonomers is the nature of the polymerization function. The other parameter is the nature of the hydrophobic group that indicates the strength of hydrophobicity and hydrophobic interactions. Also the nature of the connecting group between polymerizable function and hydrophobic comonomer is of importance. As it was mentioned earlier, in micellar copolymerization hydrophobic monomers will randomly distribute along the backbone as blocks rather than as single molecules. This pattern takes place as a result of high local concentration of hydrophobic molecules within the micelles.

It was mentioned that the increasing trend of viscosity, observed during the addition of salt, is due to the increase of the micelles' size and formation of worm-like micelles. Figure 31 shows the viscosity of solutions as a function of the shear rate upon the addition of different concentrations of SM. Unlike the effect of salt, the decreased

viscosity with increasing SM concentration is believed to be due to the reorganization of the micelles. The formation of smaller micelles containing molecules of SM through the emulsion process decreases the viscosity.

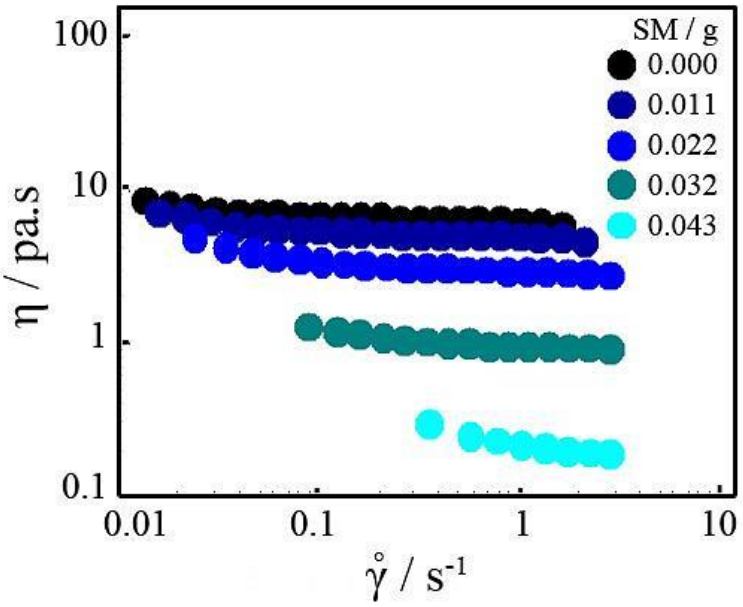

Figure 31. Viscosity variation versus shear rate with different SM amounts for systems containing 3.3 w/v% of CTAB and 0.3 M of $NaNO_3$ at 25 °C.

Also the transparency of the solutions increased by increasing the SM concentration which can be related to the smaller size of newly formed micelles. A further increase in the amount of SM resulted in a stronger decrease of viscosity due to the shrinkage of the worm-like micelles. This clearly resulted in a higher transparency of the solutions.

5.2.3 Step by Step DLS characterization of hydrogel synthesis solutions

In order to have an evaluation of the effect of the substances used on the physical gels processing, DLS analysis was performed on each step of the solution preparation. Figure 32 (a) and (b) shows the resulted normalized intermediate ensemble-average scattering function $f(\tau)$, and characteristic decay time distribution function, G(Γ), calculated immediately after addition of surfactant, salt, hydrophobic monomer, and hydrophilic monomer, respectively. The concentration of each substance is mentioned in Table 1. The solution of CTAB in water shows both fast and slow relaxations. The slow relaxation of CTAB solution is a reflectance of the surfactant agglomerates in the solution. The addition of $NaNO_3$ to the CTAB containing solution merged two relaxations into one, which obviously confirms the enhancement of aggregation

compared to the salt-free condition. This can be explained by disappearance of the slow mode and shift of the fast mode to the right (longer times).

The addition of stearyl methacryate to the surfactant and salt containing solution also shifted the fast mode relaxation to longer times compared to the parent solution. It reflects the formation of the hydrophobic associations besides the surfactant aggregates. After addition of AAm the system exhibited again both fast and slow relaxation modes. Slow relaxation occurs even in longer time scales.

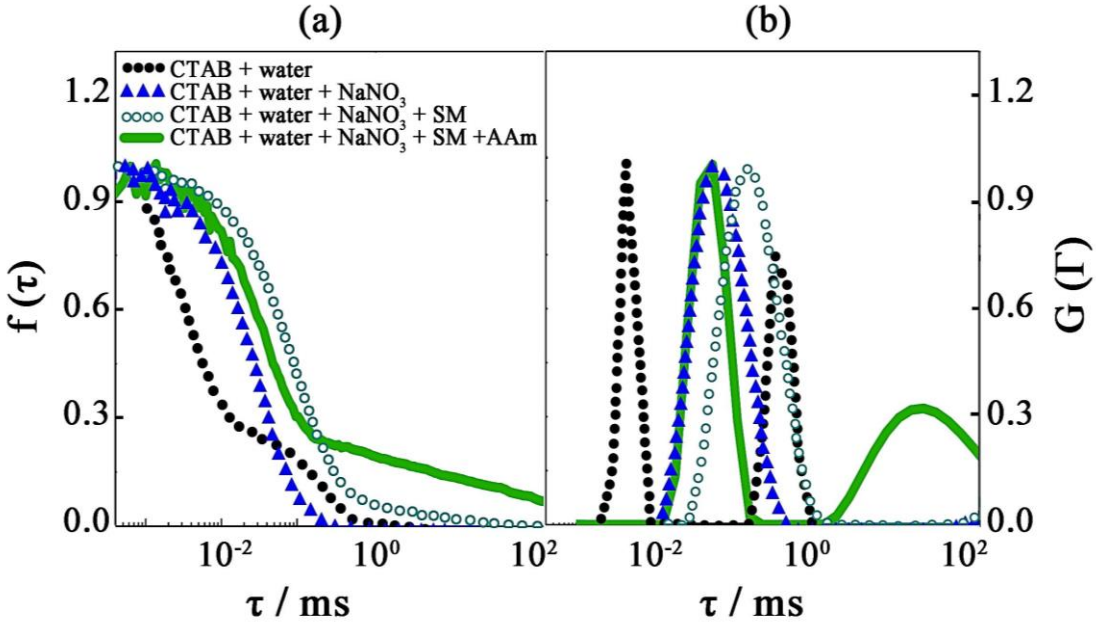

Figure 32. (a) Normalized intermediate ensemble-average scattering function $f(\tau)$, calculated from $g_T^{(2)}(\tau)$ for various preparation steps at scattering angle of 90°. (b) Characteristic decay time distribution function, G(Γ), obtained with a measurement time of 2 h at θ = 90° for different steps of solution preparation. Temperature = 25 °C.

The latter DLS analysis were performed on hydrogels utilizing time periods of 7200 seconds and longer, because the time range of this analysis does not completely illustrate the slow relaxation of formed hydrogels.

5.3 Gel formation

5.3.1 Effect of salt concentration

Polymerization of acrylamide in the presence of CTAB, $NaNO_3$ and SM was carried out. At room temperature (25 °C), no gel was formed in the absence of $NaNO_3$ and just

a turbid polymer solution resulted as shown in Figure 33. By increasing the temperature up to 35 °C in the absence of salt, however a very weak gel formed. It is believed that at lower temperatures the solubility of SM within the micelles is too low to cause the gelation, while at 35 °C the solubilization of SM in the micellar structure is enhanced which leads to the formation of gels. In the presence of salt, however, gelation occurs even at room temperature. The formation of gels in the presence of $NaNO_3$ was studied by varying the salt concentration (C_{salt}) from 0.1 to 1.0 M while the temperature was kept constant at 25 °C. Rheological analyses performed on each prepared hydrogel clearly showed that the degree of gel formation was enhanced with increasing the C_{salt}. As it can be seen from optical image shown in Figure 33, for gels synthesized at 25 °C and C_{salt} from 0.1 to 0.3 M, transparent systems were obtained, while at higher salt concentrations, opaque gels were formed.

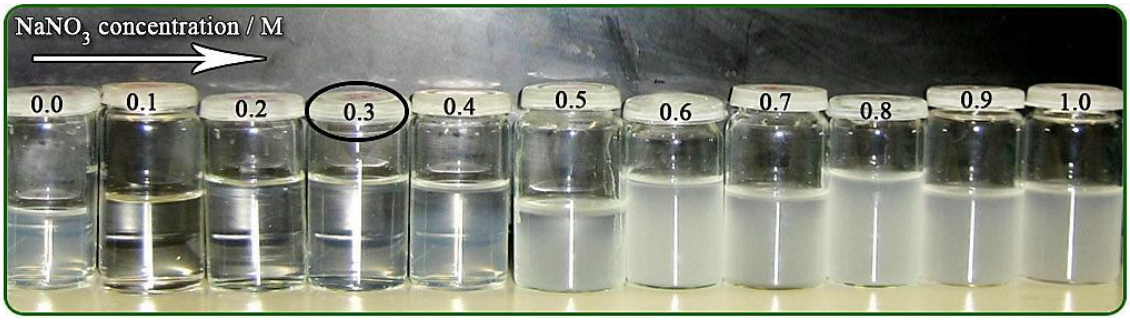

Figure 33. Optical image of synthesized physical gels at different salt concentrations ranging from 0.1 to 1.0 M at room temperature.

The formation of gels in the presence of salt indicates that SM is solubilized within the micelles which are consistent with previous reports [24-26]. The higher concentration of salt results in higher SM solubilization in the micelles which plays a key role in the formation of physical cross-links within the hydrogel network. Higher salt concentrations lead to the enhanced elasticity and viscosity and higher opacity of the gels. This indicates that a phase separation has occurred because of the aggregation of micelles [158].

The above-mentioned results were also investigated by performing rheological measurements on each gel in order to evaluate the copolymerization reaction. Although the oscillatory deformation tests were carried out on all obtained gels, only the results obtained from transparent gels ($C_{salt} \leq 0.3$ M) are presented in Table 2. The reaction time for all measured values of G′ and G″ is 10,000 seconds.

Table 2. Elastic (G´) and viscous (G˝) moduli resulting from different salt concentration.

Contents	Concentration	$NaNO_3$ / M	G´ / Pa	G˝ / Pa
CTAB	3.3 w/v%	0.1	1600	230
AAm + SM	11 w/v%	0.2	1639	251
ASP / TEMED	3.5 mM / 0.168 M	0.3	1758	335

The elastic modulus (G´) ascended as C_{salt} was increased. That demonstrates the formation of a more rigid cross-linked gel in higher salt concentrations. The elastic modulus of the gel with C_{salt} of 0.3 M, increased dramatically compared to the other transparent gels with C_{salt} 0.1 and 0.2 M. This implies that this level of salt causes more effective micellization and formation of the most rigid gel among all obtained transparent gels. The increased level of G˝ also indicates that the higher viscosity results from higher salt concentrations. This is due to the incorporation of hydrophobic blocks into the hydrophilic backbones which develops inter-molecular associations.

5.3.2 Variation of initial monomer concentration

In order to investigate the effect of the initial monomer concentration on the copolymerization, different amounts of C_0 = AAm + SM were used for preparing the physical gels. The applied monomer concentrations were varied between 5 to 13 w/v%. During this procedure concentrations of all other materials were fixed at 3.3 w/v% of CTAB, 3.5 mM of APS and 0.168 M of TEMED. The salt concentration was also kept constant at 0.3 M. The ratio of SM to total monomer (AAm + SM) in all monomer concentrations was 2 mol%, [19,159].

The gels were synthesized at 25 and 35 °C and oscillatory deformation tests were carried out on each gel at the same temperature of the synthesis. Figure 34 shows the resulted plots of G´ and G˝ after completion of copolymerization reaction at 10,000 seconds as well as tan δ (loss factor) as functions of monomer concentration at 35 °C. The results show that both the elastic and the viscous moduli increase with increasing the monomers concentration. In cases that C_0 was between 5 to 7 w/v% the formed gels were still too weak although gelation was enhanced with increasing the monomers concentration. The dramatic upward trend of G´ and G˝ versus C_0 was continued up to monomer concentration of 11 w/v%. It is notable that no significant difference was observed between the rheological results of the gels with monomer concentrations of 11 and 12 w/v%. Therefore the following discussions will be focused on the monomer concentrations of 7, 9 and 11 w/v%. The increasing trend of G´ and G˝ as a function of the monomer concentration can be explained by the fact that a higher monomer

concentration enhances the occurrence of copolymerization reaction as well as inter-molecular associations of the network.

As mentioned above both G′ and G″ increase when the monomer concentration is increased from 5 to 13 w/v%. The growing rate of the elastic modulus (G′) was faster than that of the viscous modulus (G″) and therefore the difference becomes more significant at higher amounts of C_0. The resulted data for tan δ demonstrates that when C_0 is 5 w/v%, tan δ is more than 1 that indicates a viscoelastic liquid is formed. At a monomer concentration of 6 w/v%, the loss factor is below 1 indicating that a gel is formed, although it is too weak (tan δ = 1 concerns to gel point). By increasing C_0 to higher concentrations, elasticity rises and tan δ drops consequently. The loss factor continually approached 0.2 by an additional increase in C_0, which indicates the formation of stronger hydrogels with a behavior closer to a viscoelastic solid.

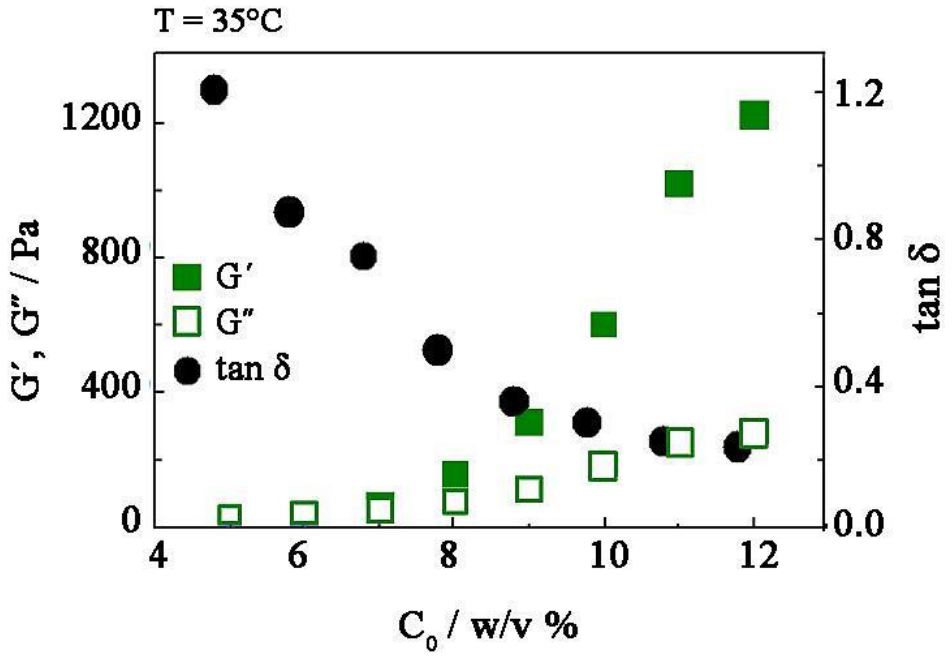

Figure 34. Values of G′ and G″ and the loss factor (tan δ) of hydrogels as a function of initial monomers concentration at 35 °C. $NaNO_3$ = 0.3 M, CTAB = 3.3 w/v%, ω = 6.3 $rad.s^{-1}$ and γ_0 = 0.01.

Figure 35 shows the results of the elastic modulus versus time (a) and its dependence on frequency (b) for different amounts of monomer concentrations at 35 °C. These plots contain only the results of the three analyzed hydrogels with initial monomer concentrations of 7, 9 and 11 w/v%. The curves represent typical gelation profiles,

which clearly demonstrate the enhancement of G´ with increasing monomer concentration. The plot of the lowest monomer concentration (AAm + SM = 7 w/v%) represents the least amount of G´, which markedly increases by increasing the monomer concentration. The reaction time before performing the frequency-sweep test was 3 hours. The range of frequency was between 0.01 and 100 Hz and γ_0 was 0.01. As it can be seen from the Figure 35, b, at lower monomer concentrations, G´ increases as a function of the frequency. However, its dependence on the frequency lowers by increasing the C_0. These combined results confirm the formation of stronger gels by increasing the initial monomer concentration.

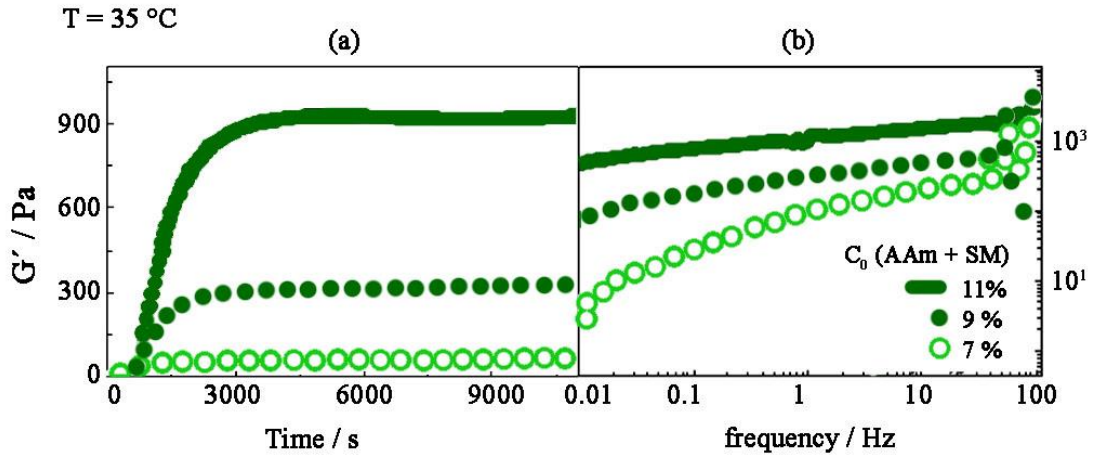

Figure 35. Characterization of the elastic modulus of hydrogels with different initial monomer concentrations by rheological measurements. Elastic modulus (G´) as a function of reaction time (a) and frequency ω (b) measured after 3 hours of reaction time. $NaNO_3$ = 0.3 M, CTAB = 3.3 w/v%.

The relaxation modulus (stress/strain) of the prepared gels was measured as a function of time for gels with monomer concentrations between 7 and 11 w/v% which is illustrated in Figure 36. The relaxation modulus increases with increasing monomer concentration owing to the enhancement of the cross-linking. The time dependent patterns of the relaxation modulus in each gel witnesses the fact that hydrophobic associations can be locally solubilizesd which causes the cross-links to be reversible. The presence of surfactant molecules prevents direct exposure of hydrophobic associations to the aqueous environment resulting in a decreased lifetime of the hydrophobic associations. A similar behavior was observed by others [20,160]. As it can be seen in Figure 36, as G(t) raises with increasing initial monomer concentration, its

dependence on time also reduces that indicates the temporary nature of hydrophobic associations.

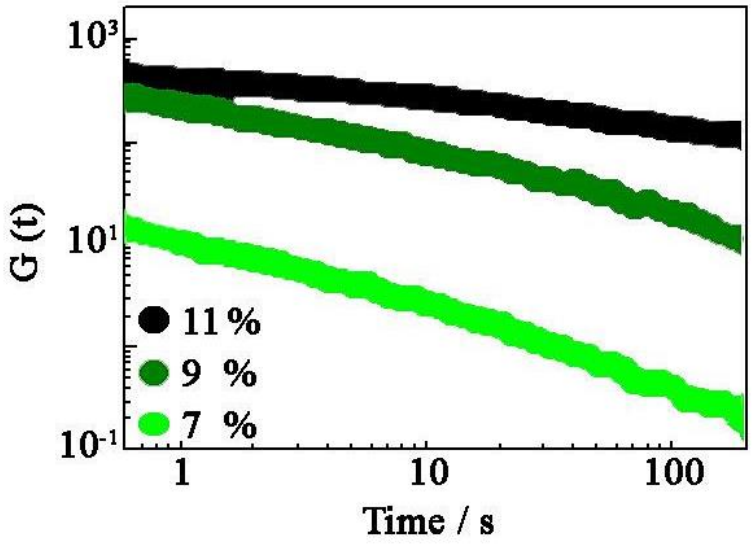

Figure 36. Relaxation modulus G(t) as a function of time for various monomer concentrations. In prepared gels $NaNO_3$ = 0.3 M, CTAB = 3.3 w/v%.

Increasing of storage modulus with frequency that's results has been presented in Figure 35 (b) agrees the observed results of relaxation time modulus that decreases versus time. It also indicates that life time of hydrophobic associations is in order of seconds. This temporary nature of hydrophobic associations leads to formation of tough hydrogels.

5.3.3 Formation of physical gels at different temperatures

The dependence of the rheological properties on the temperature was also investigated. For this purpose, elastic and viscous moduli of hydrogels synthesized with different initial monomer concentrations at different temperatures were analyzed (Figure 37, a and b). As it is obvious gels prepared in higher temperature (35 °C) exhibit a lower elastic modulus so the stored elastic energy in that gels is lower than that of the gels synthesized at 25 °C. The measurements were carried out at the same temperature at which the gels were synthesized.

It has been claimed that the formation of gels occurs after the formation and consequently association of helixes that form junction zones. The junctions become more rigid at lower temperatures [49]. It should also be mentioned that the difference between G´ of gels synthesized at different temperatures, with the same monomer concentration, raised as C_0 increased. By increasing C_0 from 9 to 11 w/v%, the elastic

modulus of the gels which were synthesized at 25 °C showed a dramatic increase while at higher reaction temperature (35 °C) the raise of the elastic modulus was much limited, suggesting that cross-linking is relatively enhanced at the lower temperature with higher monomer concentration.

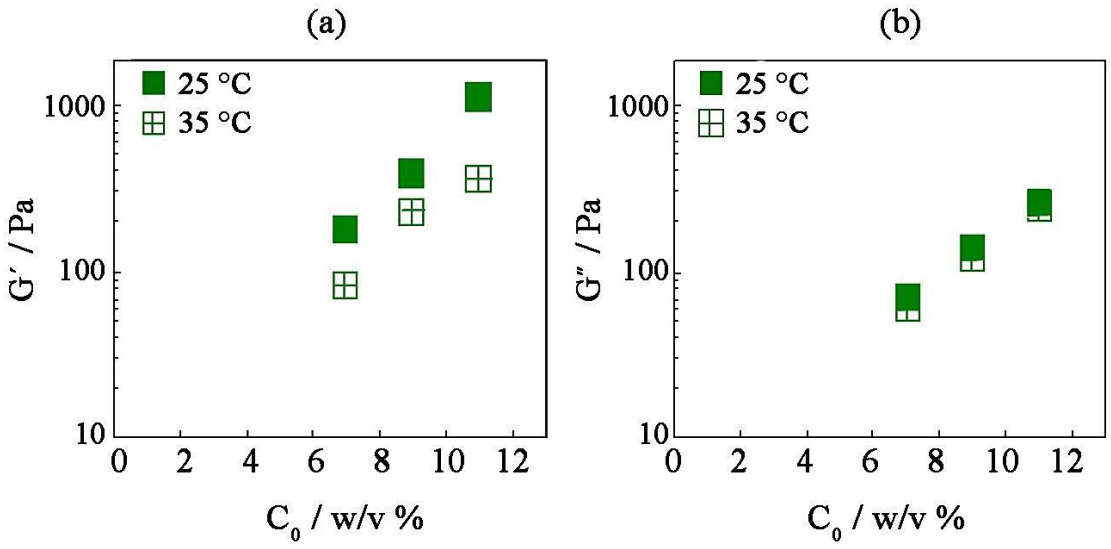

Figure 37. Temperature dependence of the static (a) and viscous (b) moduli of hydrogels as a function of the monomer concentration. $NaNO_3$ = 0.3 M, CTAB = 3.3 w/v%.

The variation of the viscous modulus of the prepared gels was measured at 25 and 35 °C for different monomer concentrations (Figure 37, b). The values of G″ show a decrease at higher temperature. Also in the analyzed range of monomer concentration, G″ increased steadily versus C_0. The dependence of G′ on the investigated parameters (Figure 37, a) was more intense than that of G″ which implies that at lower temperature and with increasing the initial monomer concentration, the hydrogels become more solid-like, owing to the formation of higher density of cross-links and a more rigid network.

5.4 Dynamic light scattering (DLS)

5.4.1 Structural inhomogeneity of physical gels

In order to evaluate the microstructure and inhomogeneity of the prepared gels, dynamic light scattering analysis was carried out. As it was stated in previous sections through DLS measurements, speckles will appear by the formation of a gel which is due to the random fluctuations in the intensity of the scattered light. Synthesized gels with various

monomer concentrations ranging between 5 and 13 w/v% were studied. All measurements were carried out at an observation temperature of 35 °C, scattering angle of $\theta = 90°$ and in 100 random sample positions. Measured data of gels formed with C_0 between 7 and 13 w/v% are presented in Figure 38 in which the variations of time-averaged scattering intensity, $\langle I \rangle_T$, versus random sample position for each initial monomer concentration is illustrated. The measurements were taken with short measuring times through which the inhomogeneity on a short time scale, shorter than the time necessary for rearrangement of the hydrophobic associations, is presented.

In addition the ensemble-averaged scattering intensity, $\langle I \rangle_E$, is shown as a solid line that is obtained by averaging of $\langle I \rangle_T$ within all sample positions. Dashed lines, $\langle I_F \rangle_T$, indicate the part of the scattering intensities which is originated from liquid-like concentration fluctuations. As it is expected, for the sample with C_0 = 7 w/v%, small fluctuations in $\langle I \rangle_T$ appear, indicating the formation of a very weak gel as a non-ergodic medium (Figure 38 (a)). It seems that in the mentioned monomer concentration (7 w/v%) and in the presence of 3.3 w/v% CTAB, stearyl methacrylate is solubilized within the micelles to achieve cross-linking via hydrophobic blocks, although in low amount. Figure 38 (b) shows that the ensemble-averaged scattering intensity, $\langle I \rangle_E$, increases significantly with increasing the monomer concentration up to 9 w/v% in which the typical speckle pattern of non-ergodic system appears, owing to the increased density of cross-links. In contrast the fluctuating component, $\langle I_F \rangle_T$, remains almost constant. As it can be seen in Figure 38 (c) and (d), for monomer concentrations of 11 and 13 w/v%, $\langle I \rangle_T$ decreased significantly, that is believed to be because of the slighter concentration variations between regions with high and low density of cross-links [161].

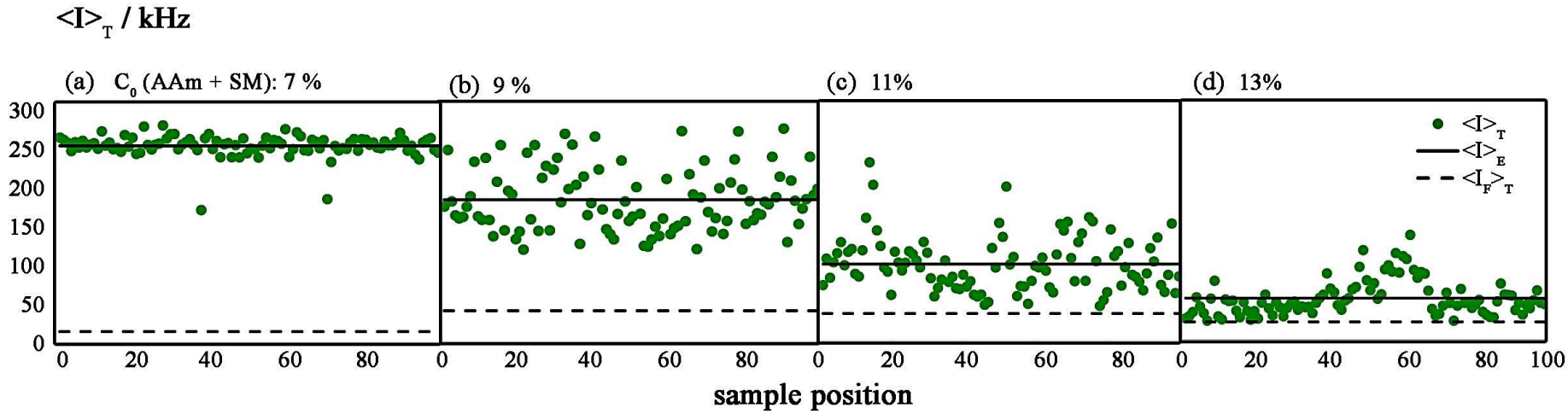

Figure 38. Variation of the time averaged scattering intensities, $\langle I \rangle_T$, with sample position of physical gels synthesized with different initial monomer concentration. The solid line indicates the ensemble-averaged scattering intensity, $\langle I \rangle_E$ and the dashed line represents the fluctuating components of the scattering intensity, $\langle I_F \rangle_T$. $\theta = 90°$ and $T = 35°C$.

5.4.2 Dynamics of physical gels

It is known that the universal features of a non-ergodic system can be more accurately presented through the normalized intermediate scattering function, $f(q,\tau)$, that has been directly calculated from the ensemble-averaged ICFs, $g_T^{(2)}(q,\tau)-1$, proposed by Pusey and Van Megen [129]. The distribution of relaxation rates, G (Γ), can be extracted by an inverse Laplace transform of $g_T^{(2)}(q,\tau)-1$ from which the relaxation rates of fast (Γ_{fast}) and slow (Γ_{slow}) modes can be obtained from the peak positions. The normalized intermediate scattering functions were obtained at a scattering angle of 90° for the initial monomer concentrations between 5 to 13 w/v%, among which the data obtained for C_0 = 7, 9 and 11 w/v% are shown in Figure 39. For all samples fast relaxations below 10^{-3} s and several slow relaxations can be observed. The dependency of the relaxation rate (Γ) on q^2 shown in Figure 41, obviously indicates that both relaxations take place through a diffusive process which will be mentioned later.

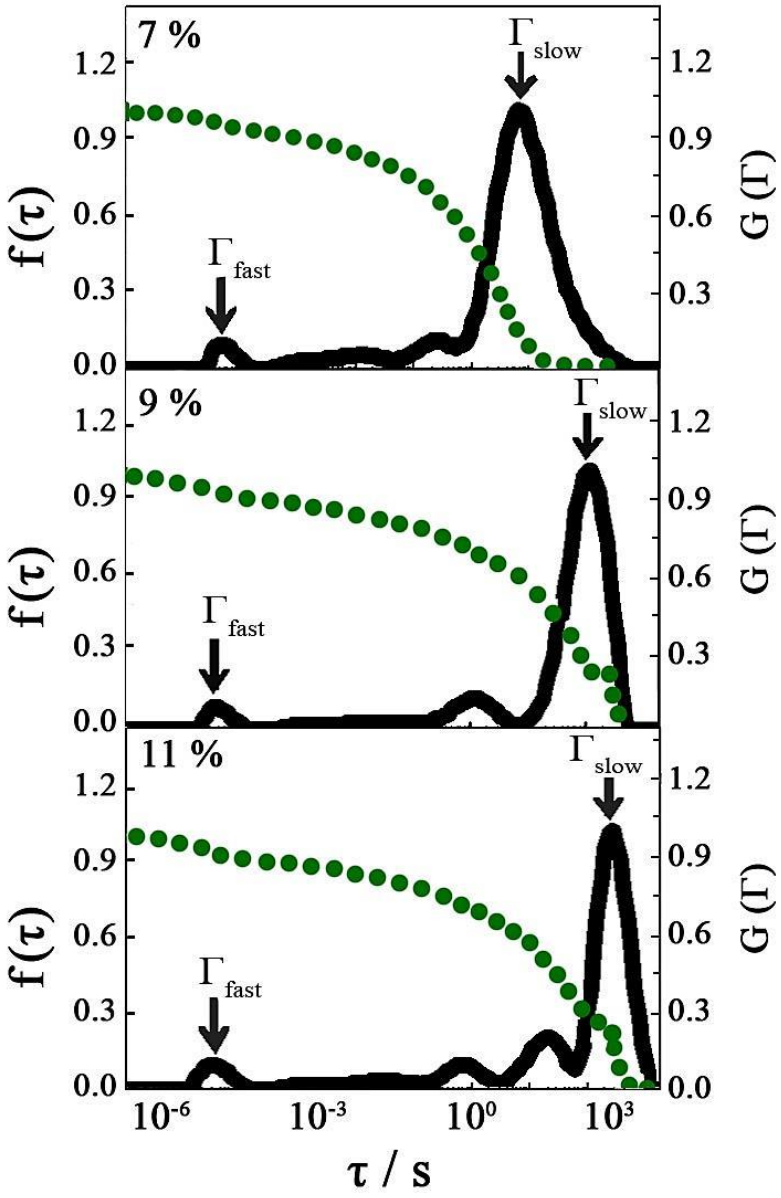

Figure 39. Normalized intermediate ensemble-average scattering function $f(\tau)$, calculated from $g_T^{(2)}(\tau)$ for different monomer concentration at a scattering angle of 90° (green curves) and characteristic decay time distribution function, G(Γ), obtained with a measurement time of 2 h at θ = 90° on a gel formed with different initial monomer concentrations. Temperature = 35 °C.

As it is can be seen in Figure 39 the monomer concentration has nearly no effect on the fast mode decay time. It is also claimed that the characteristic decay time of fast relaxation mode of hydrogels is independent of cross-linking, temperature and swelling. It indicates that slow relaxation is due to the thermally activated motions of sub-chains. It is known that the fast mode relaxation is a consequence of the cooperative diffusion

of chain segments between two adjacent entanglement or junction points. The sub-chains or “blobs” are shown schematically in Figure 40 [113,162-164].

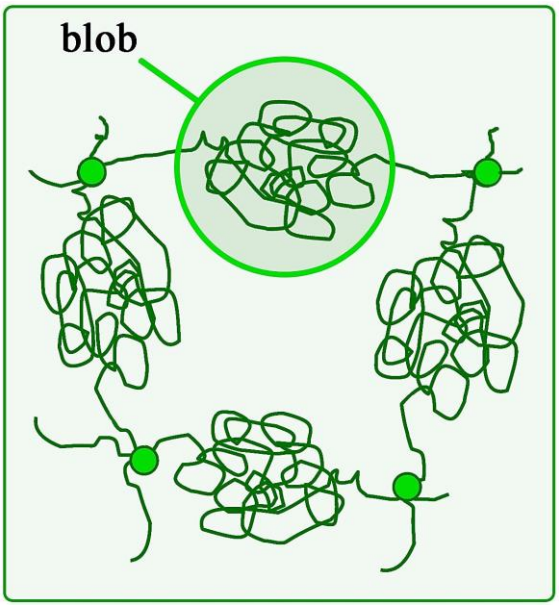

Figure 40. Sub-chains or blobs whose motion between two entangled or cross-linked point leads to fast relaxation [163].

Since the tails of the curves of $f(\tau)$ in Figure 39 are not reaching a constant level parallel to the time axis, it can be deduced that there is a slow relaxation during studied time that includes a broad range from 10^0 to 10^3 s. The slow mode relaxation of hydrogels is originated from the temporary nature of cross-links which are based on local solubilized hydrophobic associations. It has also been suggested previously that slow relaxation in micellar kinetics that lasts from scale of seconds to million seconds, is due to the dissolution of micelles into individual surfactant molecules [160]. In a study performed by D. C. Tuncaboylu et al., the surfactant molecules were extracted from the system after preparation of the gels which caused the slow relaxation mode to be removed, resulting in the formation of gels with a behavior similar to chemically cross-linked gels [20]. This observation confirms the effect of micellar kinetics on the relaxation behavior of hydrogels.

Increasing the initial monomer concentration shifts the peaks of the slow relaxation to the right (longer times). This indicates the formation of stronger gels owing to the formation of a higher density and longer life time of the physical cross-links at higher concentrations. This is also in agreement with the results of the rheological analysis that

shows the temporary nature of hydrophobic associations. Rheological observation indicated that with increasing the initial monomer concentration, time dependency of relaxation decreases.

The dependency of the relaxation rate on the scattering vector provides more information about the origin of the relaxations. Plotted Γ_{fast} and Γ_{slow} against q^2 are illustrated in Figure 41 (a). For a diffusive process the relaxation rate is dependent on q^2. Both Γ_{fast} and Γ_{slow} are proportional to q^2 which demonstrates that both modes are diffusive. Probably the motion of individual molecules and small association of chains reflects the fast relaxation time. The dependency of Γ_{fast} on q^2 also increases slightly by increasing the initial monomer concentration that indicates enhanced cross-link density and inter-molecular interactions.

The relaxation rate is given by following equation:

$$\Gamma = Dq^2 \tag{29}$$

The curves of the diffusion coefficient were also plotted (Figure 41 (b)) through which it is clear that higher monomer concentrations lead to an increase of the diffusion coefficient of the fast mode. In contrast the diffusion coefficient of the slow relaxation mode decreases markedly with increasing the monomer concentration. Increasing of D_{fast} with the monomer concentration indicates the decreasing trend of the mesh size of network. Also significant decrease of D_{slow} with raising the concentration shows that the life time of the physical cross-links is considerably larger at higher concentration.

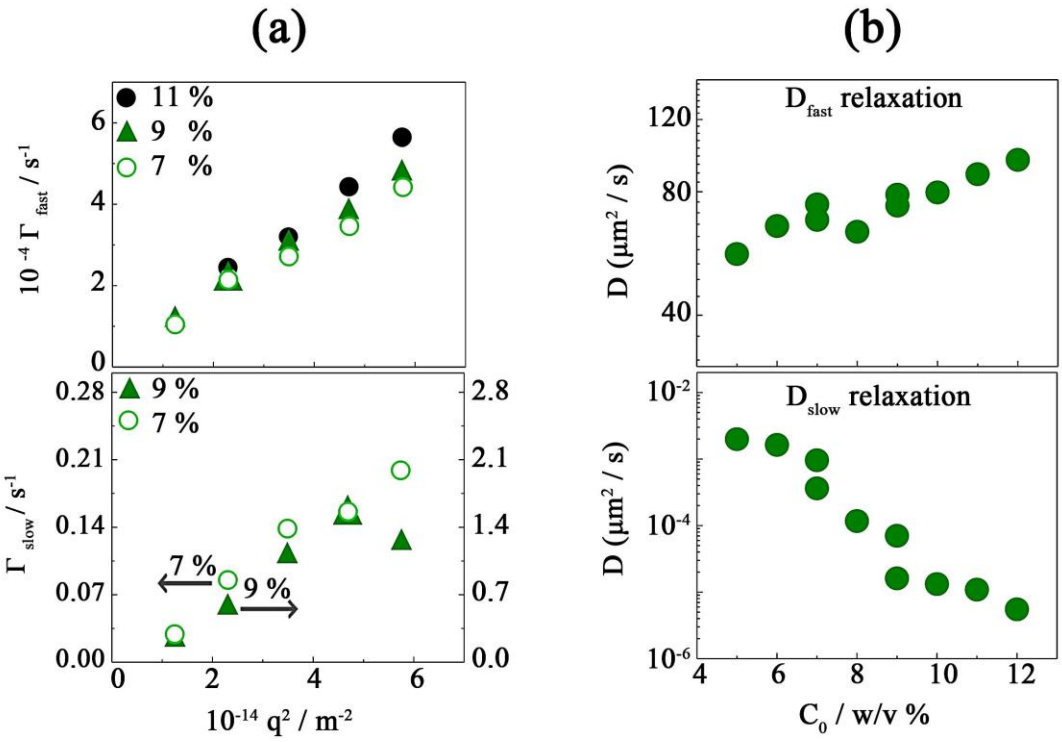

Figure 41. (a) Relaxation rate of the fast (Γ_{fast}) and slow (Γ_{slow}) modes plotted versus q^2 for different monomer concentration. (b) Diffusion coefficient of each relaxation mode plotted against initial monomer concentration.

6 Conclusion

Copolymerization of acrylamide was carried out with large hydrophobes in a micellar solution containing $NaNO_3$ as electrolyte. Presence of salt enhanced the micellar growth and solubilization of hydrophobic monomers within the micelles that provides the possibility of incorporation of hydrophobic blocks into the chains of hydrophilic PAAm.

As the first step of this study micellar solutions of water / CTAB / $NaNO_3$ were prepared and evaluated to determine the optimum concentration of each substance and its effect on the micellization process. Viscosity measurements of the solutions with various salt concentrations showed an increase in viscosity against C_{salt} from 0.3 to 0.5 M that is related to the formation and growth of worm-like micelles as C_{salt} was increased. On the other hand a further increase in $NaNO_3$ concentration up to 0.6 M resulted in a sudden drop in viscosity which is related to the branching of the micelles. Solutions with different amounts of the hydrophobic monomer (SM) were also prepared and studied with viscosity measurements. A continuous decreasing trend of viscosity versus SM concentration was observed that shows a reorganization of worm-like micelles into smaller micelles and solubilization of SM molecules within them to form hydrophobic blocks as a consequence of hydrophobic interactions. The distribution of the formed hydrophobic blocks along hydrophilic backbones occurs through the micellar copolymerization process.

Hydrogel synthesis solutions were studied step by step via dynamic light scattering (DLS). Comparison of the resulting normalized intermediate ensemble-average scattering functions and characteristic decay time distribution functions showed that surfactant agglomerates exist in water / CTAB solution that can be seen by a slow relaxation as well as fast relaxation modes. The slow relaxation mode did not appear in solutions after addition of salt and SM that confirms enhancement of aggregation. Formation of hydrophobic associations also shifted the fast relaxation to the longer times. Inclusion of hydrophilic monomers in the solutions resulted in appearance of both fast and slow relaxation modes indicating formation of hydrogels.

Evaluation of the gel formation was carried out in the second part of the experimentations. Effect of the salt concentration on the gelation was investigated at 25 and 35 °C. In salt free solutions no gel was formed at 25 °C and only a weak gel was formed at 35 °C due to enhanced solubilization of SM at the higher temperature. In the presence of salt at 25 °C and C_{salt} between 0.1 and 0.3 M formation of transparent gels also occurred. It indicates that the solubilization of SM into the micelles that leads to the

formation of physical cross-links in the gel network is higher in the presence of salt. Even higher amounts of salt resulted in formation of opaque gels.

Variation of the initial monomer concentration (C_0 = AAm + SM) from 5 to 13 w/v % also affected the properties of the gels. Both measured elastic and viscous moduli of obtained hydrogels increased with increasing C_0 because of higher inter-molecular associations of the network. The elastic modulus and frequency-sweep versus time also indicated a dramatic increase in the gel formed with C_0 = 11 % compared with lower monomer concentrations. Higher monomer concentrations led to the formation of stronger gels with smaller loss factors.

Relaxation modulus, G(t), of the gels as a function of time showed reversible cross-links resulting from the fact that hydrophobic associations can be locally solubilized. Increasing the monomer concentration led to an increase in the amount of G(t) and reduction of its dependency on time. Effect of the temperature on the synthesized gels was also investigated. Higher elastic modulus of the gels was observed at a lower temperature that is due to the enhanced cross-linking. It was found that G″ also decreased with increasing the temperature but its dependency on temperature is smaller than elastic modulus.

Evaluation of the microstructure and inhomogeneity of the gels were studied via DLS analysis. It was found that at 35 °C and with total monomer concentration of 5 w/v% no gel was formed. With a monomer concentration of 7 w/v% only a weak gel was formed and with C_0 = 9 w/v% a typical speckle pattern for the gels appeared due to the increased density of cross-links and consequently increased inhomogeneity of the hydrogels. The normalized intermediate scattering function, $f(q,\tau)$, as well as the distribution of relaxation rates, G (Γ), of the gels were obtained for various monomer concentrations. It was shown that the monomer concentration has likely no effect on the fast relaxation modes of the gels. In contrast the slow relaxation mode varied with variation of the monomer concentration. Slow relaxation mode of the physical gels is due to dissolution of micelles into individual surfactant molecules. Higher density and longer life-time of cross-links shift the slow relaxation peaks towards longer times. As diffusive modes, both fast and slow relaxation modes are proportional to the scattering vector, q^2. Moderate increase of D_{fast} with raising monomer concentration also showed that the mesh size of network becomes smaller and also significant decrease of D_{slow} with raising the concentration is an evidence of the fact that life time of the physical cross-links is considerably larger at higher concentration. To add, the hydrophobic associations have finite lifetime, so we obtain gels with high degree of toughness and self-healing property.

7 References

1. *Facile Fabrication of Tough Hydrogels Physically Cross-Linked by Strong Cooperative Hydrogen Bonding.* **G. Song, L. Zhang, C. He, D. C. Fang, P. G. Whitten, H. Wang.** 2013, Macromolecules, Vol. 46 (18), pp. 7423–7435.

2. **I. Mattiasson, B. Galaev.** *Smart Polymers. Applications in Biotechnology and Biomedicine.* 2. s.l. : CRC Press, Taylor & Francis Group, Boca Raton, 2008.

3. *Threshold fracture energies for elastomers.* **A. Ahagon, A. N. Gent.** 1975, Journal of Polymer Science: Polymer Physics Edition, Vol. 13, pp. 1903–1911.

4. *A model of the fracture of double network gels.* **H. R. Brown.** 2007, Macromolecules, Vol. 40, pp. 3815-3818.

5. *Sacrificial Bonds and Hidden Length: Unraveling Molecular Mesostructures in Tough Materials.* **G. E. Fantner, E. Oroudjev, G. Schitter, L. S. Golde, Ph. Thurner, M. M. Finch, P. Turner, Th. Gutsmann, D. E. Morse, H. Hansma, P. K. Hansma.** 2006, Biophysical Journal, Vol. 90, pp. 1411-1418.

6. *The kinetic approach to fracture in transient networks.* **S. Mora.** 2011, Soft Matter, Vol. 7, pp. 4908-4917 .

7. *Complexation of Poly(vinyl alcohol)-Congo Red Aqueous Solutions. 2. SANS and SAXS Studies on Sol-Gel Transition.* **M. Shibayama, F. Ikkai, Sh. Nomura.** 1994, Macromolecules, Vol. 27, pp. 6383–6388.

8. *Effect of degree of cross-linking on spatial inhomogeneity in charged gels. I. Theoretical predictions and light scattering study.* **M. Shibayama, F. Ikkai, Y. Shiwa, Y. Rabin.** 1997, The Journal of Chemical Physics, Vol. 107, p. 5227.

9. *Effect of Degree of Cross-Linking on Spatial Inhomogeneity in Charged Gels. 3. Ionization Effect.* **F. Ikkai, O. Iritani, M. Shibayama, C. C. Han.** 1998, Macromolecules, Vol. 31, pp. 8526–8530.

10. *Structural inhomogeneities in the range 2.5-2500 .ANG. in polyacrylamide gels.* **A. M. Hecht, R. Duplessix, E. Geissler.** 1985, Macromolecules, Vol. 18, pp. 2167–2173.

11. *Influence of the Cross-Linker Reactivity on the Formation of Inhomogeneities in Hydrogels.* **B. Lindemann, U. P. Schröder, W. Oppermann.** 1997, Macromolecules, Vol. 30, pp. 4073–4077.

12. *Structural and Dynamic Properties of Partially Charged Poly(acrylic acid) Gels: Nonergodicity and Inhomogeneities.* **A. Moussaid, S. J. Candau, J. G. H. Joosten.** 1994, Macromolecules, Vol. 27, pp. 2102–2110.

13. *Small-Angle Neutron-Scattering Study on Preparation Temperature Dependence of Thermosensitive Gels.* **S. Takata, T. Norisuye, M. Shibayama.** 2002, Macromolecules, Vol. 35, pp. 4779–4784.

14. **R. Baron, P. Setny, J. A. McCammon.** *Protein-Ligand Interactions, First Edition.* s.l. : John Wiley & Sons, Inc., 2012.

15. *Construction and Properties of Hydrophobic Association Hydrogels with High Mechanical Strength and Reforming Capability.* **G. Jiang, C. Liu, X. Liu, G.**

Zhang, M. Yang, F. Liu. 2009, Macromolecular Materials and Engineering, Vol. 294, pp. 815–820.

16. *Latex particles by miniemulsion ring-opening metathesis polymerization.* **D. Quémener, V. Héroguez, Y. Gnanou.** 2005, Macromolecules, Vol. 38 (19), pp. 7977-7982.

17. *Polyreactions in miniemulsions.* **M. Antonietti, K. Landfester.** 2002, Progress in polymer science, Vol. 27 (4), pp. 689-757.

18. *Role of surfactant type and concentration for the mean drop size during emulsification in turbulent flow.* **S. Tcholakova, N.D. Denkov, T. Danner.** 2004, Langmuir, Vol. 20 (18), pp. 7444-7458.

19. *Tough and Self-Healing Hydrogels Formed via Hydrophobic Interactions.* **D. C. Tuncaboylu, M. Sari, W. Oppermann, O. Okay.** 2011, Macromolecules, Vol. 44, pp. 4997–5005.

20. *Dynamics and Large Strain Behavior of Self-Healing Hydrogels with and without Surfactants.* **D. C. Tuncaboylu, M. Sahin, A. Argun, W. Oppermann, O. Okay.** 2012, Macromolecules, Vol. 45 (4), pp. 1991–2000.

21. *Polyacrylamide-Clay Nanocomposite Hydrogels: Rheological and Light Scattering Characterization.* **O. Okay, W. Oppermann.** 2007, Macromolecules, Vol. 40, pp. 3378-3387.

22. *Covalent Cross-Linked Polymer Gels with Reversible Sol−Gel Transition and Self-Healing Properties.* **G. Deng, Ch. Tang, F. Li, H. Jiang, Y. Chen.** 2010, Macromolecules, Vol. 43, pp. 1191–1194.

23. *Aggregation behavior of hexadecyltrimethylammonium surfactants with various counterions in aqueous solution.* **N. Jiang, P.X. Li, Y.L. Wang, J.B. Wang, H.K. Yan, R.K. Thomas.** 2005, Journal of Colloid and Interface Science, Vol. 15, pp. 755–760.

24. *Solubilization in aqueous solutions of amphiphiles.* **R. Nagarajan.** 1996, Current Opinion in Colloid and Interface Science, Vol. 1, pp. 391-401.

25. *Micellization of block copolymers.* **G. Riess.** 2003, Progress in Polymer Science, Vol. 28, pp. 1107–1170.

26. *Association of nonionic polymers with micelles, bilayers, and microemulsions.* **R. Nagarajan.** 1989, The Journal of Chemical Physics, Vol. 90, pp. 1980-1994.

27. *Phase-Transitions of Gels.* **T. Tanaka.** 1992, Acs Symposium Series, Vol. 480, pp. 1-21.

28. *Hydrogels for controled drug delivery.* **N. B. Graham, M. E. McNeil.** 1984, Biomaterials, Vol. 5, pp. 27-36.

29. *A Fluorescence Study on Swelling of Hydrogels (PAAm) at Various Cross-Linker Contents.* **D. K. Aktaş, G. A. Evingür, Ö. Pekcan.** 2009, Advances in Polymer Technology, Vols. 28, No. 4, pp. 215–223.

30. *A visible light photoinitiator system to produce acrylamide based smart hydrogels: Ru(bpy)3 probe of hydrogel microenvironments.* **C. R. Rivarola, M. A. Biasutti, C. A. Barbero.** 2009, Polymer, Vol. 50, pp. 3145–3152.

31. *Hydrogels.* **D. Ceylan.** 2009, Polymer, Vol. 51, pp. 1-28.

32. *Liquid Diffusion Applied to Analysis.* **T. Graham.** 1861, Philosophical Transactions of the Royal Society of London, Vol. 151, pp. 183–224.

33. *Thermodynamics of Polymer Solutions.* **P. J. Flory.** 1970, Discussions of the Faraday Society, pp. 7-29.

34. *Thermodynamics of High Polymer Solutions.* **P. J. Flory.** 1941, Journal of Chemical Physics, Vol. 9, pp. 660-661.

35. *Properties of Rubber Solutions and Gels.* **M. L. Huggins.** 1943, Industrial and Engineering Chemistry, Vol. 35, pp. 216-220.

36. *Theory of Solutions of High Polymers.* **M. L. Huggins.** 1941, Journal of the American Chemical Society, Vol. 64, pp. 1712-1719.

37. *The Thermodynamic Study Of Rubber-Like Elasticity.* **L. R. G. Treloar.** 1952, Proceedings of the Royal Society of London Series B-Biological Sciences, Vol. 139, pp. 506-521.

38. *The Physical Properties of Amorphous Polymer Networks.* **L. R. G. Treloar.** 1951, Chemistry & Industry, pp. 955-958.

39. *Responsive Gels: Volume Transitions 1*. **M. Shibayama, T. Tanaka.** 1993, Advances in Polymer Science, Vol. 109.

40. *Transitionin Swollen Polymer Networks Induced by Intramolecular Condensation.* **K. Dusek, D. Patterson.** 1968, Journal of Polymer Science, Part a-2-Polymer Physics, Vol. 6, pp. 1209-1216.

41. *Gels.* **T. Tanaka.** 1981, Scientific American, Vol. 1981, pp. 124-138.

42. *Studies on Mechanical and Swelling Behavior of Polymer Networks on the Basis of the Scaling.* **F. Horkay, M. Zrinyi.** 1988, Macromolecules, Vol. 21, pp. 3260-3266.

43. *Double-network hydrogels with extremely high mechanical strength.* **J. P. Gong, Y. Katsuyama, T. Kurokawa, Y. Osada.** 2003, Advanced Materials, Vol. 15, pp. 1155-1158.

44. *The polyrotaxane gel: A topological gel by figure-of-eight cross-links.* **Y. Okumura, K. Ito.** 2001, Advanced Materials, Vol. 13, pp. 485-487.

45. *Synthesis and rheological behavior of new hydrophobically modified hydrogels with tunable properties.* **G. Miquelard-Garnier, S. Demoures, C. Creton, D. Hourdet.** 2006, Macromolecules, Vol. 39, pp. 8128-8139.

46. *Nanocomposite Hydrogels: A Unique Organic–Inorganic Network Structure with Extraordinary Mechanical, Optical, and Swelling/De-swelling Properties.* **K. Haraguchi, T. Takehisa.** 2002, Advanced Materials, Vol. 14, pp. 1120–1124.

47. *Hydrogels for biomedical applications.* **A. S. Hoffman.** 2002, Advanced Drug Delivery Review, Vol. 54, pp. 3-12.

48. *Reentrant phase transition of strong polyelectrolyte poly(N-isopropylacrylamide) gels in PEG solutions.* **D. Melekaslan, O. Okay.** 2001, Macromolecular Chemistry and Physics, Vol. 202, pp. 304-312.

49. **S. K. H. Gulrez, S. Al-Assaf, G. O. Phillips.** Hydrogels: Methods of Preparation, Characterisation and Applications. [book auth.] Angelo Carpi. *Progress in*

Molecular and Environmental Bioengineering – From Analysis and Modeling to Technology Applications. s.l. : InTech, 2011, pp. 117-150.

50. *Mechanically strong hydrogels with reversible behaviour under cyclic compression with MPa loading.* **K. Harrass, R. Krüger, M. Möller, K. Albrecht, J. Groll.** 2013, Soft Matter, Vol. 9, p. 2869.

51. *Novel hydrogels with excellent mechanical performance.* **Y. Tanaka, J. Ping Gong, Y. Osada.** 2005, Progress in Polymer Science, Vol. 30, pp. 1-9.

52. *Design and Fabrication of a High-Strength Hydrogel with Ideally Homogeneous Network Structure from Tetrahedron-like Macromonomers.* **T. Sakai, T. Matsunaga, Y. Yamamoto, C. Ito, R. Yoshida, S. Suzuki, N. Sasaki, M. Shibayama and U. I. Chung.** 2008, Macromolecules, Vol. 41, pp. 5379–5384.

53. *Hydrogels and Biodegradable Polymers for Bioapplications.* **R. M. Ottebrite, S. J. Huang, K. Park.** 1996, ACS Symposium Series, Vol. 627.

54. *Hydrophilic Gels for Biological Use.* **O. Wichterle, D. Lim.** 1960, Nature, Vols. 185, No. 4706, pp. 117-118.

55. *Polymer architecture and drug delivery.* **L. Y. Qiu, Y.H. Bae.** 2006, Pharmaceutical Research, Vol. 23 (1), pp. 1-30.

56. *Hydrogels in Biology and Medicine: From Molecular Principles to Bionanotechnology.* **N. A. Peppas, J. Z. Hilt, A. Khademhosseini, R. Langer.** 2006, Advanced Materials, Vol. 18 (11), pp. 1345–1360.

57. *Synthetic hydrogels VI. Hydrogel composites as wound dressings and implant materials.* **P. H. Corkhill, C.J. Hamilton, B.J. Tighe.** 1989, Biomaterials, Vol. 10 (1), pp. 3-10.

58. *Biodegrable Hydrogels for Drug Delivery.* **T. G. Park, S. W. Shalaby.** 1993, Technomic Publishing.

59. *Hydrogels in biomedical applications.* **D. G. Pedley, P. J. Skelly, B. Tighe.** 1980, British Polymer Journal, Vol. 12, pp. 99-110.

60. *Microgels - Intramolecularly crosslinked macromolecules with a globular structure.* **W. Funke, O. Okay,B. Joos-Muller.** 1998, Microencapsulation - Microgels - Iniferters, Vol. 136, pp. 139-234.

61. **D. DeRossi, K. Kajiwara, Y. Osada, A. Yamauchi.** *Polymer Gels.* New York : Plenum, 1991.

62. **Y. Osada, K. Kajiwara.** *Gel Handbook.* New York : Academic Pres, 2001.

63. *The potential of polymeric cryogels in bioseparation.* **V. I. Lozinsky, F. M. Plieva, I. Y. Galaev, B. Mattiasson.** 2001, Bioseparation, Vol. 10, pp. 163-188.

64. *Poly (2-Hydroxyethyl Methacrylate) Sponges as Implant Materials - Invivo and Invitro Evaluation of Cellular Invasion.* **T. V. Chirila, I. J. Constable, G. J. Crawford, S. Vijayasekaran, D.E. Thompson, Y. C. Chen, W. A. Fletcher, B. J. Griffin.** 1993, Biomaterials, Vol. 14, pp. 26-38.

65. *Macroporous Hydrogels for Biomedical Applications - Methodology and Morphology.* **H. R. Oxley, P. H. Corkhill, J. H. Fitton, B. J. Tighe.** 1993, Biomaterials, Vol. 14, pp. 1064-1072.

66. *Effect of salt and temperature on viscoelasticity of gelatin hydrogels.* **S. Chatterjee, H. B. Bohidar.** 2006, Journal of Science and Technology, Vol. 22, pp. 1-13.

67. **W. Kauzmann.** *The Mechanism of Enzyme Action.* s.l. : The John Hopkins Press, 1953. pp. 70–110.

68. *Hydrophobic interaction chromatography of proteins.* **J. A. Queiroz, C. T. Tomaz, J. M. S. Cabral.** 2001, Journal of Biotechnology, Vol. 87, pp. 143–159.

69. *Effect of salt addition on strength and dynamics of hydrophobic interactions.* **T. Fujita, H. Watanabe, S. Tanaka.** 2007, Chemical Physics Letters, Vol. 434, pp. 42-48.

70. *A View of the Hydrophobic Effect.* **N. T. Southall, K. A. Dill, A. D. J. Haymet.** 2002, The Journal of Physical Chemistry B, Vol. 106, pp. 521-533.

71. **R. Winter, F. Noll, C. Czeslik.** *Methoden der Biophysikalischen Chemie.* s.l. : Teubner-Verlag, 1998.

72. *Design of high-toughness polyacrylamide hydrogels by hydrophobic modification.* **S. Abdurrahmanoglu, V. Can, O. Okay.** 2009, Polymer, Vol. 50, pp. 5449-5455.

73. *Shape and Size of Highly Concentrated Micelles in CTAB/NaSal Solutions by Small Angle Neutron Scattering (SANS).* **N. Ch. Das, H. Cao, H. Kaiser, G. T. Warren, J. R. Gladden, P. E. Sokol.** s.l. : American Chemical Society, 2012, Langmuir, Vol. 28, p. 11962−11968.

74. **R. Mandavi.** Critical Micelle Concentration of Surfactant, Mixed Surfactantand Polymer By Different Methods at Room Temperature And Its Importance. *Kinetic studies of some Esters and Amides in presence of micelles.* 2011, 2.

75. *Viscoelastic surfactant solutions: model systems for rheological research.* **H. Rehage, H. Hoffmann.** s.l. : Taylor & Francis, 1991, Molecular Physics, Vols. 24, No. 9, pp. 933-973.

76. *Investigation of SDS, DTAB and CTAB micelle microviscosities by electron spin resonance.* **M. A. Bahri, M. Hoebeke, A. Grammenos, L. Delanaye, N. Vandewalle, A. Seret.** 2006, Colloids and Surfaces A: Physicochemical and Engineering Aspects, Vol. 290, pp. 206–212.

77. *Importance of Micellar Kinetics in Relation to Technological Processes.* **A. Patist, J. R. Kanicky, P. K. Shukla, D. O. Shah.** 2002, Journal of Colloid and Interface Science, Vol. 245, pp. 1-15.

78. **W. J. Peer.** 1987, Polymer Materials Science and Engineering, Vol. 57, p. 492.

79. *Properties of Hydrophobically Associating Polyacrylamides: Influence of the Method of Synthesis.* **A. Hill, F. Candau, J. Selb.** 1993, Macromolecules, Vol. 26, pp. 4521-4532.

80. **S. R. Turner, D. B. Siano and J. Bock (Exxon Research and Engineering Company, United States).** *A Microemulsion Process for Producing Acrylamide-Alkyl Acrylamide Copolymers. 4,521,580* U. S. Patent, June 1985.

81. *Thermo-Sensitive Hydrogel: Control of Hydrophilic-Hydrophobic Transition.* **W. Siriwatwechakul, N. Teraphongphom, V. Ngaotheppitak, S. Kunataned.** 2008, International Journal of Chemical and Biological Engineering, pp. 1-4.

82. *Emulsion polymerization of hydrophobic monomers like stearyl acrylate with cyclodextrin as a phase transfer agent.* **R. J. Leyrer, W. Machtle.** 2000, macromolecular chemistry and physics, Vol. 201, pp. 1235-1243.

83. *Emulsion polymerization of hydrophobic monomers.* **W. Lau.** 2002, Macromolecular Symposia, Vol. 182, pp. 283-289.

84. *Effect of Ostwald ripening on styrene Effect of Ostwald ripening on styrene.* **C. S. Chern, T. J. Chen.** 1998, Colloids Surfaces A: Physicochemical and Engineering Aspects, Vol. 138, pp. 65-74.

85. *Self-healing hydrogels formed in catanionic surfactant solutions.* **G. Akay, A. Hassan-Raeisi, D. C. Tuncaboylu, N. Orakdogen, S. Abdurrahmanoglu, W. Oppermann, O. Okay.** 2013, Soft Matter, Vol. 9, pp. 2254-2261.

86. *The effect of organic additives on paraffin chain electrolyte solutions. VI. Light scattering measurements on viscoelastic solubilized solutions of methyl naphthalene in aqueous hexadecyl trimethyl ammonium bromide.* **A. J. Hyde, D.W.M Johnstone.** 1975, Journal of Colloid and Interface Science, Vol. 53, pp. 349-357.

87. **T. Cosgrove, [ed.].** *Colloid Science Principles, methods and applications.* s.l. : John Wiley & Sons Ltd, 2010.

88. *Structure and Flow in Surfactant Solutions.* **C. A. Herb, R. K. Prud'homme.** 1994, ACS Symposium Series, Vol. 578.

89. *Rheological properties of viscoelastic surfactant systems.* **H. Rehage, H. Hoffmann.** 1988, Journal of Physical Chemistry, Vol. 92, pp. 4712-4719.

90. *Viscoelastic behavior of surfactant threadlike micellar solutions: effects of additives.* **T. Shikata, M. Shiokawa, S. Imai.** 2003, Journal of Colloid and Interface Science, Vol. 259, pp. 367–373.

91. *Effects of Sodium Salicylate on the Microstructure of an Aqueous Micellar Solution and Its Rheological Responses.* **W. J. Kim, S. M. Yang.** 2, 2000, Journal of Colloid and Interface Science, Vol. 232, pp. 225-234.

92. *Effect of C12EOn mixed surfactant systems on the formation of viscoelastic worm-like micellar solutions in sucrose alkanoate– and CTAB–water systems.* **S. Engelskirchen, D.P. Acharya, M. Garcia-Roman, H. Kunieda.** 2006, Colloids and Surfaces A: Physicochemical and Engineering Aspects, Vol. 279, pp. 113–120.

93. *Formation of Viscoelastic Wormlike Micellar Solutions in Mixed Nonionic Surfactant Systems.* **D. P. Acharya, H. Kunieda.** 2003, Journal of Physical Chemistry, Vol. 107 (37), pp. 10168–10175.

94. *Formation and Disruption of Viscoelastic Wormlike Micellar Networks in the Mixed Surfactant Systems of Sucrose Alkanoate and Polyoxyethylene Alkyl Ether.* **A. Maestro, D. P. Acharya, H. Furukawa, J. M. Gutiérrez, M. A. López-Quintela, M. Ishitobi, H. Kunieda.** 2004, Journal of Physical Chemistry, B, Vol. 108 (37), pp. 14009–14016.

95. *Effects of Protonation on the Viscoelastic Properties of Tetradecyldimethylamine Oxide Micelles.* **H. Maeda, A. Yamamoto, M. Souda, H. Kawasaki, Kh. S. Hossain, N. Nemoto, M. Almgren.** 2001, Journal of Physical Chemistry, Vol. 105 (23), pp. 5411–5418.

96. *Viscoelastic micellar water/CTAB/NaNO3 solutions: Rheology, SANS and cryo-TEM analysis.* **K. Kuperkar, L. Abezgauz, D. Danino, G. Verma, P.A. Hassan, V.K. Aswal, D. Varade, P. Bahadur.** 2008, Journal of Colloid and Interface Science, Vol. 323, pp. 403–409.

97. *Mechanical properties of hydrogels and their experimental determination.* **K. S. Anseth, Ch. N. Bowman, L. Brannon-Peppas.** 1996, Biomaterials, Vol. 17, pp. 1647-1657.

98. **L. H. Sperling.** *Introduction to Physical Polymer Science.* 2005.

99. **I. M. Ward, J. Sweeney.** *An Introduction to the Mechanical Properties of Solid Polymers.* 2004.

100. **M. Rubinstein, R. Colby.** *Polymer Physics.* New York : Oxford University Press, 2008.

101. **D. I. Bower.** *An Introduction to Polymer Physics.* s.l. : Cambridge University Press, 2002.

102. **H. Murata.** Rheology – Theory and Application to Biomaterials. [book auth.] Ailton De Souza Gomes. *Polymerization.* 2012.

103. **R. S. Lakes.** *Viscoelastic Materials.* s.l. : Cambridge University Press, 2009.

104. *Composition dependence of the viscoelasticity of end-linked poly(dimethylsiloxane) at the gel point.* **J. C. Scanlan, H. H. Winter.** 1991, Macromolecules, Vol. 24, pp. 47–54.

105. *Viscoelasticity of Dental Tissue Conditioners during the Sol-gel Transition.* **H. Murata, H. Chimori, T. Hamada, J. F. McCabe.** 2005, Journal of Dental Research, Vol. 84 Issue 4, p. 376.

106. *Stress-relaxation behavior in gels with ionic and covalent crosslinks.* **X. Zhao, N. Huebsch, D. J. Mooney, Zh. Suo.** 2010, Journal of Applied Physics, Vol. 107.

107. *Small-angle x-ray and neutron scattering studies of the volume phase transition in thermosensitive core–shell colloids.* **S. Seelenmeyer, I. Deike, S. Rosenfeldt, Ch. Norhausen, N. Dingenouts, M. Ballauff, T. Narayanan, and P. Lindner.** 2001, Journal of Chemical Physics, Vol. 114, pp. 10471-10478.

108. *Clustering induced collapse of a polymer brush.* **T. J. Wu, C. Hu.** 1999, Physical Review Letters, Vol. 83, pp. 4105-4107.

109. **B. Chu.** *Laser Light Scattering; Basic Principles and Practice.* 2nd. San Diego : Academic Press, 1991.

110. **B. J. Berne, R. Pecora.** *Dynamic light scattering.* New York : Wiley, 1976.

111. *Cross-link Density Dependence of Spatial Inhomogeneities and Dynamic Fluctuations of Poly(N-isopropylacrylamide) Gels.* **M. Shibayama, T. Norisuye, Sh. Nomura.** 1996, Macromolecules, Vol. 29, pp. 8746–8750.

112. *Preparation of Homogeneous Hydrogels by Controlling the Crosslinker Reactivity and Availability.* **S. Abdurrahmanoglu, O. Okay.** 2008, Journal of Macromolecular Science, Part A, Vol. 45, pp. 769-775.

113. *Spatial inhomogenity and dynamic fluctuations of polymer gels.* **M. Shibayama.** 1998, Macromolecular Chemistry and Physics, Vol. 199, pp. 1-30.

114. *Spatial Inhomogeneities of Polystrene Gels Prepared from Semidilute Solutions.* **R. G. Liu, W. Oppermann.** 2006, Macromolecules, Vol. 39, pp. 4159-4167.

115. *Gel Formation Analyses by Dynamic Light Scattering.* **M. Shibayama, T. Norisuye.** 2002, bulletin of chemical society of japan, Vol. 75, pp. 641-659.

116. **E. Geissler.** *Dynamic Light Scattering, the methods and applications.* [ed.] W. Brown Oxford University. s.l. : Oxford, 1993.

117. *An Audiofrequency Resonance in the Quasielastic Light Scattering of Polymer Gels.* **W. Prins, L. Rimai, A. F. Chompff.** January 1972, Macromolecules, Vol. 5 (1), pp. 104-106.

118. *Spectrum of light scattered from a viscoelastic gel.* **T. Tanaka, L. Hocker, G. Benedek.** 1973, Journal of Chemical Physics, Vol. 59, p. 5151.

119. *The Poisson ratio in polymer gels. 2.* **E. Geissler, A. M. Hecht.** January 1981, Macromolecules, Vol. 14, pp. 185–188.

120. *Rayleigh light scattering from concentrated solutions of polystyrene in cyclohexane.* **E. Hecht, A.M. Geissler.** 1976, Journal of Chemical Physics, Vol. 65, p. 103.

121. *Dynamic light scattering from polyacrylamide-water gels.* **A. M. Hecht, E. Geissler.** 1978, Journal de Physique, Vol. 39 (6), p. 631.

122. *Scattering and swelling properties of inhomogeneous polyacrylamide gels.* **S. Mallam, F. Horkay, A. M. Hecht, E. Geissler.** 1989, Macromolecules, Vol. 22, pp. 3356–3361.

123. *Inhomogenity control in polymer gels.* **F. Ikkai, M. Shibayama.** 2005, Journal of Polymer Science: Part B: Polymer Physics, Vol. 43, pp. 617-628.

124. *Characterization of inhomogeneous polyacrylamide hydrogels.* **Y. Cohen, O. Ramon, I. J. Kopelman and S. Mizrahi.** 1992, Journal of Polymer Science Part B: Polymer Physics, Vol. 30, pp. 1055–1067.

125. *Swelling and cross-linking density effects on the structure of partially ionized gels.* **F. Schosseler, R. Skouri, J. P. Munch and S. J. Candau.** 1994, Journal de Physique II, Vols. 4, No. 7, p. 1221.

126. *Neutron Scattering Properties of Randomly Cross-Linked Polyisoprene Gels.* **F. Horkay, G. B. McKenna, P. Deschamps, E. Geissler.** 2000, Vol. 33, pp. 5215–5220.

127. *Small-angle neutron scattering study on weakly charged temperature sensitive polymer gels.* **M. Shibayama, T. Tanaka, C. C. Han.** 1992, The Journal of Chemical Physics [1], Vol. 97, p. 6842 .

128. *Effects of cyclization and electrostatic interactions on the termination rate of macroradicals in free-radical crosslinking copolymerization.* **M. Keskinel, O. Okay.** 1998, Polymer Bulletin, Vol. 40, pp. 491-498.

129. *Dynamic light scattering by non-ergodic media.* **P. N. Pusey, W. van Megen.** 1989, Physica A, Vol. 157, pp. 705-741.

130. *Dynamic and Static Light Scattering by Aqueous Polyacrylamide Gels.* **J. G. H. Joosten, J. L. McCarthy, P. N. Pusey.** 1991, Macromolecules, Vol. 24, pp. 6690-6699.

131. *Dynamic light scattering by permanent gels: heterodyne and nonergodic medium methods of data evaluation.* **L. Fang, W. Brown.** 1992, Macromolecules, Vol. 25, pp. 6897–6903.

132. *Dynamic light scattering by nonergodic media: Brownian particles trapped in polyacrylamide gels.* **J. G. H. Joosten, E. T. F. Geladé, P. N. Pusey.** 1990, Physical Review A, Vol. 42, pp. 2161–2175.

133. *Universality and Specificity of Polymer Gels Viewed by Scattering Methods.* **M. Shibayama.** 2006, Bulletin of Chemical Society of Japan, Vol. 79, pp. 1799–1819.

134. *Hydrophobically-modified polyacrylamides prepared by micellar polymerization.* **F. Candau, J. Selb.** 1999, Advances in Colloid and Interface Science, Vol. 79, pp. 149-172.

135. *Water-soluble copolymers. 37. Synthesis and characterization of responsive hydrophobically modified polyelectrolytes.* **C. L. McCormick, J. C. Middleton, D. F. Cummins.** 1992, Macromolecules, Vol. 25, pp. 1201–1206.

136. *Water soluble copolymers: 38. Synthesis and characterization of electrolyte responsive terpolymers of acrylamide, N-(4-butyl)phenylacrylamide, and sodium acrylate, sodium-2-acrylamido-2-methylpropanesulphonate or sodium-3-acrylamido-3-methylbutanoate.* **C. L. McCormick, J. C. Middleton, C. E. Grady.** 1992, Polymer, Vol. 33, pp. 4184-4190.

137. *Water-soluble polymers: 59. Investigation of the effects of polymer microstructure on the associative behaviour of amphiphilic terpolymers of acrylamide, acrylic acid and N-[(4-decyl)phenyl]acrylamide.* **K. D. Branham, D. L. Davis, J. C. Middleton, C. L. McCormick.** 1994, Polymer, Vol. 35, pp. 4429-4436.

138. *Water-Soluble Copolymers. 61. Microstructural Investigation of Pyrenesulfonamide-Labeled Polyelectrolytes. Variation of Label Proximity Utilizing Micellar Polymerization.* **K. D. Branham, G. S. Shafer, Ch. E. Hoyle, Ch. L. McCormick.** 1995, Macromolecules, Vol. 28, pp. 6175–6182.

139. **M. W. Urban, Th. Provder, [ed.].** *Multidimensional Spectroscopy of Polymers, Vibrational, NMR, and Fluorescence Techniques.* Washington, DC : ACS Symposium Series, American Chemical Society, 1995. Vol. 598.

140. *Water-Soluble Copolymers. 64. Effects of pH and Composition on Associative Properties of Amphiphilic Acrylamide/Acrylic Acid Terpolymers.* **K. D. Branham, H. S. Snowden, Ch. L. McCormick.** 1996, Macromolecules, Vol. 29, pp. 254–262.

141. *Stearyl Methacrylate 1618 F HS (SMA 1618 F HS).* s.l. : BASF the chemical company, 2013.

142. **Q. Shi, G. Jackowski.** Chapter 2: One–dimensional Polyacrylamide Gel Electrophoresis. [book auth.] Hames BD. *Gel Electrophoresis of Proteins: A Practical Approach.* s.l. : Oxford University Press, 1998, pp. 1-52.

143. *Role of hydration and water structure in biological and colloidal interactions.* **J. Israelachvili, H. Wennerströ.** 1996, Nature, Vol. 379, pp. 219-225.

144. *Interaction between the Strong Anionic Character of Strong Anions and the Hydrophobic Association Property of Hydrophobic Blocks in Macromolecular Chains of a Water-Soluble Copolymer.* **B. Gao, N. Wu, Y. Li.** 2005, Journal of Applied Polymer Science, Vol. 96, pp. 714–722.

145. *Synthesis, structure and properties of hydrophobically associating polymers.* **F. Candau, S. Biggs, A. Hill, J. Selb.** 1994, Progress in Organic Coatings, Vol. 24, pp. 11-19.

146. *Dynamics in polyacrylamide hydrogels formed via hydrophobic associations.* **A. Hassan-Raeisi, O. Okay, W. Oppermann.** Freiburg : s.n., February 2013, conference of MACROMOLEKULAR KOLLOQUIUM FREIBURG.

147. *Variations on a theme: Changes to electrophoretic separations that can make a difference.* **T. Rabilloud.** 2010, Journal of Proteomics, Vol. 73, pp. 1562-1572.

148. *Small-angle neutron-scattering and viscosity studies of CTAB/NaSal viscoelastic micellar solutions.* **V. K. Aswal, P. S. Goyal, P. Thiyagarajan.** 1998, The Journal of Physical Chemistry B, Vol. 102, pp. 2469–2473.

149. **W. M. Kulicke, Ch. Clasen.** *Viscosimetry of Polymers and Polyelectrolytes.* Berin : Springer, 2004.

150. *A systematic study of equilibrium structure, thermodynamics, and rheology of aqueous CTAB/NaNO3 wormlike micelles.* **M. E. Helgeson, T. K. Hodgdon, E. W. Kaler, N. J. Wagner.** 2010, Journal of Colloid and Interface Science, Vol. 349, pp. 1-12.

151. *Electrostatic Screening and Charge Correlation Effects in Micellization of Ionic Surfactants.* **A. Jusufi, A.P. Hynninen, M. Haataja, A. Z. Panagiotopoulos.** 2009, Journal of Physical Chemistry, Vol. 113, pp. 6314-6320.

152. *Effects of Protonation on the Viscoelastic Properties of Tetradecyldimethylamine Oxide Micelles.* **hazf (90) H. Maeda, A. Yamamoto, M. Souda, H. Kawasaki, Kh. S. Hossain, N. Nemoto, M. Almgren.** 2001, Journal of Physical Chemistry B, Vol. 105 (23), pp. 5411–5418.

153. *Wormlike micelles in Tween-80/CmEO3 mixed nonionic surfactant systems in aqueous media.* **D. Varade, K. Ushiyama, L. K. Shrestha, K. Aramaki.** 2007, Vol. 312, pp. 489-497.

154. *Micellar solubilization of drugs.* **C. O. Rangel-Yagui, A. Pessoa-Jr, L. C. Tavares.** 2005, Journal of Pharmaceutical Sciences, Vol. 8(2), pp. 147-163.

155. *Solubilization of poorly water-soluble drugs by mixed micelles based on hydrogenated phosphatidylcholine.* **C. Rupp, H. Steckel, B. W. Müller.** 2010, International Journal of Pharmaceutics, Vol. 395, pp. 272–280.

156. *Kinetics of Emulsion Polymerization.* **W. V. Smith, R. H. Ewart.** 1948, Journal of chemical physics, Vol. 16, p. 592.

157. *A General Theory of the Mechanism of Emulsion Polymerization.* **Harkins, W. D.** 1947, Journal of American Chemical Society, Vol. 69 (6), pp. 1428–1444.

158. *Micelle size and shape of sodium dodecyl sulfate in concentrated sodium chloride solutions.* **S. Hayashi, Sh. Ikeda.** 1980, The Journal of Physical Chemistry, Vol. 84, pp. 744–751.

159. *The Effects of Concentration, Pressure, and Temperature on the Diffusion Coefficient and Correlation Length of SDS Micelles.* **J. S. Collura, D. E. Harrison, C. J. Richards, T. K. Kole, M. R. Fisch.** 2001, The Journal of Physical Chemistry B, Vol. 105, pp. 4846–4852.

160. *Kinetics of micellization: its significance to technological processes.* **A. Patist, S.G. Oh, R. Leung, D.O. Shah.** 2001, Colloids and Surfaces A: Physicochemical and Engineering Aspects, Vol. 176, pp. 3-16.

161. **V. Can.** *Investigation of the Network Inhomogeneity of Thiol-Ene Organogels.* s.l. : Dissertation, Clausthal University of Technology, 2013.

162. *The slow relaxation mode: from solutions to gel networks.* **J. Li, T. Ngai, Ch. Wu.** s.l. : The Society of Polymer Science, Japan (SPSJ), 2010, Polymer Journal, Vol. 42, pp. 609–625.

163. *Origins of Speckles and Slow Dynamics of Polymer Gels.* **T. Ngai, Ch. Wu, Y. Chen.** 2004, The Journal of Physical Chemistry B, Vol. 45, pp. 5532-5540.

164. *Large-scale heterogeneities in randomly cross-linked networks.* **J. Bastide, L. Leibler.** 1988, Macromolecules, Vol. 21, pp. 2647–2649.

List of symbols

AAm	Acrylamide
APS	Ammonium persulfate
CTAB	Cetyltrimethylammoniumbromide
$NaNO_3$	Sodium nitrate
SM	Stearyl methacrylate
C16	n-hexadecyl methacrylate
C18	n-octadecyl methacrylate
TEMED	Tetramethylethylenediamine
DTAB	Dodecyltrimethylammonium bromide
SDS	Sodium dodecyl sulfate
NO_3^-	Nitrate
KBr	Potassium bromide
NaSal	Sodium salicylate
PAAm	Polyacrylamide
LS	Light scattering
DLS	Dynamic light scattering
SANS	Small-angle neutron scattering
cryo-TEM	Cryo-transmission electron microscopy
PCS	Photon correlation spectroscopy
DN	Double network gel
MMC	Macromolecular microspheres composite
TP	Topological gel
PEG	Tetra-polyethylene glycol
PHEMA	Poly (2-hydroxyethyl methacrylate)
ΔG	Free energy
ΔH	Enthalpy
ΔS	Entropy
CMC	Critical micelle concentration
C	Concentration
C_{salt}	Salt concentration
G'	Elastic modulus (Storage modulus)
G''	Viscous modulus (Loss modulus)
G	Shear modulus
σ	Shear stress
ω	Angular frequency

η	Viscosity
η_0	Intrinsic viscosity
δ	Loss angle
$\tan \delta$	Loss factor
γ_0	Deformation amplitude
γ	Shear strain
$\dot{\gamma}$	Shear rate
$\dot{\gamma}_{crit}$	Critical shear rate
G (t)	Relaxation modulus
T_g	Gelation temperature
T	Absolute temperature (K)
λ	Wavelength
ICF	Intensity Correlation Function
THB theory	Theory of Tanaka, Hocker and Benedek
D_{NE}	Non-ergodic medium method
D_{HT}	Partial heterodyne method
D_{HTB}	partial heterodyne method with the instrumental coherence correction
D_{HM}	Homodyne method
q	Scattering vector
β	Coherence factor
$f(q,\infty)$	Asymptotic value
$f(q,\tau)$	Function of the normalized intermediate ensemble-average
$I(q,\tau)$	Scattered light intensity
$\langle ... \rangle_T$	Time-average
$\langle ... \rangle_E$	Ensemble-average
$\langle I \rangle_T$	Time-average scattering intensity
$\langle I \rangle_E$	Ensemble-average scattering intensity
$\langle I_F \rangle_T$	Intensity of fluctuating part
$I_C\,(q)$	Static component
$\langle I(q) \rangle_E$	Ensemble-averages intensity
$\langle I(q) \rangle_T$	Time average scattering intensity
$\langle I_F(q) \rangle_T$	Time-average of dynamic fluctuations
$g^{(2)}(\tau)$	Simple exponential function
$g^{(2)}(q,\tau)$	Intensity correlation function
τ	Intensity correlation time
$f(\tau)$	Normalized intermediate ensemble-average scattering function

D_{trans}	Translational diffusion coefficient
R_H	Hydrodynamic radius
k_B	Boltzmann's constant
kT	Boltzmann energy
ζ	Dynamic correlation length
D_A	Apparent diffusion coefficient
D	Cooperative diffusion coefficient
Γ_{fast}	Relaxation rate of fast mode
Γ_{slow}	Relaxation rate of slow mode
G(Γ)	Characteristic decay time distribution function

PERSONAL INFORMATION

Azadeh HASSAN RAEISI (polymer chemist)

136, Mühlenstrasse, Germany

0049 17620956032 00982188077263

raeisi.azadeh@yahoo.de / ahrae@tu-clausthal.de

Sex female | Date of birth 20/09/1980| Nationality German/ Iranian

WORK EXPERIENCE

2010-2013 Research Scientist and Teacher Assistant at the Clausthal University of Technology, Physical Chemistry Institute, Clausthal, Germany

2009-2010 Assistant at the Clausthal University of Technology, Technical chemistry Institute, Clausthal, Germany

2008-2009 Working at the CUTEC-Institute GmbH, Clausthal, Germany

2003-2005 Teaching inorganic chemistry, Tehran

EDUCATION AND TRAINING

06.2010-02.2014 PhD student at the physical chemistry department, Clausthal University of Technology, Clausthal, Germany

Thesis title: "**Investigation of Hydrophobically Modified Polyacrylamide Gels Prepared in Micellar Solutions of a Cationic Surfactant**".

10.2007-05.2010 Master study in polymer chemistry at technical chemistry department, Clausthal University of Technology, Germany. Master degree: good

Thesis title: "**Synthesis and modification of inorganic/ organic hybrid materials of polyhedral oligosilsesquioxanes (POSS) compounds and organic reactive polymers**".

2005-2007 Graduate course "Bachelor", at technical chemistry department, Clausthal University of Technology, Germany. Bachelor degree: good

Thesis title: "**Radical Polymerization under different conditions**".

1999-2003 Bachelor study in applied chemistry, Azad University of Tehran/Iran, ended at June 2003

2013 Business English Course (12 weeks), fulltime, Academy überlingen, Goslar, Germany.

2012 Team working workshop, Clausthal University of Technology, Clausthal, Germany.

2012 Cultural relationships among universities, Clausthal University of Technology, Clausthal, Germany.

2011 Collaboration with the Istanbul University of technology, working on collaboration projects during PhD (4 weeks) Istanbul, Turkey.

2011 Presentation skills workshop, Hannover University, Hannover, Germany

ADDITIONAL INFORMATION

Publications-Presentations

Azadeh H. Raeisi, Oguz Okay and Wilhelm Oppermann, Poster, "**Dynamics in polyacrylamide hydrogels formed via hydrophobic associations**", MACROMOLEKULARESKOLLOQUIUM FREIBURG, February 2013

GizemAkay, Azadeh H-Raeisi, Deniz C. Tuncaboylu, Nermin Orakdogen, Suzan Abdurrahmanogl, Wilhelm Oppermann and Oguz Okay, "**Self-Healing Hydrogels Formed in Catanionic Surfactant Solutions**", Soft.Matter, 2013

Azadeh Hassan-Raeisi, Seyed Pouya Mohammadi,
"Hydrogels: Fundamentals and Applications in Drug Delivery", (Published book in Persian), Tehran, 2014

Clausthal-Zellerfeld, February 2014